MEMORANDUM (DRAFT)

Tetra Tech, Inc.
10306 Eaton Place, Suite 340
Fairfax, VA 22030
Telephone (703) 385-6000
Fax (703) 385-6007

Date: November 20, 2015

To: Mark Voorhees, EPA Region I

From: Guoshun Zhang, Khalid Alvi – Tetra Tech

Subject: Update of long-term runoff time series for various land uses in New England

Under WA 4-35, Tetra Tech is tasked to update long-term pollutant runoff time series for typical land uses in the region. The time series update consists of two aspects: 1. To update annual average pollutant loading rates for Total Nitrogen (TN), Total Phosphorous (TP), Total Suspended Solids (TSS), and Zinc (Zn), and 2. To expand the time series duration of 01/01/1992-12/31/2002 to 01/01/1992-12/31/2014. This memorandum introduces the background information for the time series update, the overall strategy for the time series update, and the final results.

1. Background of the Long-Term Runoff Time Series

When developing long-term BMP performance curves for the region in a previous assignment, runoff time series for the period of 01/01/1992 to 12/31/2002 were created for simulating BMP processes (Tetra Tech, 2008). In that effort, the time series for TSS, TP, TN, and Zn were developed for 5 land uses including Commercial, Industrial, High Density Residential, Medium Density Residential, and Low Density Residential. Typical pollutant loading rates for these land uses and pollutant combinations are summarized in Table 1.

Table 1. Pollutant loading rates for previous round of long-term time series generation.

Land cover/Source category	Pollutant loading export rates (lbs/ac-yr)			
	TSS	TP	TN	Zn
Commercial	1,000	1.5	9.8	2.1
Industrial	670	1.3	4.7	0.4
High-Density Residential	420	1.0	6.2	0.7
Medium-Density Residential	250	0.3	3.9	0.1
Low-Density Residential	65	0.04	0.4	0.04

Source: Shaver et al. 2007

A set of Stormwater Management Model (SWMM) were set up to simulate the land use and pollutant combinations. Using the long-term rainfall time series as input, SWMM model buildup and washoff parameters were calibrated to match the annual average loading rates in Table 1. The calibrated time series were later used for estimating cumulative BMP performances (Tetra Tech, 2008).

A similar set of pollutant time series were developed in a later study for three communities in Upper Charles River, Massachusetts (Tetra Tech, 2009), and the rates are summarized in Table 2. In comparison with the pollutant loading rates in Table 1, the pollutant loading rates for the three Upper Charles River communities were for TP only, with more land use categories that are separated into pervious and impervious categories.

Table 2. Annual average TP loading rates for three Upper Charles River communities.

Land use	TP load export rate (kg/ha/yr)	Land surface cover	P load (kg/ha/yr)	Source of export rate
Agriculture *	0.5	Pervious	0.5	1
Commercial **	1.679	Impervious	2.5	2
		Pervious	0.3	
Forest	0.13	Impervious	1	3
		Pervious	0.1	
Freeway	0.9	Impervious	1.5	2
		Pervious	0.3	
High-density residential	1.119	Impervious	2.5	2
		Pervious	0.3	
Industrial	1.455	Impervious	2	2
		Pervious	0.3	
Low-density residential (rural)	0.30	Impervious	1	3
		Pervious	0.15	
Medium-density residential	0.560	Impervious	1.5	2
		Pervious	0.3	
Open space	0.30	Impervious	1	3
		Pervious	0.25	

Sources: (1) Budd and Meals 1994; (2) Shaver et al. 2007; (3) Mattson and Isaac 1999

Notes:

* Agriculture includes row crops, actively managed hay fields and pasture land.

** Institutional type land uses such as government properties, hospitals, and schools are included in the commercial land use category for the purpose of calculating phosphorus loadings.

2. Planned Updates to Long-Term Pollutant Runoff Time Series

EPA Region 1 continues to compile and assess representative stormwater pollutant loading information. Consequently, it is desirable to update long-term pollutant loading time series to incorporate the most recent knowledge into the stormwater management decision-making processes across the region. Consideration of factors such as rainfall concentrations of certain pollutants (e.g. TP and TN) and further assessments of stormwater runoff quality from impervious and pervious surface separately are areas where refinements to the time series can be made. Additionally, it is desirable to expand the previous time series duration, 01/01/1992 to 12/31/2002, to include current climate data for decision-makers who are interested in knowing the climate impacts from a more recent time frame.

Long-term pollutant runoff time series are updated in recognition of the practical needs. The updates modify pollutant loading rates in reflection of more recent loading rate estimations and expand the duration of loading rates to a more recent ending time (e.g. 12/31/2014).

Tables 3 to 6 below present the updated annual average pollutant loading rates for TP, TN, TSS, and Zn, respectively, and the sources for the updated loading rates are also included. As shown in the tables, updated loading rates are provided for eight land uses, each with both a pervious and impervious loading rate. For each of the land use and pollutant combination, new time series are generated for the time period of 01/01/1992 to 12/31/2014.

Table 3. Proposed annual average TP loading rates (rainfall concentration of TP considered).

Phosphorus Source Category by Land Use	Land Surface Cover	Phosphorus Load Export Rate, Kg/ha/yr	Comments
Commercial (Com) Industrial (Ind) & Institutional	Directly connected impervious	2	Derived using a combination of the Lower Charles USGS Loads study and NSWQ dataset. This PLER is approximately 75% of the HDR PLER and reflects the difference in the distributions of SW TP EMCs between Commercial/Industrial and Residential.
	Pervious	See* DevPERV	
Multi-Family (MFR) and High-Density Residential (HDR)	Directly connected impervious	2.6	Largely based on loading information from Charles USGS loads, SWMM HRU modeling, and NSWQ data set
	Pervious	See* DevPERV	
Medium -Density Residential (MDR)	Directly connected impervious	2.2	Largely based on loading information from Charles USGS loads, SWMM HRU modeling, and NSWQ data set
	Pervious	See* DevPERV	
Low Density Residential (LDR) - "Rural"	Directly connected impervious	1.7	Derived in part from Mattson & Issac, HRU modeling, lawn runoff TP quality information from Chesapeake Bay and subsequent modeling to estimate PLER for DCIA (Table 14) to approximate literature reported composite rate 0.3 kg/ha/yr.
	Pervious	See* DevPERV	
Highway (HWY)	Directly connected impervious	1.5	Largely based on USGS highway runoff data, HRU modeling, information from Shaver et al and subsequent modeling to estimate PLER for DCIA for literature reported composite rate 0.9 kg/ha/yr.
	Pervious	See* DevPERV	
Forest (For)	Directly connected impervious	1.7	Derived from Mattson & Issac and subsequent modeling to estimate PLER for DCIA that corresponds with the literature reported composite rate of 0.13 kg/ha/yr (Table 14)
	Pervious	0.13	
Open Land (Open)	Directly connected impervious	1.7	Derived in part from Mattson & Issac, HRU modeling, lawn runoff TP quality

Phosphorus Source Category by Land Use	Land Surface Cover	Phosphorus Load Export Rate, Kg/ha/yr	Comments
	Pervious	See* DevPERV	information from Chesapeake Bay and subsequent modeling to estimate PLER for DCIA (Table 14) to approximate literature reported composite rate 0.3 kg/ha/yr.
Agriculture (Ag)	Directly connected impervious	1.7	Derived from Budd, L.F. and D.W. Meals and subsequent modeling to estimate PLER for DCIA to approximate reported composite PLER of 0.5 kg/ha/yr.
	Pervious	0.5	
*Developed Land Pervious (DevPERV)- Hydrologic Soil Group A	Pervious	0.03	Derived from SWMM and P8 - Curve Number continuous simulation HRU modeling with assumed TP concentration of 0.2 mg/L for pervious runoff from developed lands. TP of 0.2 mg/L is based on TB-9 (CSN, 2011), and other PLER literature and assumes unfertilized condition due to the upcoming MA phosphorus fertilizer control legislation.
*Developed Land Pervious (DevPERV)- Hydrologic Soil Group B	Pervious	0.13	
*Developed Land Pervious (DevPERV) - Hydrologic Soil Group C	Pervious	0.24	
*Developed Land Pervious (DevPERV) - Hydrologic Soil Group C/D	Pervious	0.33	
*Developed Land Pervious (DevPERV) - Hydrologic Soil Group D	Pervious	0.41	

Table 4. Proposed annual average TN loading rates (rainfall concentration of TN considered).

Nitrogen Source Category by Land Use	Land Surface Cover	Runoff Nitrogen Load Export Rate, Kg/ha/yr	Comments
Commercial (Com) Industrial (Ind) & Institutional	Directly connected impervious	16.9	WISE modeling by Geosyntec for the Squamscot River IMP, 2014. Average of NLER for rooftops and other impervious surfaces for commercial and industrial
	Pervious	See* DevPERV	
Multi-Family (MFR) and High-Density Residential (HDR)	Directly connected impervious	15.8	WISE modeling by Geosyntec for the Squamscot River IMP, 2014. Average of NLERs for rooftops and other impervious surfaces for residential
	Pervious	See* DevPERV	
Medium -Density Residential (MDR)	Directly connected impervious	15.8	WISE modeling by Geosyntec for the Squamscot River IMP, 2014. Average of

Nitrogen Source Category by Land Use	Land Surface Cover	Runoff Nitrogen Load Export Rate, Kg/ha/yr	Comments
	Pervious	See* DevPERV	NLERs for rooftops and other impervious surfaces for residential
Low Density Residential (LDR) - "Rural"	Directly connected impervious	15.8	WISE modeling by Geosyntec for the Squamscot River IMP, 2014. Average of NLERs for rooftops and other impervious surfaces for residential
	Pervious	See* DevPERV	
Highway (HWY)	Directly connected impervious	11.4	WISE modeling by Geosyntec for the Squamscot River IMP, 2014. Average of NLERs for roadways and freeway impervious surfaces
	Pervious	See* DevPERV	
Forest (For)	Directly connected impervious	12.7	WISE modeling by Geosyntec for the Squamscot River IMP, 2014. NLER for roadways
	Pervious	0.6	Derived from SWMM and P8 - Curve Number continuous simulation HRU modeling with assumed TN concentration of 0.8 mg/L for pervious runoff from forest lands. Median TN conc. of 0.8 mg/l by (Budd and Meals, 1994)
Open Land (Open)	Directly connected impervious	12.7	WISE modeling by Geosyntec for the Squamscot River IMP, 2014. NLER for roadways
	Pervious	See* DevPERV	
Agriculture (Ag)	Directly connected impervious	12.7	WISE modeling by Geosyntec for the Squamscot River IMP, 2014. NLER for roadways
	Pervious	2.9	Derived from SWMM and P8 - Curve Number continuous simulation HRU modeling with assumed TN concentration of 2.5 mg/L for pervious runoff from agriculture lands. Median TN conc. of 2.5 mg/l by (Budd and Meals, 1994)
*Developed Land Pervious (DevPERV)- Hydrologic Soil Group A	Pervious	0.3	Derived from SWMM and P8 - Curve Number continuous simulation HRU modeling with assumed TN concentration of 2.0 mg/L for pervious runoff from developed lands. TN of 2.0 mg/L is based on TB-9 (CSN, 2011), and other PLER literature and assumes 50% of unfertilized and 50% fertilized conditions.
*Developed Land Pervious (DevPERV)- Hydrologic Soil Group B	Pervious	1.3	
*Developed Land Pervious (DevPERV) - Hydrologic Soil Group C	Pervious	2.7	
*Developed Land Pervious (DevPERV) - Hydrologic Soil Group C/D	Pervious	3.4	

Nitrogen Source Category by Land Use	Land Surface Cover	Runoff Nitrogen Load Export Rate, Kg/ha/yr	Comments
*Developed Land Pervious (DevPERV) - Hydrologic Soil Group D	Pervious	4.1	

Table 5. Proposed annual average TSS loading rates.

TSS Source Category by Land Use	Land Surface Cover	Runoff TSS Load Export Rate, Kg/ha/yr	Comments
Commercial (Com) Industrial (Ind) & Institutional	Directly connected impervious	423	Derived from SWMM and P8 - Curve Number continuous simulation HRU modeling with assumed TSS concentration of 43 mg/L for impervious runoff from commercial and Industrial lands. EMC of 43 mg/L is the median EMC for commercial and industrial from the NSQD, 2008 for Rainfall regions 1 and 2
	Pervious	See* DevPERV	
Multi-Family (MFR) and High-Density Residential (HDR)	Directly connected impervious	492	Derived from SWMM and P8 - Curve Number continuous simulation HRU modeling with assumed TSS concentration of 50 mg/L for impervious runoff from residential lands. EMC of 50 mg/L is the median EMC for residential from the NSQD, 2008 for Rainfall regions 1 and 2
	Pervious	See* DevPERV	
Medium -Density Residential (MDR)	Directly connected impervious	492	
	Pervious	See* DevPERV	
Low Density Residential (LDR) - "Rural"	Directly connected impervious	492	
	Pervious	See* DevPERV	
Highway (HWY)	Directly connected impervious	1659	Derived for MassDOT by VHB "Long-Term Continuous Simulation for Pollutant Loading and Treatment for MassDOT Impaired Waters Program" (June 2012) using highway runoff data collected by the USGS for MassDOT
	Pervious	See* DevPERV	
Forest (For)	Directly connected impervious	728	Derived from SWMM and P8 - Curve Number continuous simulation HRU modeling with assumed TSS concentration of 74 mg/L for impervious runoff from forest lands. EMC of 74 mg/L is the median EMC for open land from the NSQD, 2008 for Rainfall regions 1 and 2
	Pervious	See* DevPERV	
Open Land (Open)	Directly connected impervious	728	
	Pervious	See* DevPERV	
Agriculture (Ag)	Directly connected impervious	728	

TSS Source Category by Land Use	Land Surface Cover	Runoff TSS Load Export Rate, Kg/ha/yr	Comments
	Pervious	See* DevPERV	
*Developed Land Pervious (DevPERV)- Hydrologic Soil Group A	Pervious	8	Derived from SWMM and P8 - Curve Number continuous simulation HRU modeling with assumed TSS concentration of 50 mg/L for pervious runoff from developed lands. TSS EMC of 50 mg/L is the median EMC for residential from the NSQD, 2008 for Rainfall regions 1 and 2
*Developed Land Pervious (DevPERV)- Hydrologic Soil Group B	Pervious	33	
*Developed Land Pervious (DevPERV) - Hydrologic Soil Group C	Pervious	67	
*Developed Land Pervious (DevPERV) - Hydrologic Soil Group C/D	Pervious	85	
*Developed Land Pervious (DevPERV) - Hydrologic Soil Group D	Pervious	102	

Table 6. Proposed annual average Zn loading rates.

Zinc Source Category by Land Use	Land Surface Cover	Runoff Zinc Load Export Rate, Kg/ha/yr	Comments
Commercial (Com) Industrial (Ind) & Institutional	Directly connected impervious	1.54	Derived from SWMM and P8 - Curve Number continuous simulation HRU modeling with assumed Total Zinc concentration of 156 µg/L for impervious runoff from commercial and Industrial lands. Zn of 156 µg/L is based on the median EMCs for commercial and industrial categories from the NSQD, 2008 for Rainfall regions 1 and 2
	Pervious	See* DevPERV	
Multi-Family (MFR) and High-Density Residential (HDR)	Directly connected impervious	0.79	Derived from SWMM and P8 - Curve Number continuous simulation HRU modeling with assumed Total Zinc concentration of 80 µg/L for impervious runoff from residential lands. Zn of 80 µg/L is based on the median EMC for residential from the NSQD, 2008 for Rainfall regions 1 and 2
	Pervious	See* DevPERV	
Medium -Density Residential (MDR)	Directly connected impervious	0.79	
	Pervious	See* DevPERV	
Low Density Residential (LDR) - "Rural"	Directly connected impervious	0.79	

Zinc Source Category by Land Use	Land Surface Cover	Runoff Zinc Load Export Rate, Kg/ha/yr	Comments
	Pervious	See* DevPERV	
Highway (HWY)	Directly connected impervious	1.97	Derived from SWMM and P8 - Curve Number continuous simulation HRU modeling with assumed Total Zinc concentration of 200 µg/L for impervious runoff from highways. Zn of 200 µg/L is based on Table 3-10 from Fundamentals of Urban Runoff, 2007.
	Pervious	See* DevPERV	
Forest (For)	Directly connected impervious	0.79	Derived from SWMM and P8 - Curve Number continuous simulation HRU modeling with assumed Total Zinc concentration of 80 µg/L for impervious runoff from residential lands. Zn of 80 µg/L is based on the the median EMC for residential from the NSQD, 2008 for Rainfall regions 1 and 2
	Pervious	0.05	
Open Land (Open)	Directly connected impervious	1.11	Derived from SWMM and P8 - Curve Number continuous simulation HRU modeling with assumed Total Zinc concentration of 113 µg/L for impervious runoff from open lands. Zn of 113 µg/L is based on the on the the median for open land for the NSQD, 2008 for Rainfall regions 1 and 2
	Pervious	See* DevPERV	
Agriculture (Ag)	Directly connected impervious	0.79	
	Pervious	See* DevPERV	
*Developed Land Pervious (DevPERV)- Hydrologic Soil Group A	Pervious	0.006	Derived from SWMM and P8 - Curve Number continuous simulation HRU modeling with assumed Total Zinc concentration of 39 µg/L for pervious runoff from developed lands. Zn of 39 µg/L is based on Table 3-10 from Fundamentals of Urban Runoff, 2007.
*Developed Land Pervious (DevPERV)- Hydrologic Soil Group B	Pervious	0.025	
*Developed Land Pervious (DevPERV) - Hydrologic Soil Group C	Pervious	0.052	
*Developed Land Pervious (DevPERV) - Hydrologic Soil Group C/D	Pervious	0.066	
*Developed Land Pervious (DevPERV) - Hydrologic Soil Group D	Pervious	0.08	

3. Strategy for Pollutant Time Series Update

Similar to the pollutant time series creation in previous BMP performance curve development (Tetra Tech, 2008) and the three Upper Charles River communities study (Tetra Tech, 2009), the update of pollutant time series consists of setting up the SWMM model for unit-area land uses, calibrating the SWMM buildup and washoff parameters to match the pollutant loading rates specified in Tables 3 to 6, and processing the SWMM outputs for SUSTAIN input. There are two additional steps in SWMM model calibration in comparison to the two previous calibration exercises for TP and TN: inclusion of rainfall concentrations of TN and TP, and using the calibrated buildup and washoff parameters for impervious surfaces against the TP and TN EMCs from the Region's representative SW database. A separate study was performed under Task 9 to calibrate the SWMM buildup and washoff parameters for a generic impervious cover. The detailed methodology and the outcome of that study is reported in a technical memo 9.1 "*Memo_Buildup Washoff Calibration Approach*" and technical memo 9.2 "*Memo_Buildup Washoff Calibration Results*". A scaling factor (calibration parameter) was introduced to the maximum buildup possible under different impervious land use categories to further calibrate the annual average loading rates for TN and TP long-term timeseries developed under this task.

Rainfall concentrations of TN and TP are specified as constant values in SWMM model setup. According to the Region, the TN rainfall concentration is set as 0.31 mg/L, and the TP rainfall concentration is set as 0.017 mg/L.

4. Results

The time series for TN, TP, Zn, and TSS have been calibrated against the target values specified in Tables 3 to 6. The buildup and washoff parameters for TP and TN were selected from the calibrated parameters identified under Task 9 effort. The maximum storage capacity was adjusted iteratively until the long-term average annual loading rate matched the targeted values. Table 7 to Table 10 show the calibrated buildup and washoff parameters used in SWMM model for developing the long-term timeseries for eight land use categories.

Table 7. Calibrated Buildup and Washoff Parameters for TN.

	Buildup Parameters		Washoff Parameters	
Land Use Type	Max Storage (lb/acre)	Buildup Rate (per day)	Washoff Coeff.	Washoff Exponent
Commercial (Com), Industrial (Ind) & Institutional (Ins)	0.517	0.2	2	1
Multi-Family (MFR) and High-Density Residential (HDR)	0.476	0.2	2	1
Medium -Density Residential (MDR)	0.476	0.2	2	1
Low Density Residential (LDR) - "Rural"	0.476	0.2	2	1
Highway (HWY)	0.310	0.2	2	1
Forest (For)	0.359	0.2	2	1
Open Land (Open)	0.359	0.2	2	1
Agriculture (Ag)	0.359	0.2	2	1

Land Use Type	Buildup Parameters		Washoff Parameters	
	Max Storage (lb/acre)	Buildup Rate (per day)	Washoff Coeff.	Washoff Exponent
Forest (ForPERV) Pervious	0.698	0.1	1	2
Agriculture (AgPERV) Pervious	4.383	0.1	1	2
Developed Land Pervious (DevPERV)-Hydrologic Soil Group A	1.630	0.1	1	2
Developed Land Pervious (DevPERV)-Hydrologic Soil Group B	1.765	0.1	1	2
Developed Land Pervious (DevPERV) - Hydrologic Soil Group C	1.753	0.1	1	2
Developed Land Pervious (DevPERV) - Hydrologic Soil Group C/D	1.714	0.1	1	2
Developed Land Pervious (DevPERV) - Hydrologic Soil Group D	1.564	0.1	1	2

Table 8. Calibrated Buildup and Washoff Parameters for TP.

Land Use Type	Buildup Parameters		Washoff Parameters	
	Max Storage (lb/acre)	Buildup Rate (per day)	Washoff Coeff.	Washoff Exponent
Commercial (Com), Industrial (Ind) & Institutional (Ins)	0.069	0.2	2	1
Multi-Family (MFR) and High-Density Residential (HDR)	0.093	0.2	2	1
Medium -Density Residential (MDR)	0.075	0.2	2	1
Low Density Residential (LDR) - "Rural"	0.056	0.2	2	1
Highway (HWY)	0.052	0.2	2	1
Forest (For)	0.056	0.2	2	1
Open Land (Open)	0.056	0.2	2	1
Agriculture (Ag)	0.056	0.2	2	1
Forest (ForPERV) Pervious	0.194	0.1	1	2
Agriculture (AgPERV) Pervious	0.798	0.1	1	2
Developed Land Pervious (DevPERV)-Hydrologic Soil Group A	0.174	0.1	1	2
Developed Land Pervious (DevPERV)-Hydrologic Soil Group B	0.194	0.1	1	2
Developed Land Pervious (DevPERV) - Hydrologic Soil Group C	0.170	0.1	1	2
Developed Land Pervious (DevPERV) - Hydrologic Soil Group C/D	0.185	0.1	1	2
Developed Land Pervious (DevPERV) - Hydrologic Soil Group D	0.175	0.1	1	2

Table 9. Calibrated Buildup and Washoff Parameters for Zn.

Land Use Type	Buildup Parameters		Washoff Parameters	
	Max Storage (lb/acre)	Buildup Rate (per day)	Washoff Coeff.	Washoff Exponent
Commercial (Com), Industrial (Ind) & Institutional (Ins)	0.253	0.3	1	2
Multi-Family (MFR) and High-Density Residential (HDR)	0.130	0.3	1	2
Medium -Density Residential (MDR)	0.130	0.3	1	2
Low Density Residential (LDR) - "Rural"	0.130	0.3	1	2
Highway (HWY)	0.323	0.3	1	2
Forest (For)	0.134	0.2	1	2
Open Land (Open)	0.187	0.2	1	2
Agriculture (Ag)	0.134	0.2	1	2
Forest (ForPERV) Pervious	0.083	0.1	1	2
Agriculture (AgPERV) Pervious	0.041	0.1	1	2
Developed Land Pervious (DevPERV)-Hydrologic Soil Group A	0.038	0.1	1	2
Developed Land Pervious (DevPERV)-Hydrologic Soil Group B	0.041	0.1	1	2
Developed Land Pervious (DevPERV) - Hydrologic Soil Group C	0.042	0.1	1	2
Developed Land Pervious (DevPERV) - Hydrologic Soil Group C/D	0.042	0.1	1	2
Developed Land Pervious (DevPERV) - Hydrologic Soil Group D	0.038	0.1	1	2

Table 10. Calibrated Buildup and Washoff Parameters for TSS.

Land Use Type	Buildup Parameters		Washoff Parameters	
	Max Storage (lb/acre)	Buildup Rate (per day)	Washoff Coeff.	Washoff Exponent
Commercial (Com), Industrial (Ind) & Institutional (Ins)	69.159	0.3	1	2
Multi-Family (MFR) and High-Density Residential (HDR)	80.440	0.3	1	2
Medium -Density Residential (MDR)	80.440	0.3	1	2
Low Density Residential (LDR) - "Rural"	80.440	0.3	1	2
Highway (HWY)	271.238	0.3	1	2
Forest (For)	122.362	0.2	1	2
Open Land (Open)	122.362	0.2	1	2
Agriculture (Ag)	122.362	0.2	1	2
Forest (ForPERV) Pervious	54.009	0.1	1	2
Agriculture (AgPERV) Pervious	54.009	0.1	1	2
Developed Land Pervious (DevPERV)-Hydrologic Soil Group A	49.490	0.1	1	2

Land Use Type	Buildup Parameters		Washoff Parameters	
	Max Storage (lb/acre)	Buildup Rate (per day)	Washoff Coeff.	Washoff Exponent
Developed Land Pervious (DevPERV)- Hydrologic Soil Group B	54.009	0.1	1	2
Developed Land Pervious (DevPERV) - Hydrologic Soil Group C	53.309	0.1	1	2
Developed Land Pervious (DevPERV) - Hydrologic Soil Group C/D	53.065	0.1	1	2
Developed Land Pervious (DevPERV) - Hydrologic Soil Group D	49.738	0.1	1	2

Figures 1 to Figure 4 show the box and whisker plots for the calibrated annual pollutant loading time series for both impervious and pervious land use categories. Figure 1 shows that the targeted TN loading rates (annual average value) for impervious areas are slightly lower than the median values and for pervious areas they are close to the median values. The targeted loading rates for TP, Zn, and TSS are aligned with the median values.

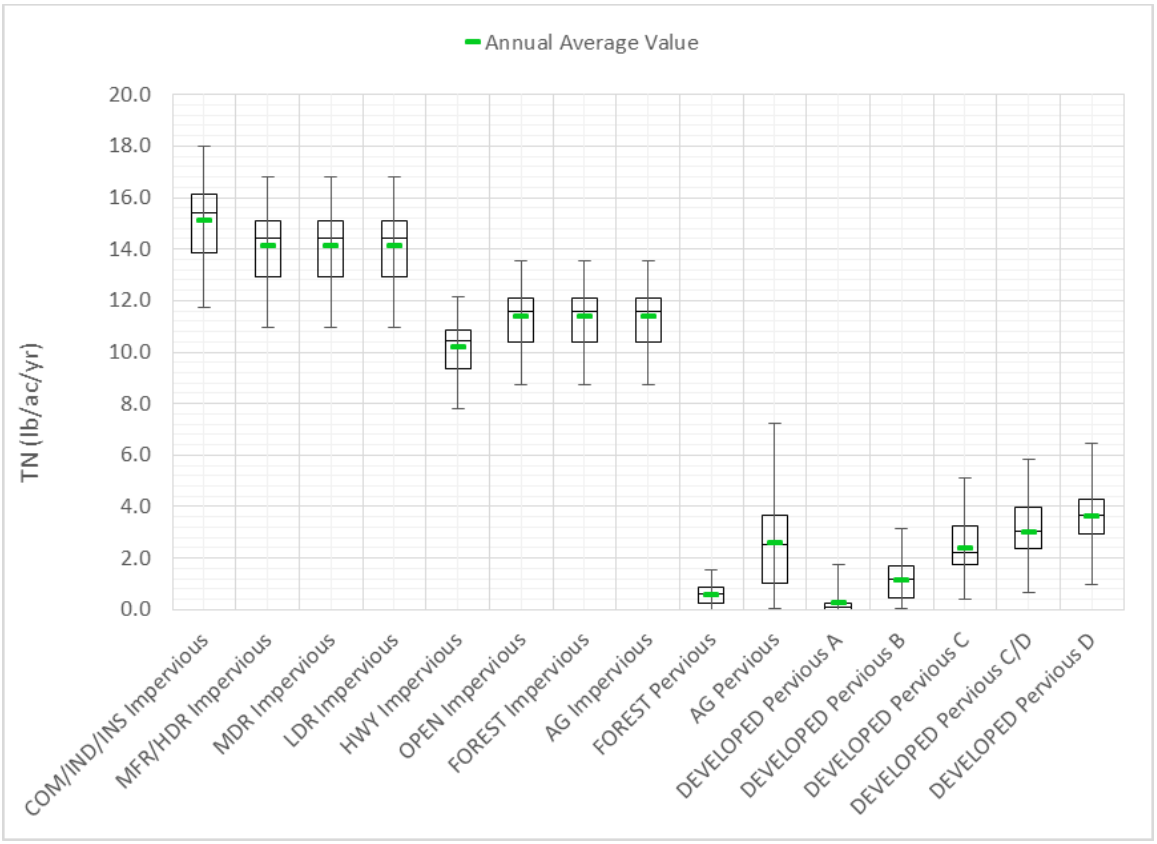

Figure 1. Box and whisker plot for calibrated TN loading time series for the period of 01/01/1992 to 12/31/2014.

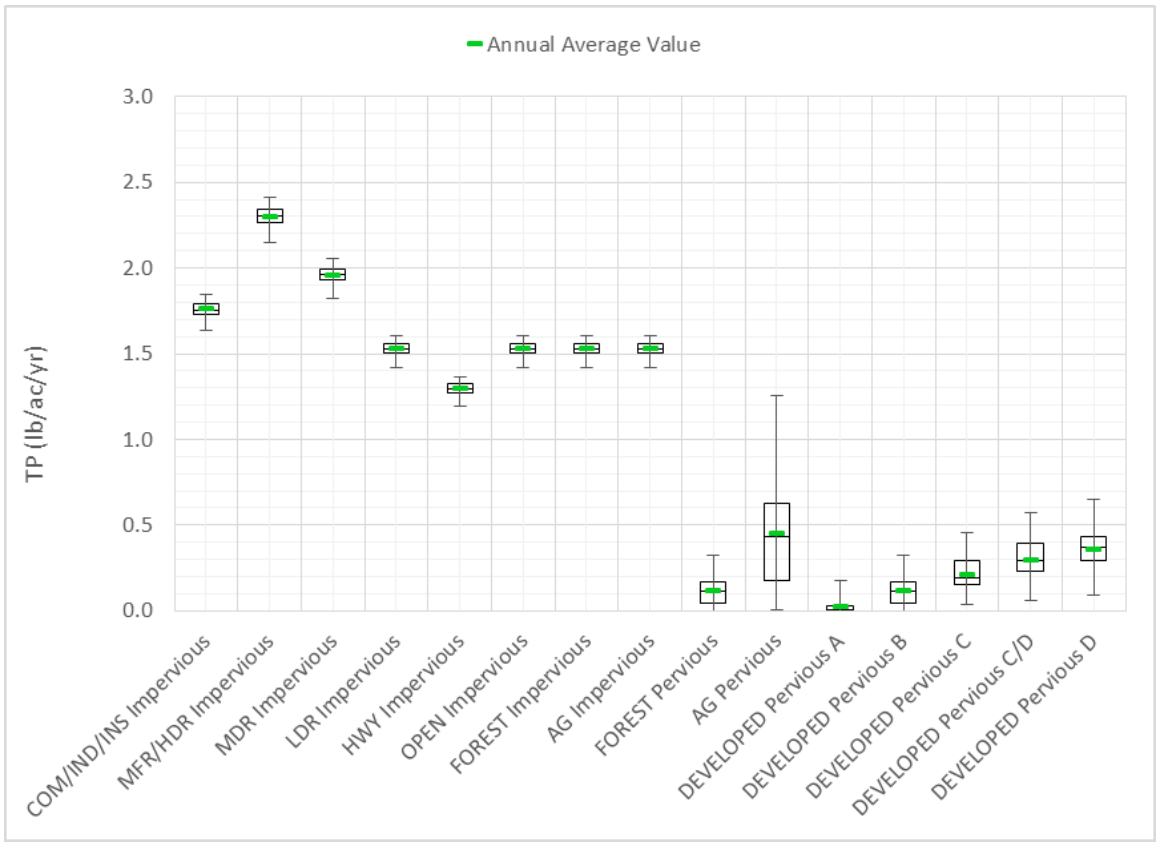

Figure 2. Box and Whisker plot for calibrated TP loading time series for the period of 01/01/1992 to 12/31/2014.

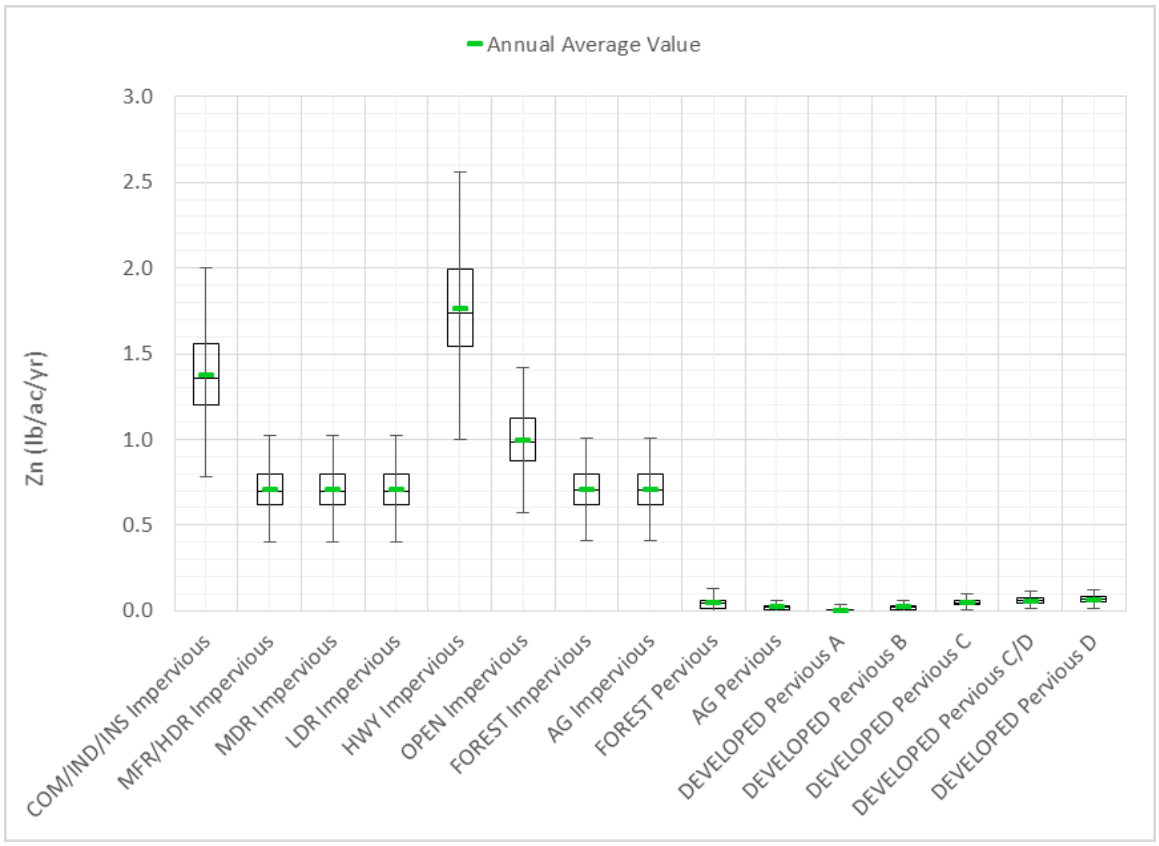

Figure 3. Box and Whisker plot for calibrated Zn loading time series for the period of 01/01/1992 to 12/31/2014.

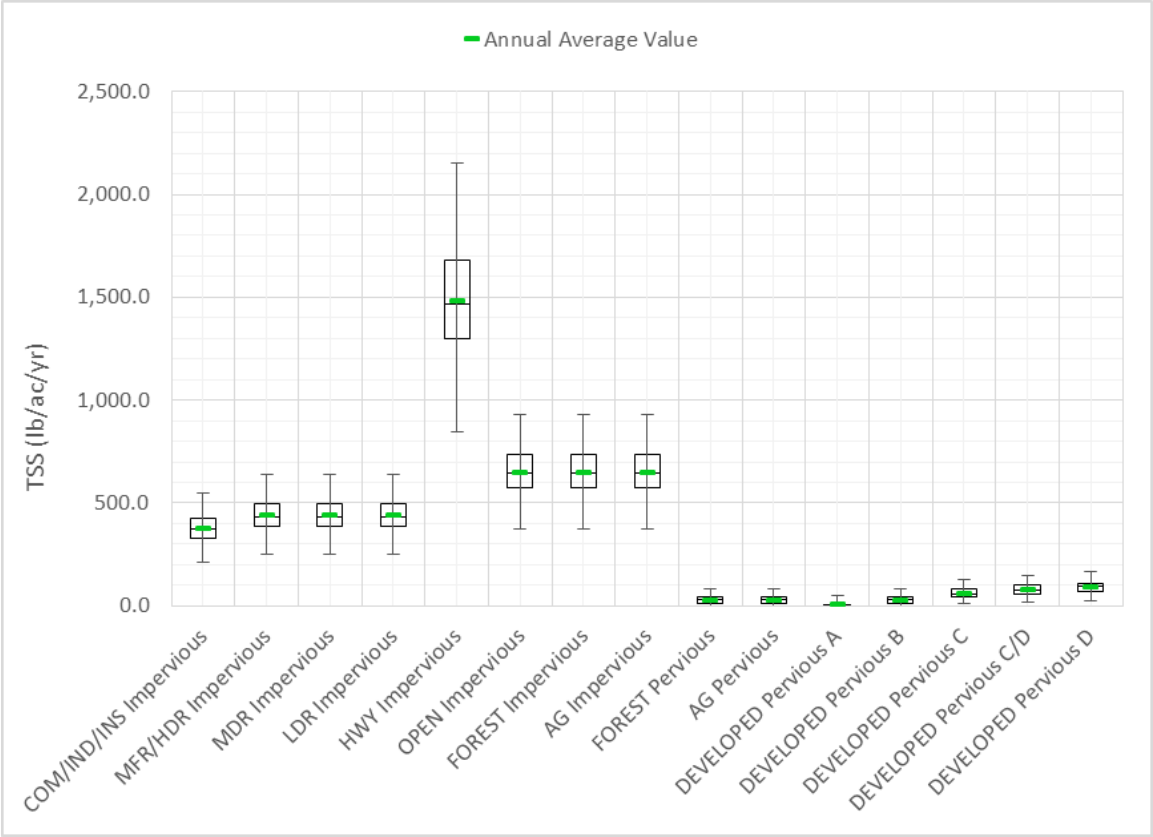

Figure 4. Box and Whisker plot for calibrated TSS loading time series for the period of 01/01/1992 to 12/31/2014.

In order to compare the observed and simulated EMC statistics (25th percentile, median, 75th percentile, average), the simulated time series results were summarized on daily basis (average daily concentration) and on event basis (6 hour inter event duration). Figure 5 to Figure 12 show the box and whisker plots for those comparisons. It seems daily- and event- based statistics are very similar compared to each other and show a similar distribution. The simulated average values for TN and TP are very close to the median values showing a good distribution; whereas, the observed average values for TN and TP are much higher than the observed median values. The simulated average values for Zn and TSS are slightly higher than the simulated median values; whereas, the observed average values for Zn and TSS are closer to the 75th percentile observed values.

In order to estimate what percentile value of the simulated pollutant concentration would generate the targeted annual average loading rate using the long-term annual average flow volume, the simulated event-based average concentration values were ranked and EMC percentile values were multiplied with the annual average flow volume to generate a polluting loading curve. The pollutant loading curves for TN, TP, Zn, and TSS were generated for each impervious land use category and are shown in Figures 13 to 36. The trend in the simulated time series shows that 27th percentile EMC values for TN and TP and 80th percentile EMC values for Zn and TSS can be used as representative EMC values to generate the annual average loading rate from the corresponding impervious land use category.

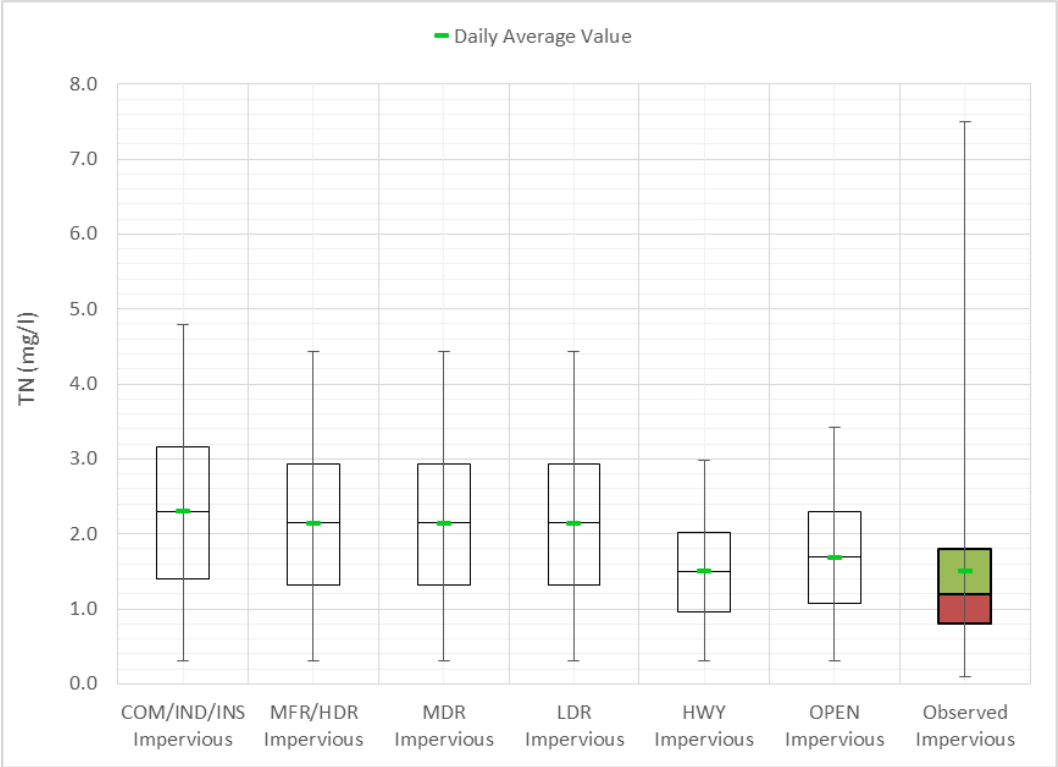

Figure 5. Comparison of calibrated daily TN concentration time series against the monitored EMC values.

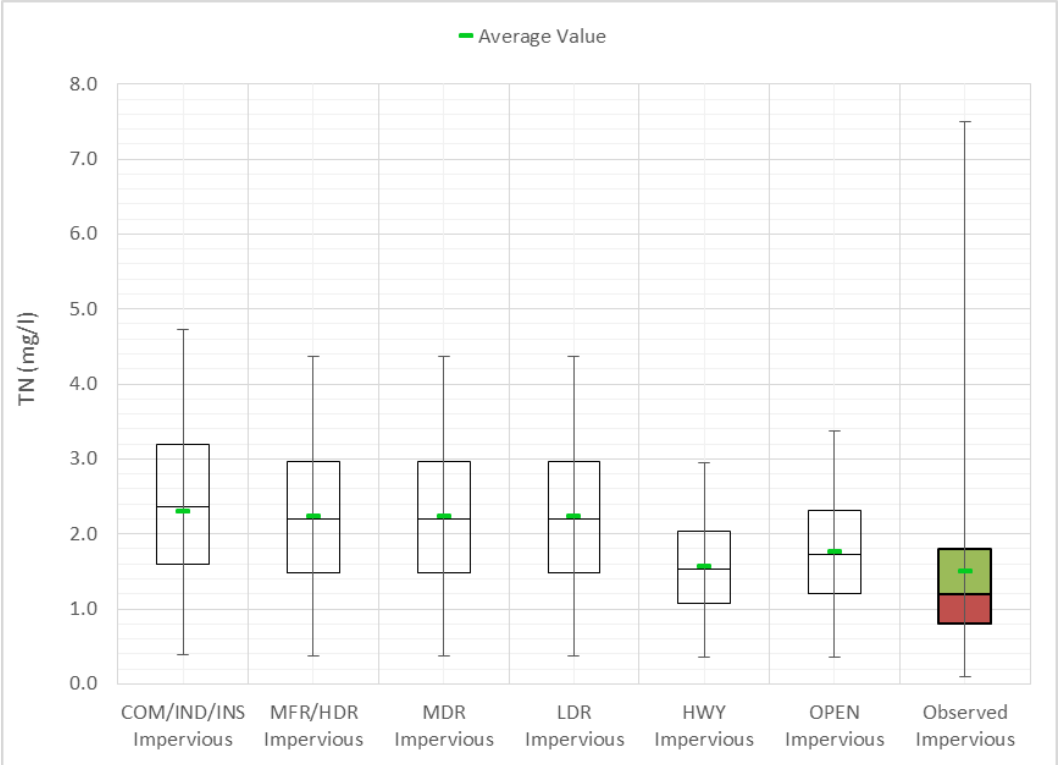

Figure 6. Comparison of calibrated timeseries EMC (minimum 6 hour inter event duration) against the monitored EMC values for TN.

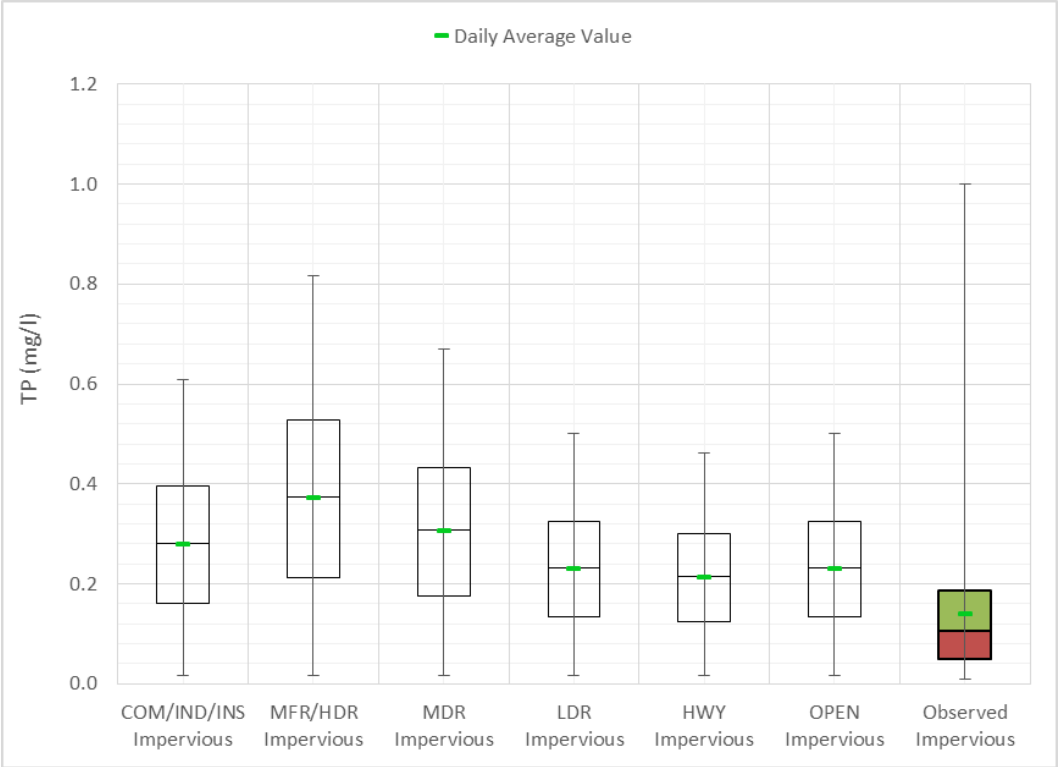

Figure 7. Comparison of calibrated daily TP concentration time series against the monitored EMC values.

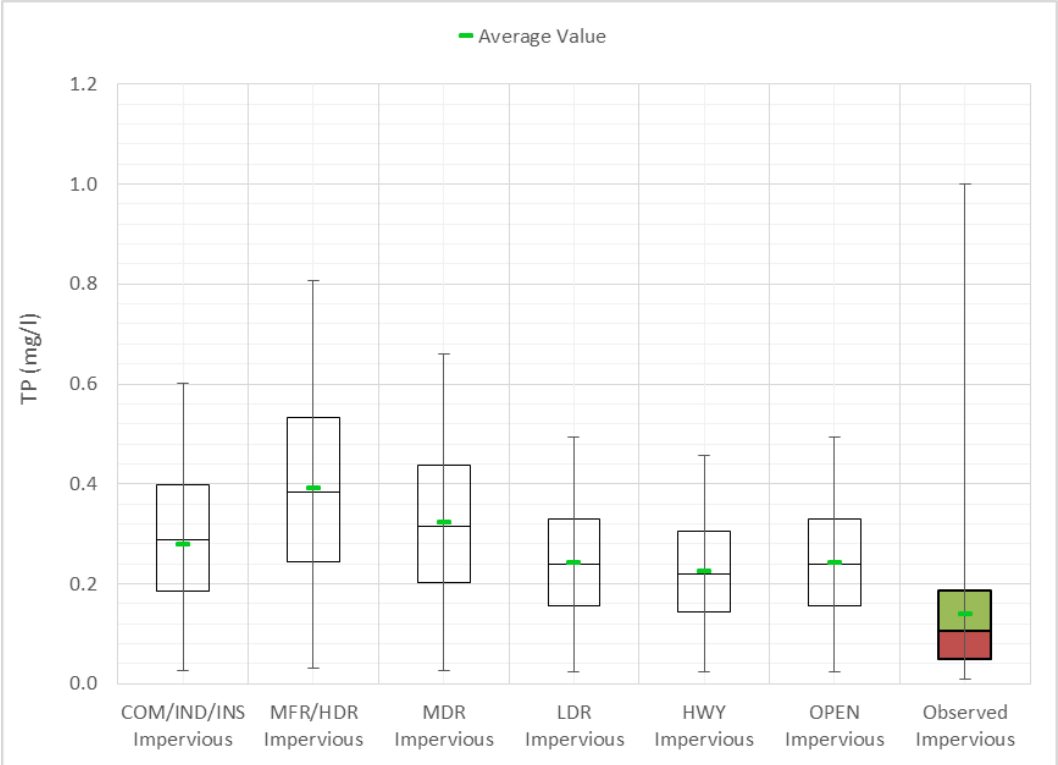

Figure 8. Comparison of calibrated timeseries EMC (minimum 6 hour inter event duration) against the monitored EMC values for TP.

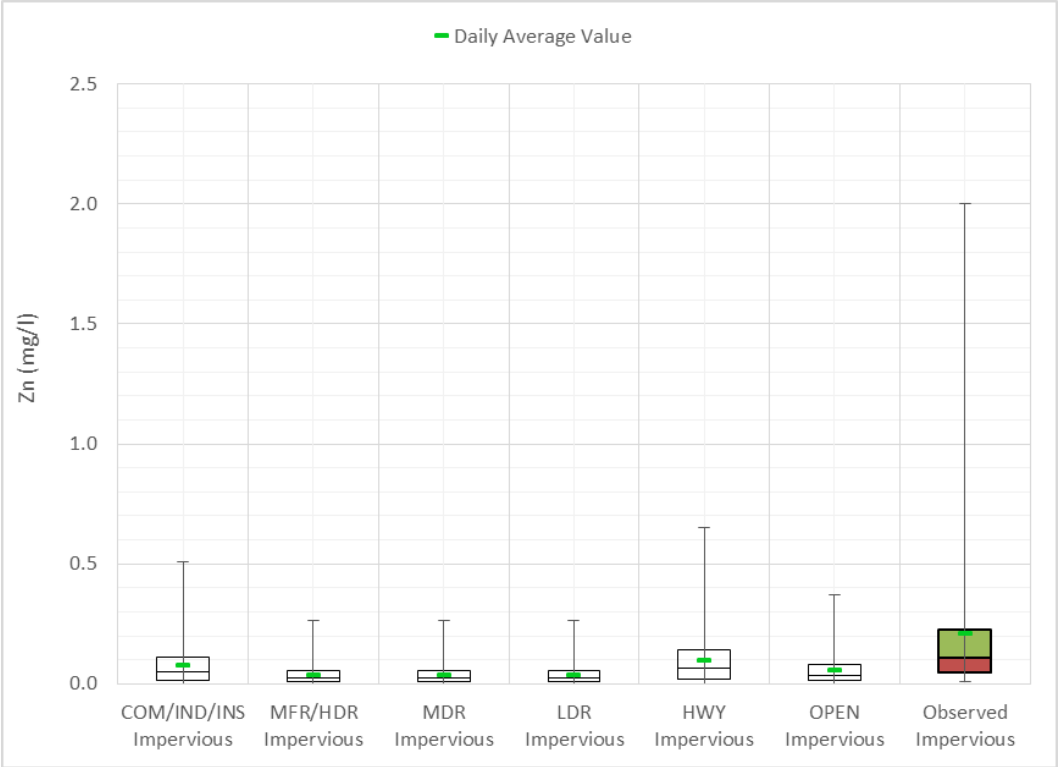

Figure 9. Comparison of calibrated daily Zn concentration time series against the monitored EMC values.

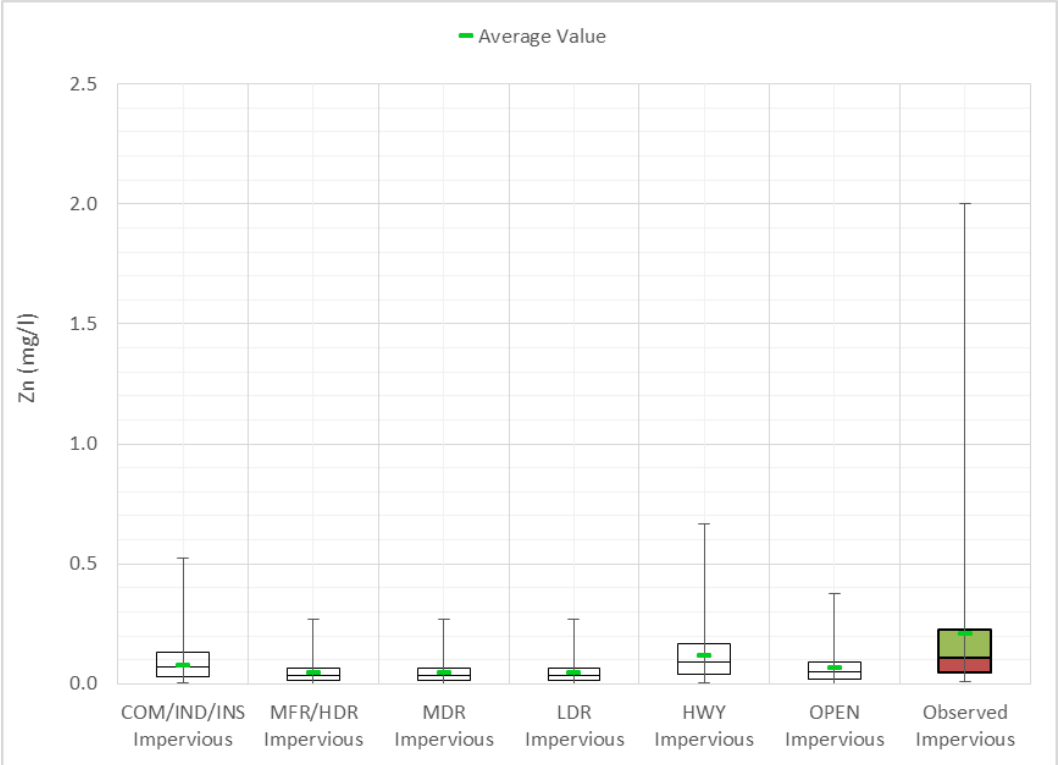

Figure 10. Comparison of calibrated timeseries EMC (minimum 6 hour inter event duration) against the monitored EMC values for Zn.

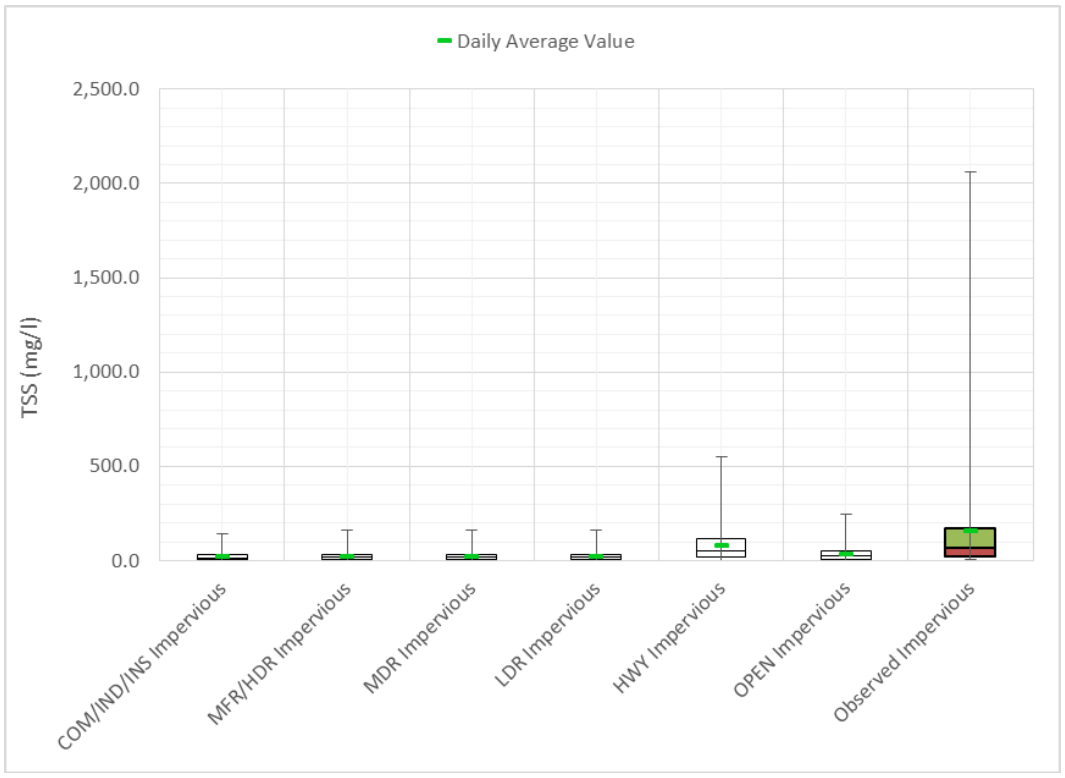

Figure 11. Comparison of calibrated daily TSS concentration time series against the monitored EMC values.

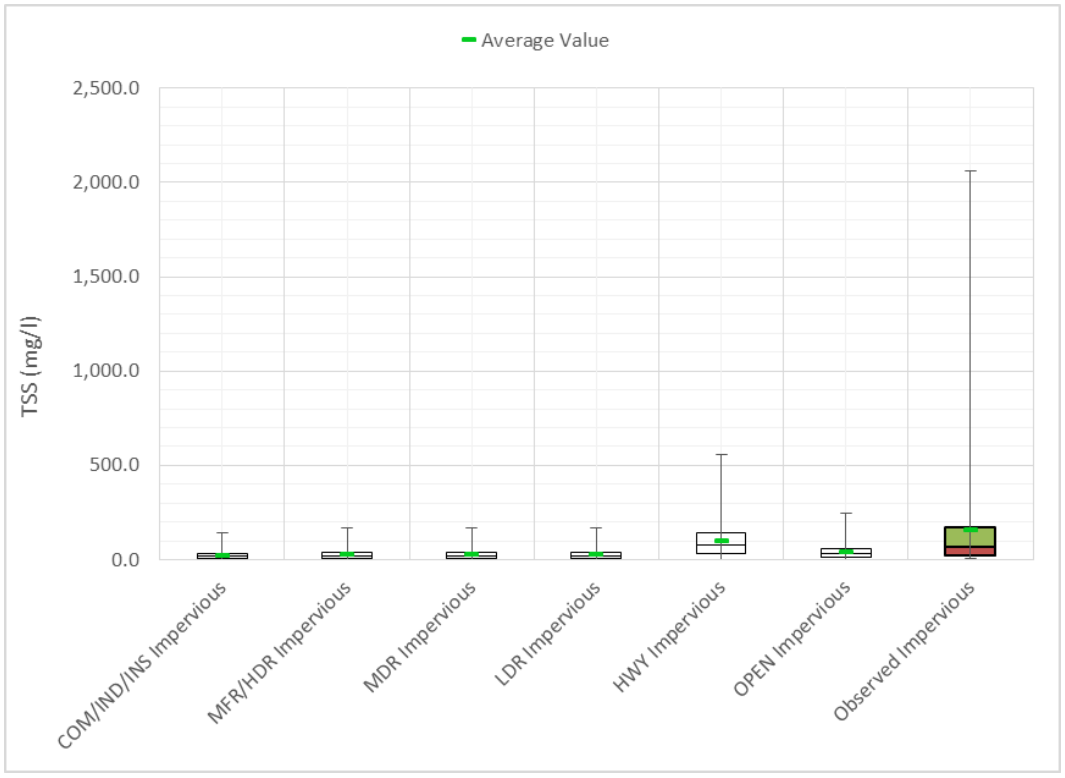

Figure 12. Comparison of calibrated timeseries EMC (minimum 6 hour inter event duration) against the monitored EMC values for TSS.

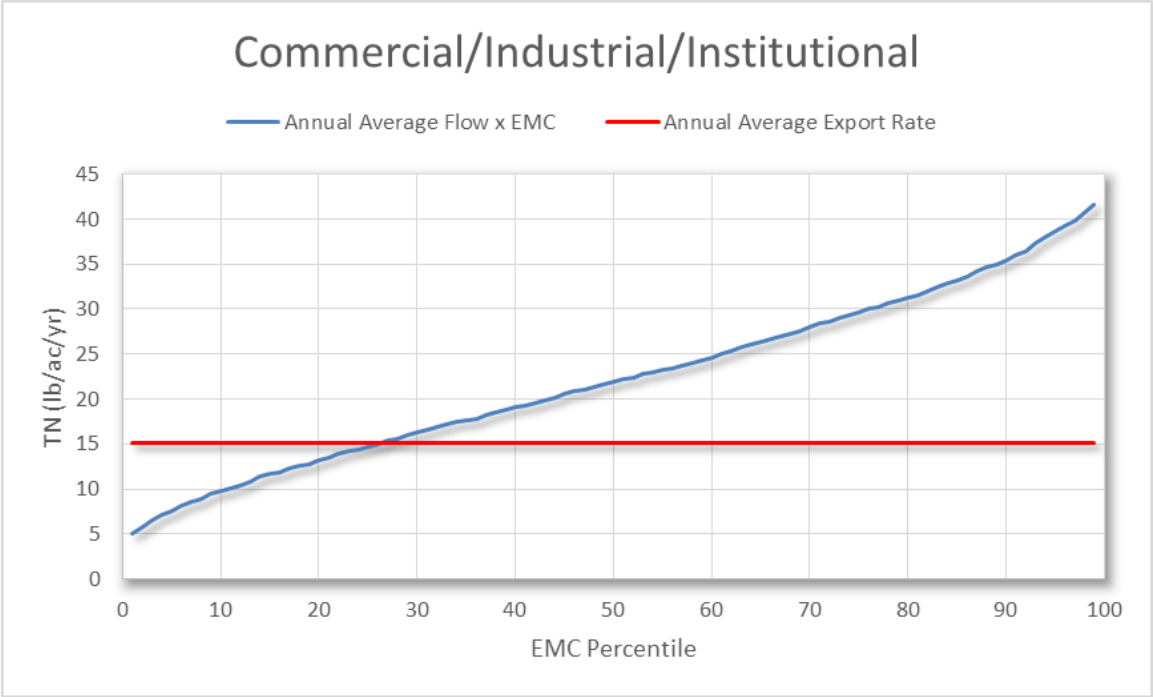

Figure 13. Comparison of calibrated TN timeseries EMC based annual average load against the targeted annual average export rate for COM/IND/INS impervious cover.

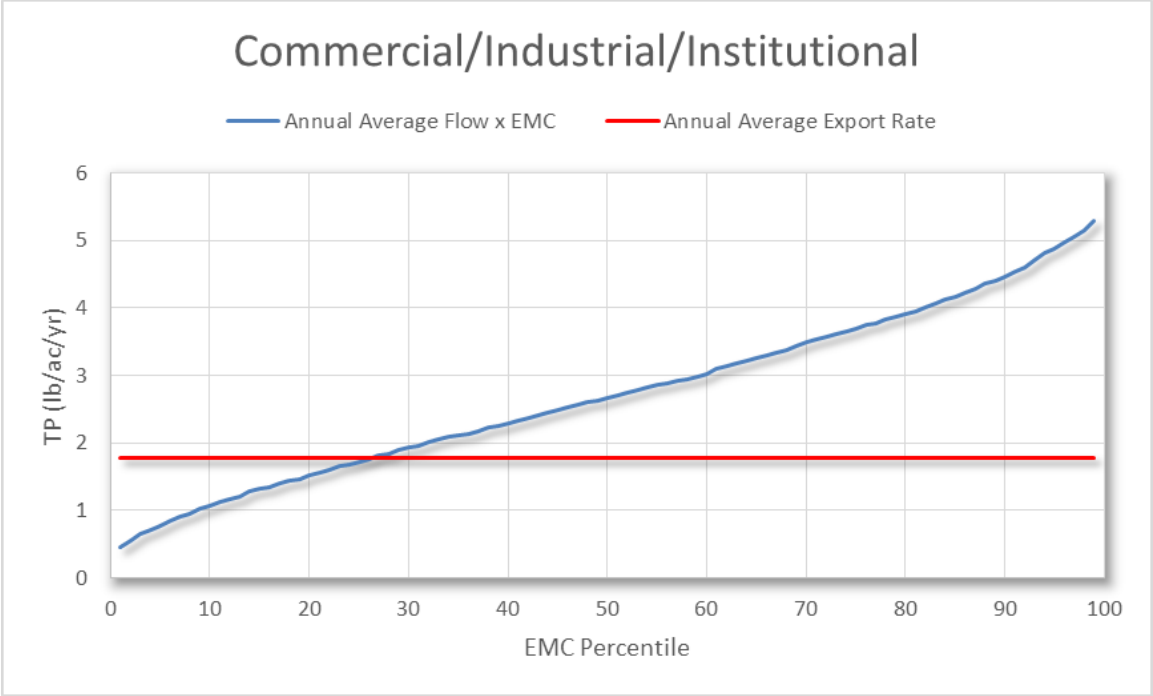

Figure 14. Comparison of calibrated TP timeseries EMC based annual average load against the targeted annual average export rate for COM/IND/INS impervious cover.

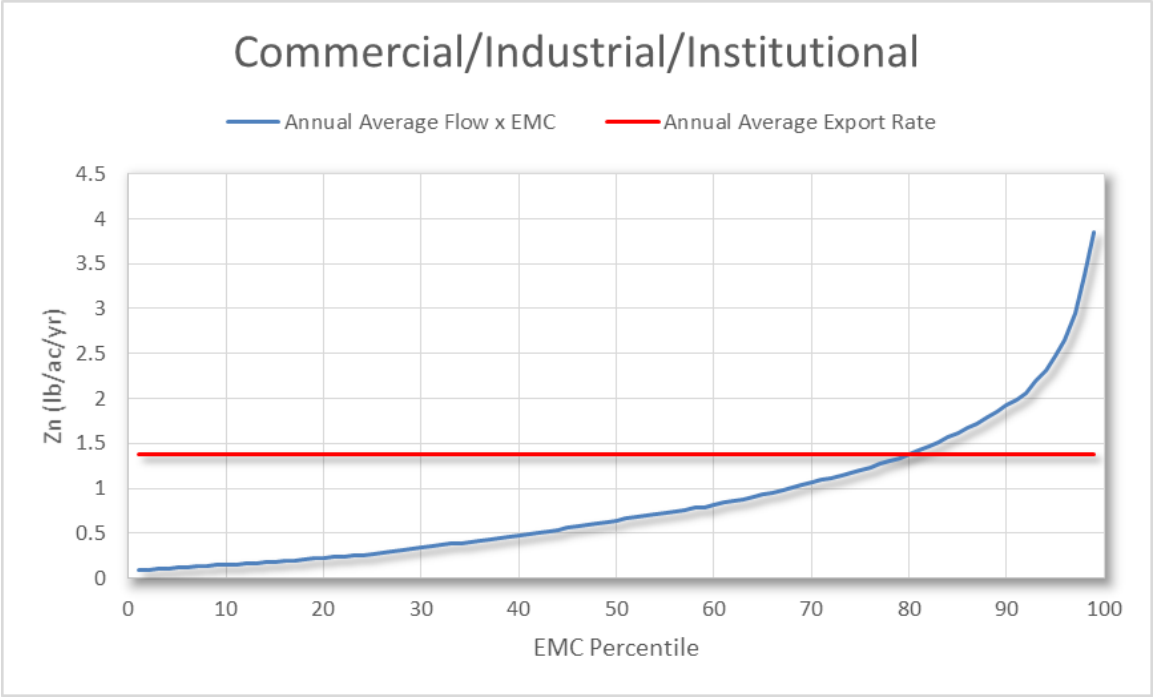

Figure 15. Comparison of calibrated Zn timeseries EMC based annual average load against the targeted annual average export rate for COM/IND/INS impervious cover.

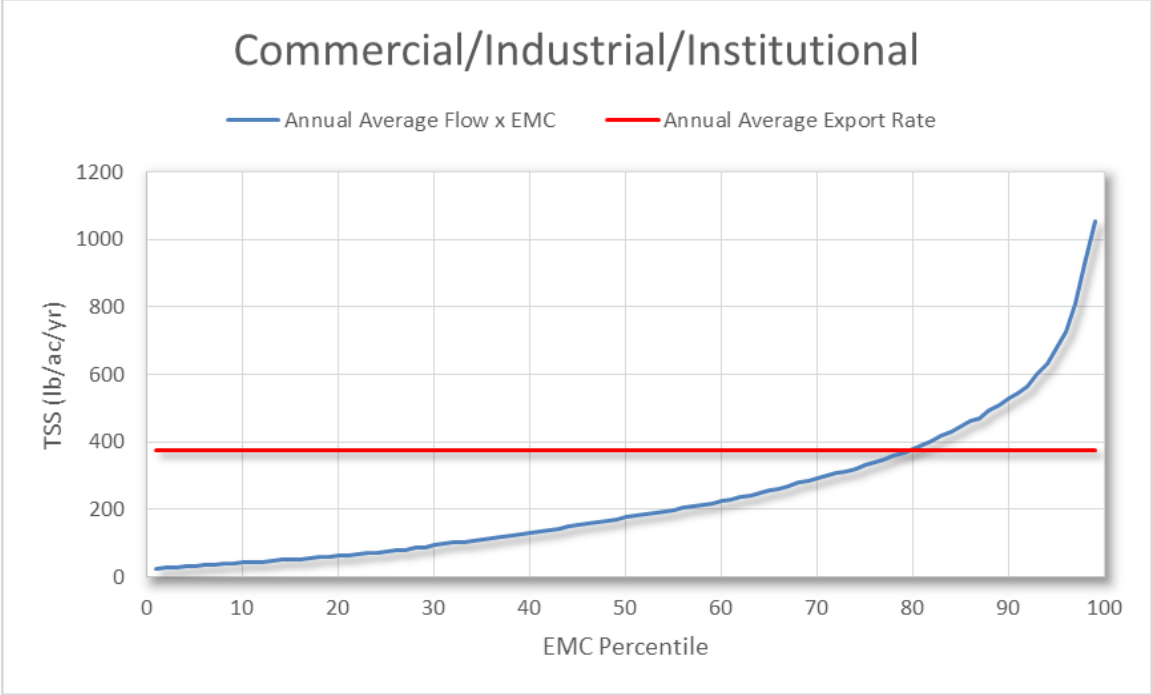

Figure 16. Comparison of calibrated TSS timeseries EMC based annual average load against the targeted annual average export rate for COM/IND/INS impervious cover.

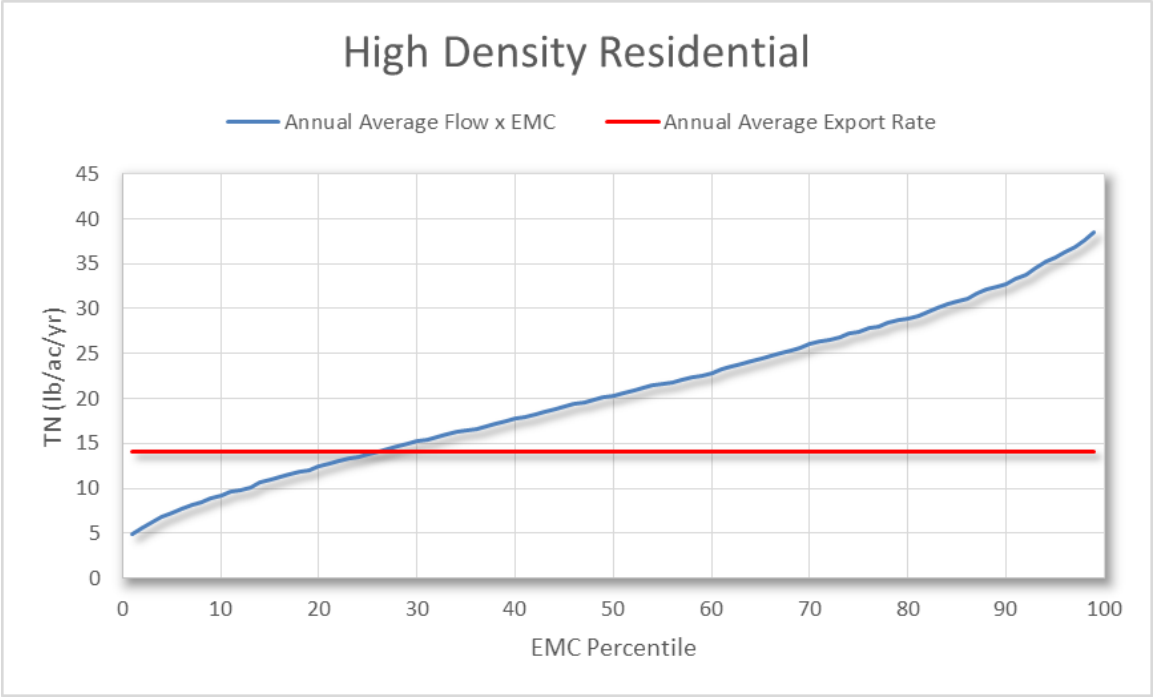

Figure 17. Comparison of calibrated TN timeseries EMC based annual average load against the targeted annual average export rate for MFR/HDR impervious cover.

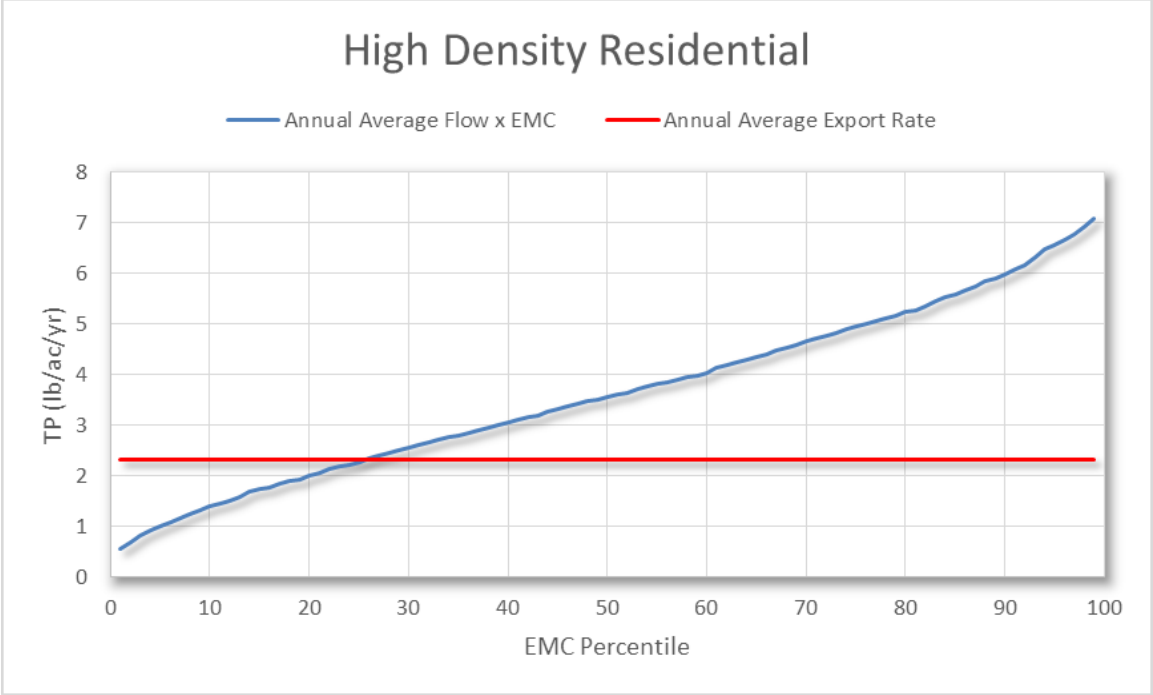

Figure 18. Comparison of calibrated TP timeseries EMC based annual average load against the targeted annual average export rate for MFR/HDR impervious cover.

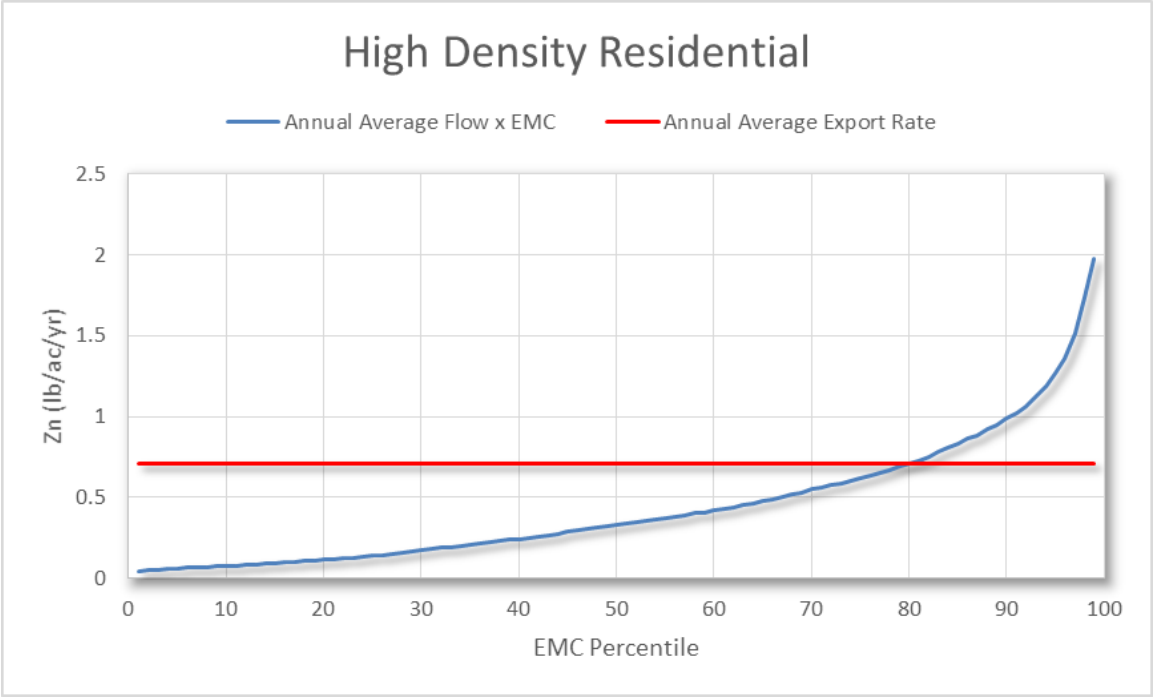

Figure 19. Comparison of calibrated Zn timeseries EMC based annual average load against the targeted annual average export rate for MFR/HDR impervious cover.

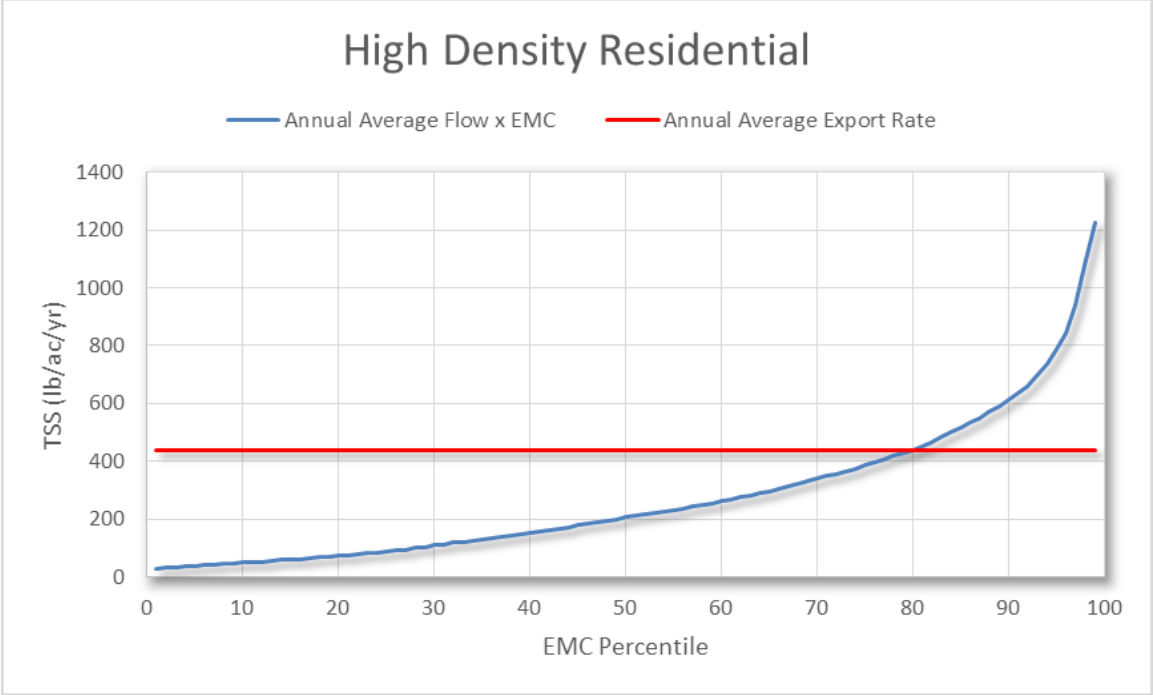

Figure 20. Comparison of calibrated TSS timeseries EMC based annual average load against the targeted annual average export rate for MFR/HDR impervious cover.

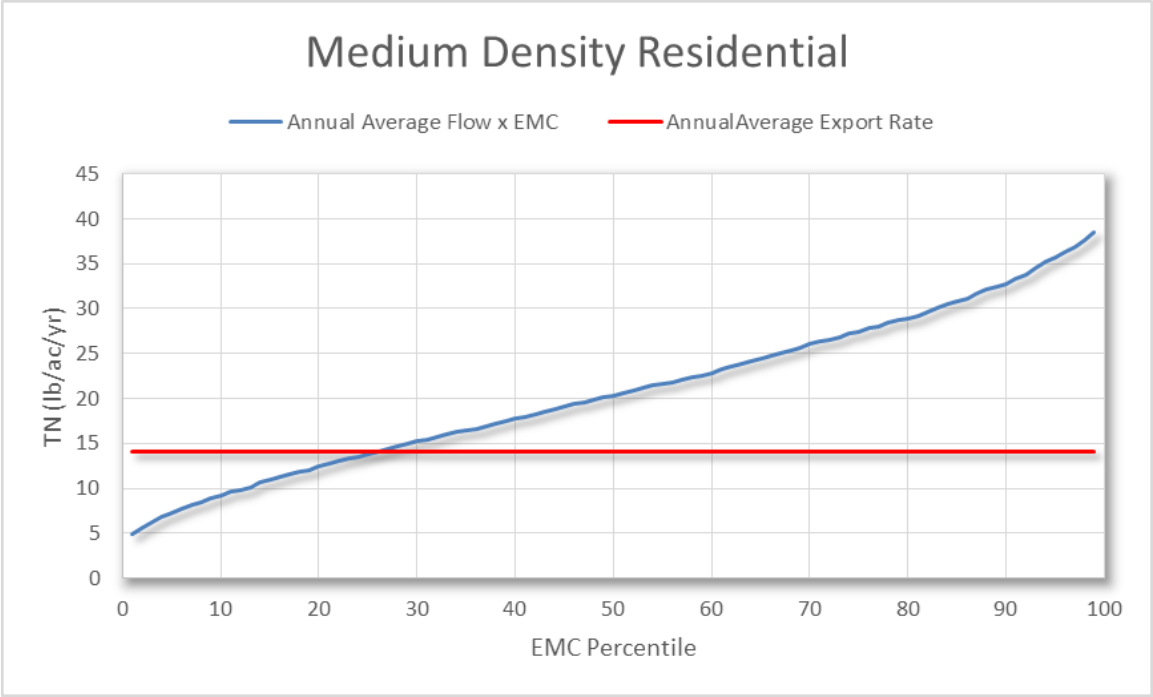

Figure 21. Comparison of calibrated TN timeseries EMC based annual average load against the targeted annual average export rate for MDR impervious cover.

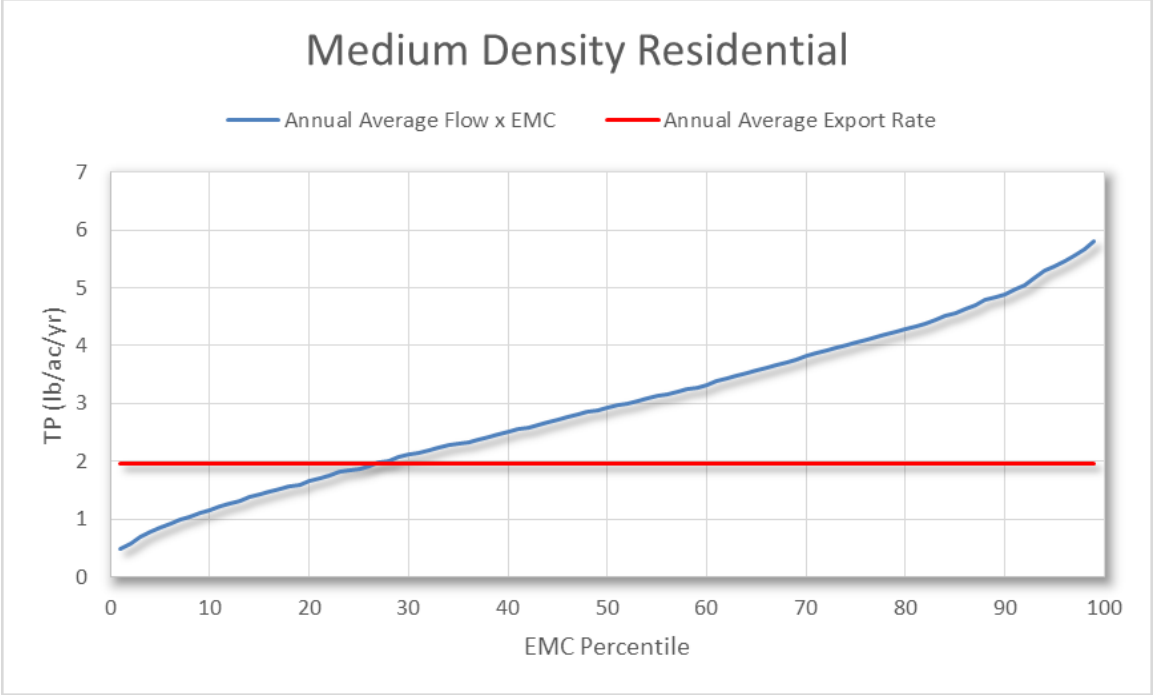

Figure 22. Comparison of calibrated TP timeseries EMC based annual average load against the targeted annual average export rate for MDR impervious cover.

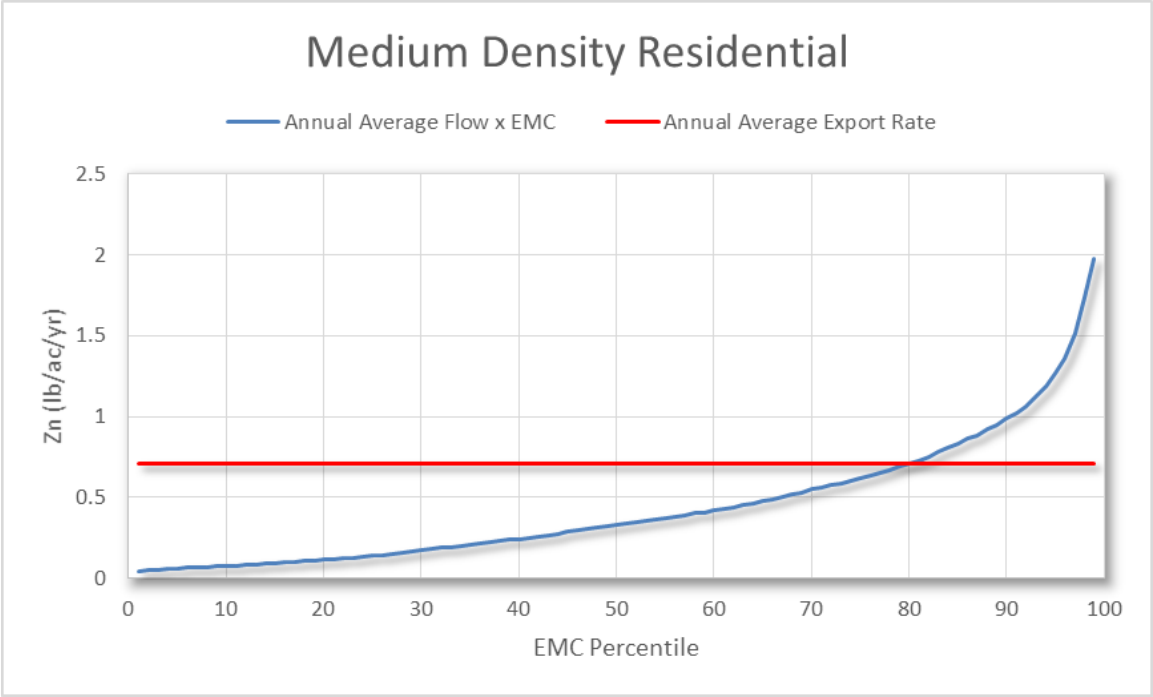

Figure 23. Comparison of calibrated Zn timeseries EMC based annual average load against the targeted annual average export rate for MDR impervious cover.

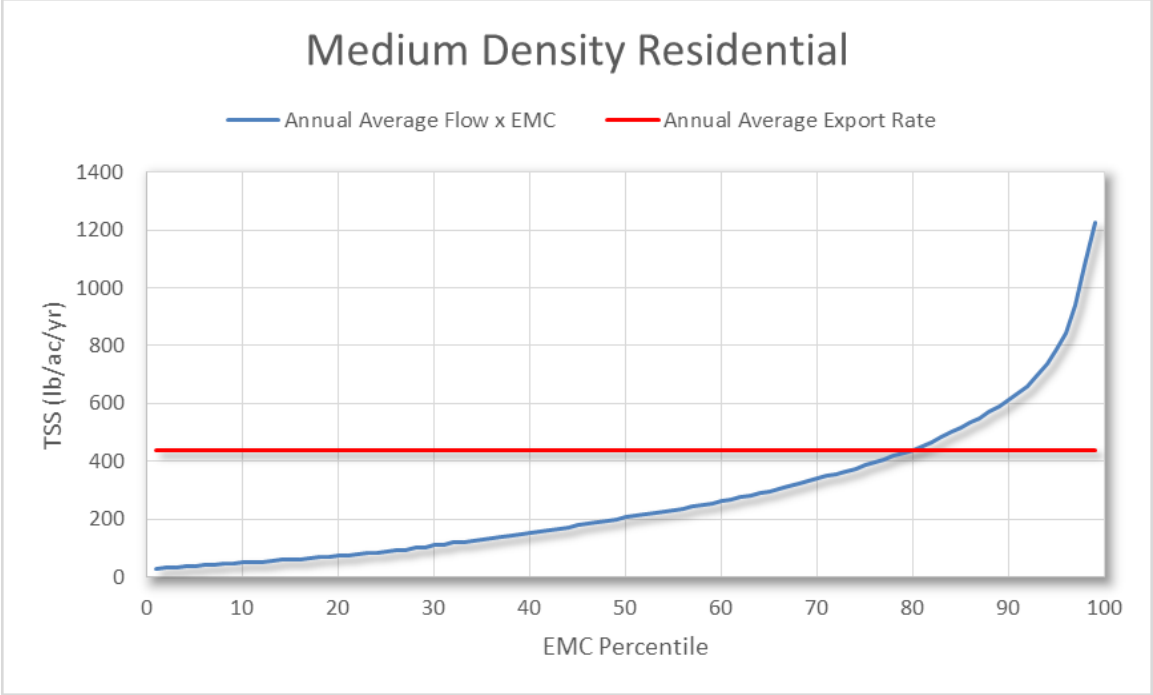

Figure 24. Comparison of calibrated TSS timeseries EMC based annual average load against the targeted annual average export rate for MDR impervious cover.

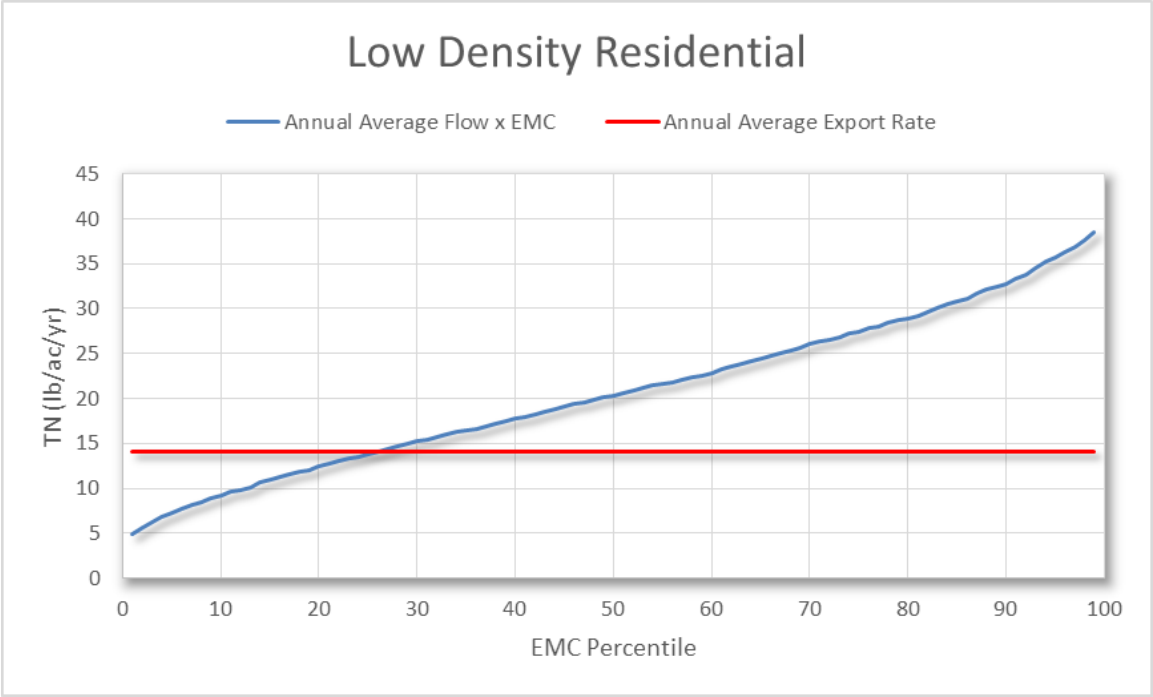

Figure 25. Comparison of calibrated TN timeseries EMC based annual average load against the targeted annual average export rate for LDR impervious cover.

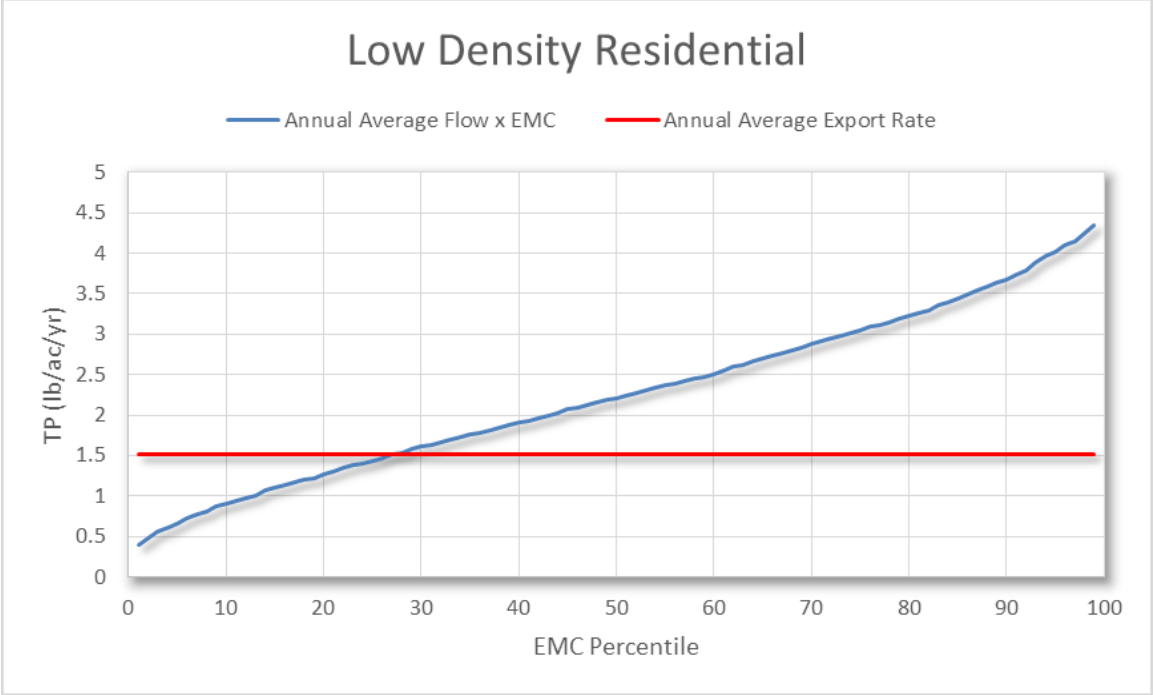

Figure 26. Comparison of calibrated TP timeseries EMC based annual average load against the targeted annual average export rate for LDR impervious cover.

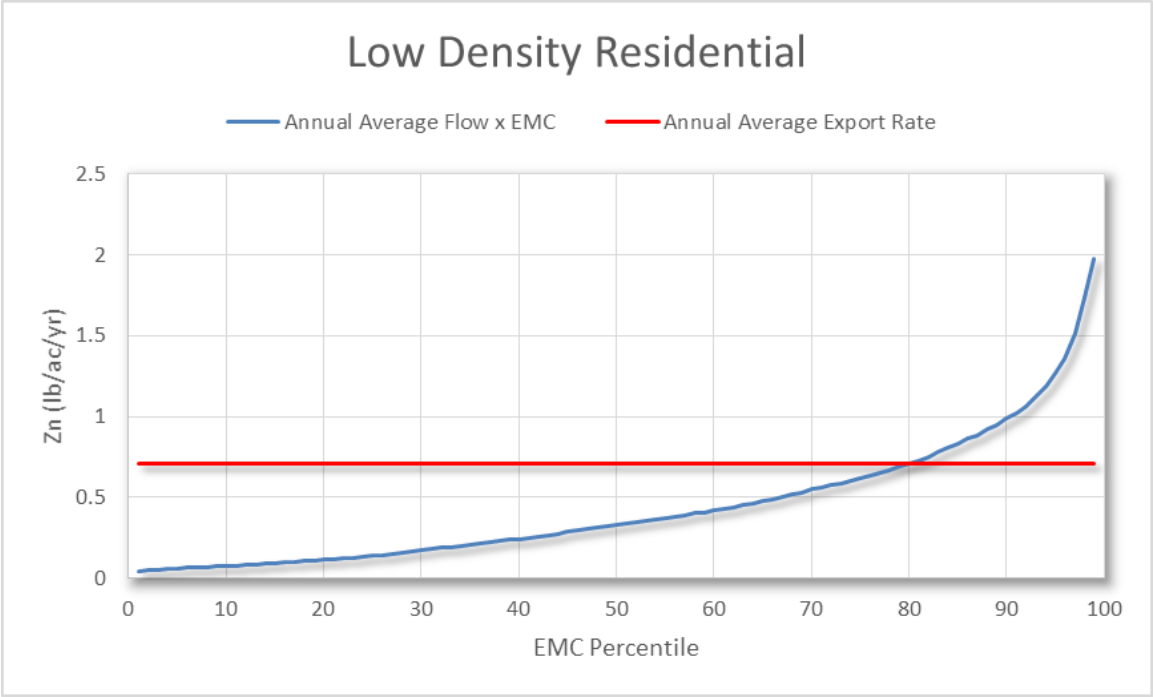

Figure 27. Comparison of calibrated Zn timeseries EMC based annual average load against the targeted annual average export rate for LDR impervious cover.

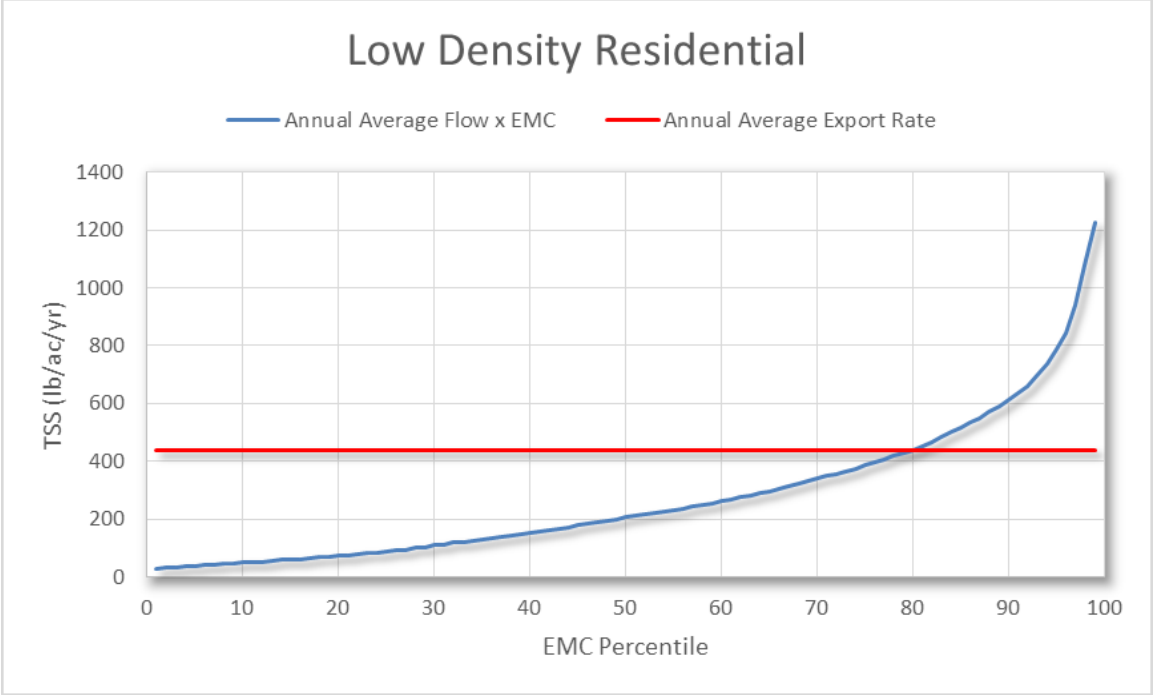

Figure 28. Comparison of calibrated TSS timeseries EMC based annual average load against the targeted annual average export rate for LDR impervious cover.

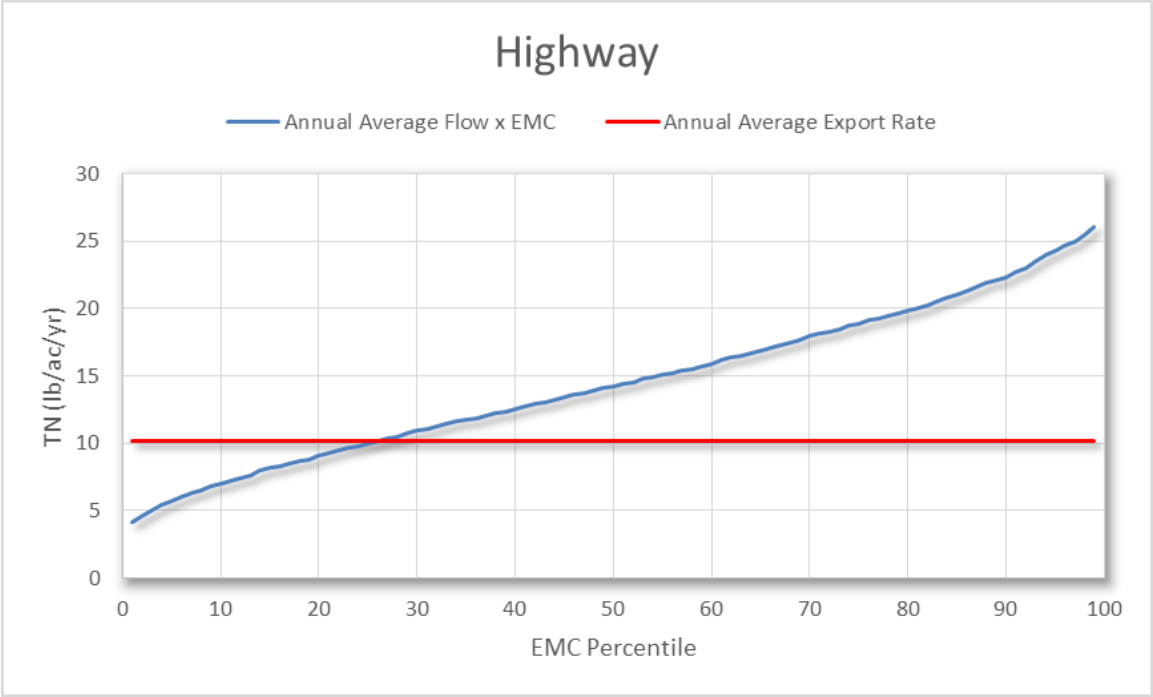

Figure 29. Comparison of calibrated TN timeseries EMC based annual average load against the targeted annual average export rate for HWY impervious cover.

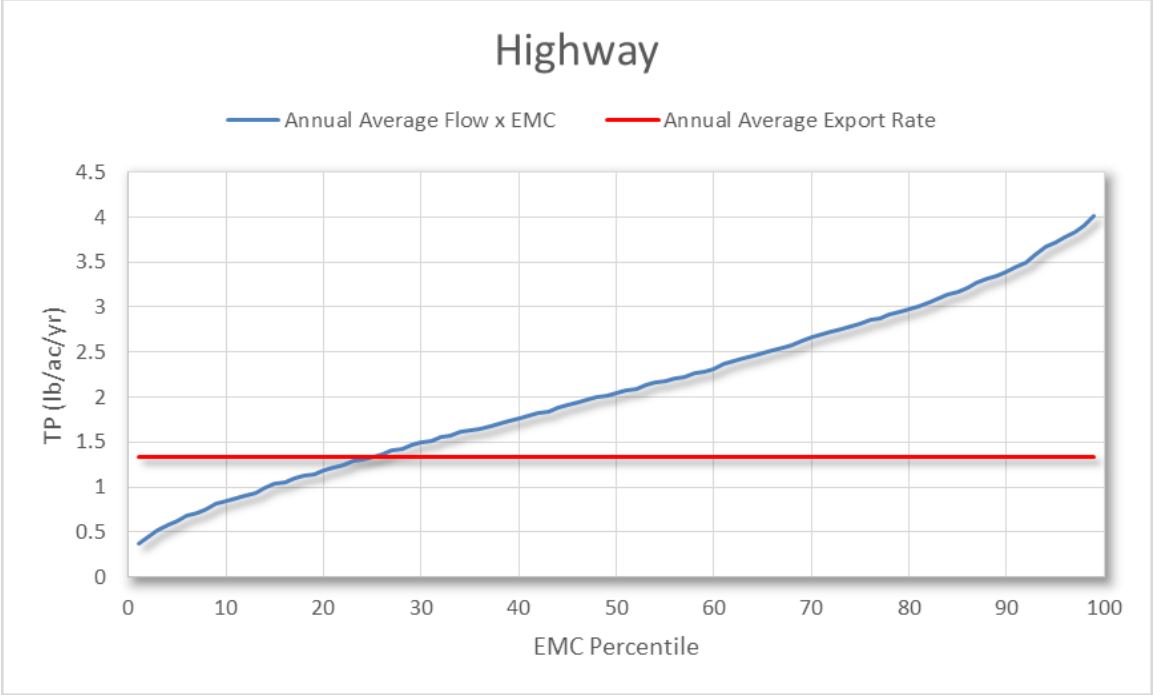

Figure 30. Comparison of calibrated TP timeseries EMC based annual average load against the targeted annual average export rate for HWY impervious cover.

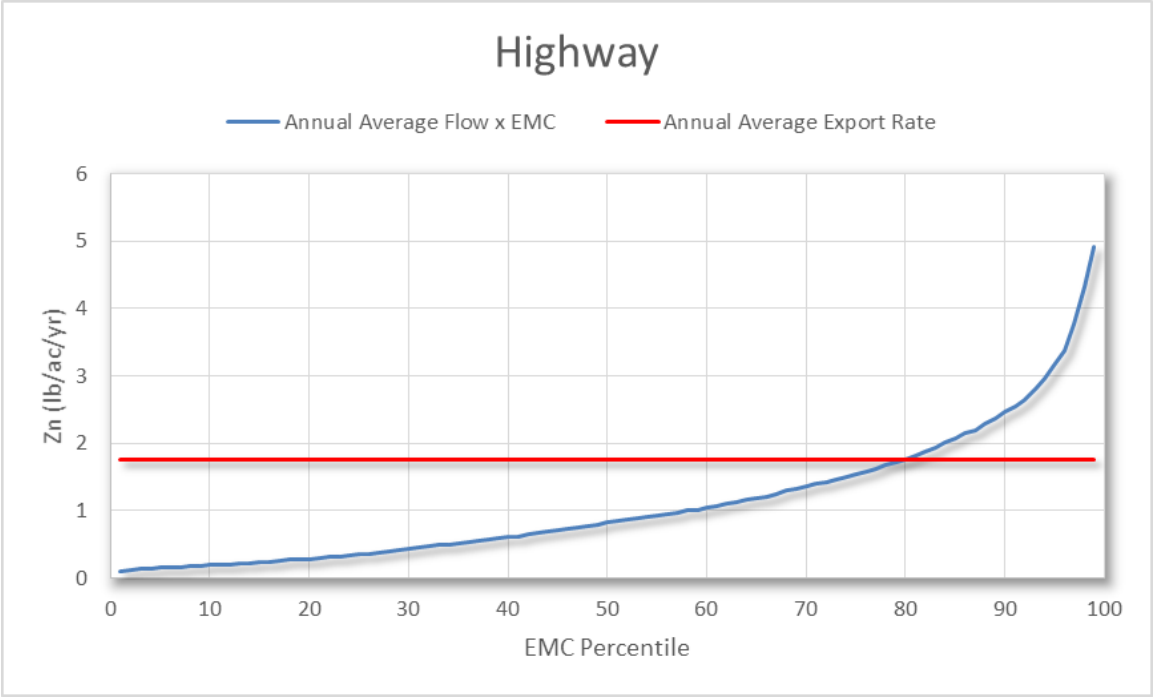

Figure 31. Comparison of calibrated Zn timeseries EMC based annual average load against the targeted annual average export rate for HWY impervious cover.

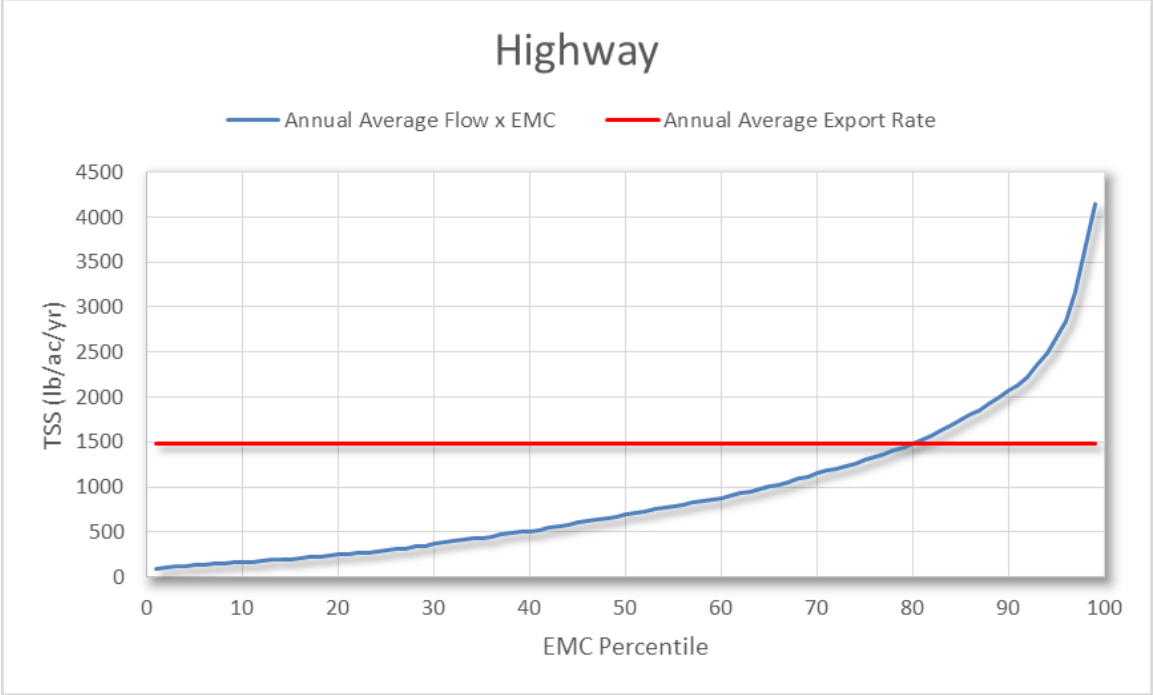

Figure 32. Comparison of calibrated TSS timeseries EMC based annual average load against the targeted annual average export rate for HWY impervious cover.

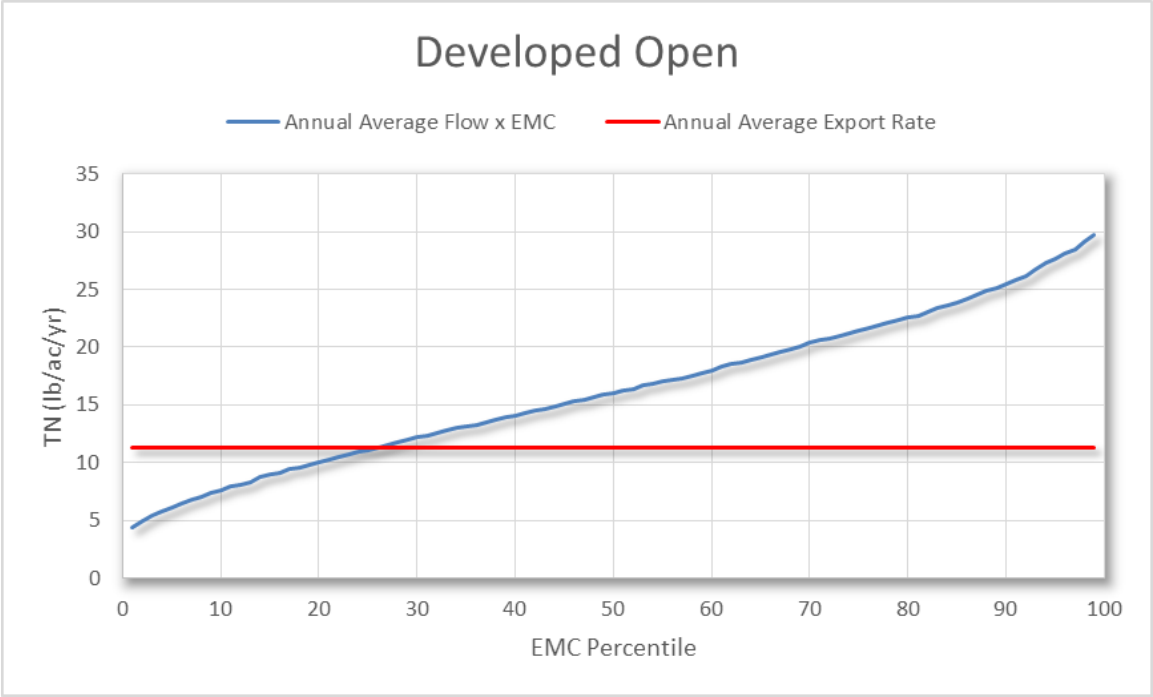

Figure 33. Comparison of calibrated TN timeseries EMC based annual average load against the targeted annual average export rate for OPEN impervious cover.

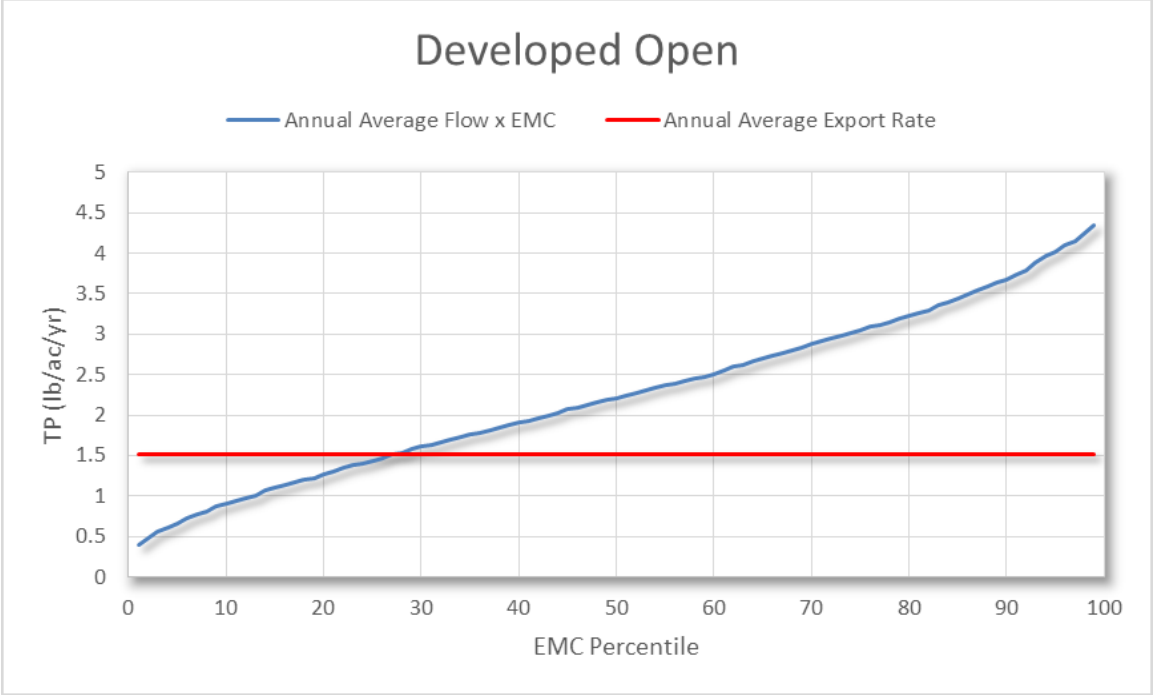

Figure 34. Comparison of calibrated TP timeseries EMC based annual average load against the targeted annual average export rate for OPEN impervious cover.

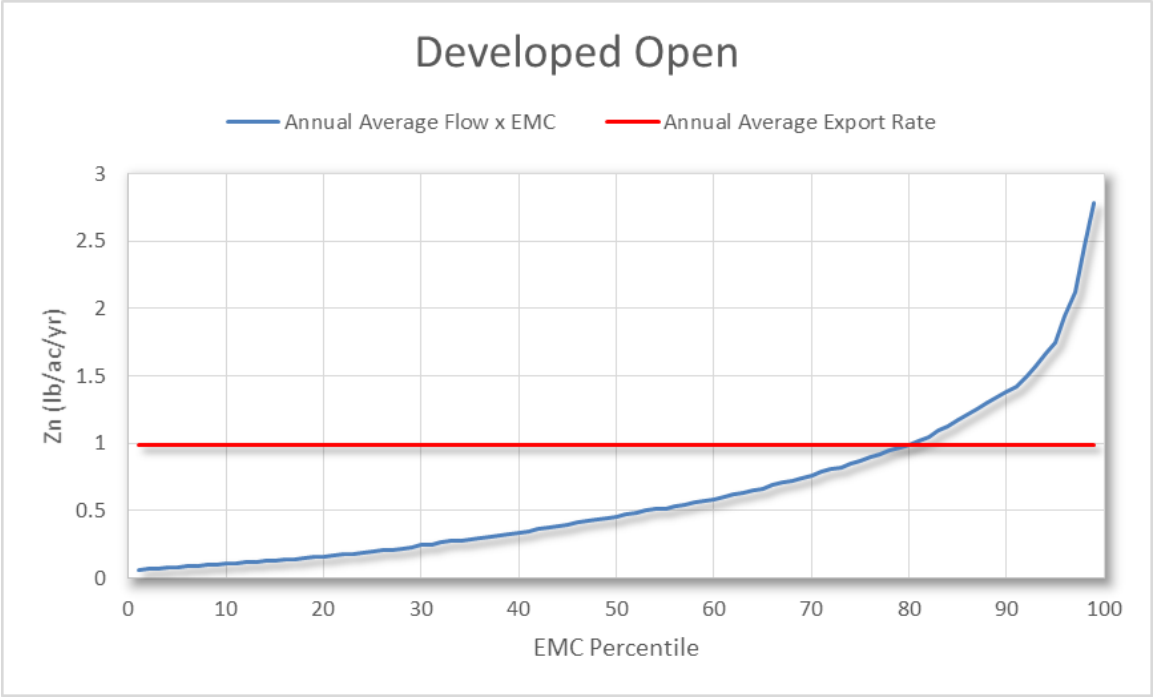

Figure 35. Comparison of calibrated Zn timeseries EMC based annual average load against the targeted annual average export rate for OPEN impervious cover.

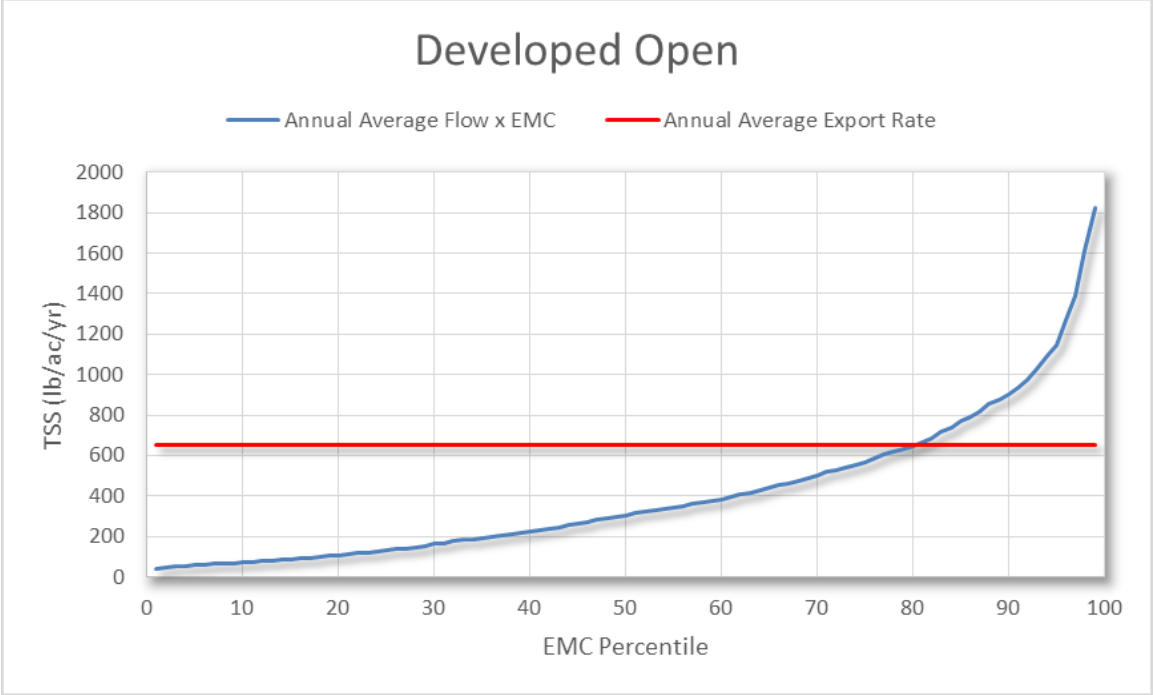

Figure 36. Comparison of calibrated TSS timeseries EMC based annual average load against the targeted annual average export rate for OPEN impervious cover.

References

Tetra Tech, 2008 (updated later in 2010). Stormwater Best Management Practices (BMP) Performance Analysis. Prepared for: U.S. EPA Region 1, Boston, MA. Prepared by: Tetra Tech, Inc. Fairfax, VA 22030.

Tetra Tech, 2009. Optimal Stormwater Management Plan Alternatives: A Demonstration Project in Three Upper Charles River Communities. Prepared for: U.S. EPA Region 1, Boston, MA. Prepared by: Tetra Tech, Inc. Fairfax, VA 22030.

MEMORANDUM

DATE: February 20, 2016

TO: Opti-Tool TAC

FROM: Karen Mateleska, EPA Region- I

SUBJECT: **Methodology for developing cost estimates for Opti-Tool**

Introduction

EPA – Region I offered to provide TetraTech with BMP cost information for the New England Stormwater Management Optimization Tool (Opti-Tool). The goal was to include the latest available information that would accurately reflect capital costs for select BMPs installed in the New England region. This document describes the approach used to determine these values.

The unit cost estimates originally developed as part of a 2010 study were used as the basis/starting-point for the cost estimates for the Opti-Tool. This study, entitled *Stormwater Management Plan for Spruce Pond Brook Subwatershed,* was produced by the Charles River Watershed Association (CRWA). The full report can be viewed at: http://www.crwa.org/hs-fs/hub/311892/file-636820515-pdf/Our_Work_/Blue_Cities_Initiative/Scientific_and_Technical/CRWA_Franklin_Plan.pdf. This subwatershed in the Town of Franklin (in eastern Massachusetts) was selected, in part, because it represented one of the many communities in the watershed that would be required to reduce nutrient (phosphorus) loads in stormwater runoff as part of EPA's Phase II MS4 General Stormwater Permit and a TMDL for Nutrients in the Upper/Middle Charles River. The cost estimates developed in the study can predominantly be attributed to CRWA and both Rich Claytor and Nigel Pickering of Horsley Witten Group (CRWA *et al.* 2010). The development of these costs was based on a literature review of BMP cost information and Claytor's extensive experience working in this field with Massachusetts communities. These values were originally reported in Appendix B of the aforementioned CRWA document. Those cost estimates have also been used in additional stormwater studies supported by EPA – Region I, including the *Sustainable Stormwater Funding Evaluation for the Upper Charles River Communities of Bellingham, Franklin, and Milford, MA (*2011). (That report can be viewed at: http://www.epa.gov/region1/npdes/charlesriver/pdfs/20110930-SWUtilityReport.pdf)

Before simply relying on the CRWA cost estimates, additional research was conducted of publicly available (online) resources to determine if more recent BMP cost information for the New England region was available. These resources included:

- EPA's LID webpage: http://water.epa.gov/polwaste/green/
- EPA's 2013 Article: *Case Studies Analyzing the Economic Benefits of Low Impact Development and Green Infrastructure Programs: http://water.epa.gov/polwaste/green/upload/lid-gi-programs_report_8-6-13_combined.pdf*

- New England Environmental Finance Center: http://efc.muskie.usm.maine.edu/
- UNC Environmental Finance Center's *Catalog of Finance Publications on Green Infrastructure Approaches to Stormwater Management* (This spreadsheet provides a catalog of 46 publications related on green infrastructure for stormwater management that have finance relevance; Several of the sources from the catalog were reviewed for this document) : http://www.efc.sog.unc.edu/reslib/item/catalog-green-infrastructure-and-stormwater-finance-publications
- Houle, *et al. Comparison of Maintenance Cost, Labor Demands, and System Performance for LID and Conventional Stormwater Management*: http://www.unh.edu/unhsc/sites/unh.edu.unhsc/files/Houle_JEE_July-2013.pdf
- University of New Hampshire Stormwater Center's *Forging the Link: Linking the Economic Benefits of LID and Community Decisions: http://www.unh.edu/unhsc/forging-link-topics*
- Center for Neighborhood Technology's *Green Values Stormwater Tool Box: http://greenvalues.cnt.org/* which included the Green Values Calculator: http://greenvalues.cnt.org/national/calculator.php
- Water Environment Research Foundation (WERF): User's Guide to the BMP and LID Whole Life Cost Models, Version 2.0: www.werf.org/bmpcost
- Low Impact Development Center: http://www.lowimpactdevelopment.org/
- ECONorthwest's *The Economics of Low-Impact Development: A Literature Review:* http://www.econw.com/our-work/publications/the-economics-of-low-impact-development-a-literature-review/
- Drexel University's Low Impact Development Rapid Assessment (LIDRA Model) http://www.lidratool.org/home/publications.aspx

A review of these resources did highlight the multitude of variables that can impact the cost of installing LID BMPs and the variety of cost analysis methods that can be used when assessing the cost effectiveness of various LID storm water controls. For example, many of the resources emphasized that costs tend to be site specific. Costs often differ significantly among different geographical locations, depending upon labor and material expenses and the constraints of a particular site. Unfortunately, most of the aforementioned resources highlighted projects outside of the New England region (with the exception of the articles by Houle of the UNHSC and New England Environmental Finance Center.)

EPA's recent (2013) report entitled *Case Studies Analyzing the Economic Benefits of Low Impact Development and Green Infrastructure Programs* listed the 7 different types of economic analyses that were represented by the 13 case studies highlighted in the report. These ranged from the simplest form of economic analysis (i.e., the capital cost assessment) to more robust forms, including the life cycle cost assessment. Whole life-cycle costs would provide a more accurate estimate of the cost of installing, operating, maintaining, and replacing a project (i.e., BMP) throughout its expected lifetime. However this type of analysis requires solid estimates for capital, land purchase, O&M, and other related costs.

Ideally, the goal was to include a more advanced economic analysis (i.e. – life cycle costs) in the Opti-Tool while still maintaining some level of simplicity for the end user. However, such a robust economic analysis does not currently appear possible because the literary search for more recent BMP cost estimates, reflective of New England states, was largely unsuccessful. However, the search was not

entirely fruitless. Jamie Houle of the UNHSC did provide extremely valuable information on capital and maintenance costs for various BMPs that have been tested at the UNHSC. Cost estimates for a particular BMP available from *both* the CRWA study and UNHSC were discussed among Mark Voorhees of EPA, Jamie Houle of UNHSC, and Karen Mateleska of EPA, and a best professional judgment decision was made.

The recommendation at this time is to use a combination of the CRWA cost estimates **and** UNHSC costs estimates as the basis for the Opti-Tool BMP cost estimates, and to use a modified capital cost assessment (which includes a fixed percentage for Design and Contingency Costs) as well as a separate field for maintenance hours (from the UNHSC). The details supporting this approach are described below.

Overview of Scope and Approach

According to a draft memo, dated 6/20/14 from Tetra Tech to EPA Region I, the current SUSTAIN BMP Cost function has seven major individual components, using a formula that would likely be useful in a more detailed design mode. For purposes of simplicity, EPA Region I is proposing the following cost function formula for the tool's "planning" mode:

General Cost Function Formula = Storage Volume of BMP* (ft^3) X Cost Estimate for BMP ($/$ft^3$)

X Adjustment Factor

* Storage Volume of BMP is more accurately defined as (Design) Physical Storage Capacity of BMP; See Section A below for more details

Initially, the intention was to include the preliminary Operations and Maintenance (O&M) costs in the general formula (page 3) by simply multiplying the formula results by our Preliminary O & M costs. However, such an approach would only include **one year's worth** of operations and maintenance, which could have been misleading because it would not have reflected the true life cycle cost of the BMP (i.e., assume life cycle of 20 years). However, simply including the 20 year life cycle cost (O&M cost *20) in the above formula would have greatly increased the cost value and perhaps have created misconceptions about BMP use and affordability.

Therefore, the subcommittee decided to include the anticipated operation and maintenance **hours** required for each BMP per year instead. This parameter was included as a completely separate field in the Opti-Tool. The rationale was that Opti-Tool users need to understand that operation and maintenance impact the overall cost-effectiveness of BMPs and should be considered when selecting a BMP. Including O&M hours (instead of costs) as a separate field, would still highlight this important consideration for stormwater managers.

A. Storage Volume and Proposed Cost Estimate Values

As highlighted above, the general cost function formula used in the Opti-Tool consists of 3 factors: the BMP storage volume, the proposed BMP storage volume cost estimate, and the adjustment factor. The first two factors will be covered together in this memo because they are so closely linked. Table 1 below summarizes the proposed BMP cost estimates for the Opti-Tool.

Table 1: Proposed BMP Cost Estimates for Opti-Tool

BMP (From Opti-Tool)	Cost ($/ft^3) [1]	Cost ($/ft^3) – 2016 dollars[6]
Bioretention (Includes rain garden)	13.37 [2,4]	15.46
Dry Pond or detention basin	5.88 [2,4]	6.80
Enhanced Bioretention (aka-Bio-filtration Practice)	13.5 [2,3]	15.61
Infiltration Basin (or other Surface Infiltration Practice)	5.4 [2,3]	6.24
Infiltration Trench	10.8 [2,3]	12.49
Porous Pavement - Porous Asphalt Pavement	4.60 [2,4]	5.32
Porous Pavement - Pervious Concrete	15.63 [2,4]	18.07
Sand Filter	15.51 [2,4]	17.94
Gravel Wetland System (aka-subsurface gravel wetland)	7.59 [2,4]	8.78
Wet Pond or wet detention basin	5.88 [2,4]	6.80
Subsurface Infiltration/Detention System (aka-Infiltration Chamber)	54.54[5]	67.85

[1] Footnote: Includes 35% add on for design engineering and contingencies

[2] Costs in 2010 dollars

[3] From CRWA Cost Estimates

[4] From UNHSC Cost Estimates; Most of original costs were from 2004 and converted to 2010 dollars using U.S. Department of Labor (USDOL). (2012). Bureau of Labor Statistics consumer price index inflation calculator. http://www.bls.gov/data/inflation_calculator.htm

[5] From Cost Estimate of MA TT Rizzo Project (2008 Dollars)

[6] 2010 costs were converted to 2016 values to adjust for inflation. The ENR Cost Index Method was used for this conversion.

Table 1 includes all of the BMPs that are included in the Opti-Tool. The unit costs represent the dollar amount ($) per cubic foot of storage volume (ft^3), where the storage volume reflects the (design) physical static storage capacity that the relevant BMP can hold. This volume includes the volume of ponding water *and* the volume of water retained in the porous media or subbase materials if applicable. (This storage volume does *not* represent the *treated* volume of stormwater, which may be significantly higher than the physical storage volume of a BMP particularly for systems that are sized dynamically or

by a water quality flow rate as opposed to a water quality volume.) This unit cost per storage volume captured by a BMP differs from other (perhaps more traditional) methods that can be used. By choosing to use the unit cost per storage volume instead of volume of water treated, we are trying to eliminate confusion over what the actual dimensions of the BMP will be for the costs being estimated. Additionally, this use of the unit cost per storage volume is consistent with the approach used in developing the BMP performance curves (used in the Opti-Tool) where the x-axis is the actual **physical storage capacity** to hold water. Lastly, expressing the unit costs in this manner will benefit users who are simply interested in using the unit costs (outside of the Opti-Tool) by eliminating the step of modeling hydrology and routing the water through the BMP, which can yield widely varying results depending on modeling approach and supporting assumptions. Attachment A describes the method used in calculating the design storage volume for each of the selected BMPs.

Also, each unit cost per storage value represents the capital cost of construction/installation of the BMP and includes a 35% design/engineering/contingency (D & E) cost. This 35% fixed percentage of the total construction cost follows a general "rule of thumb," often used by consulting firms. Based upon a conversation between Mark Voorhees and Jamie Houle (two members of the Opti-Tool cost subcommittee), a decision was made to include this D&E cost. The values in Table 1 do *not* include the cost of purchasing any land, nor does it include any O&M costs (which is discussed in more detail in a subsequent section). Therefore, each unit cost in Table 1 that was based on the CRWA's 2010 values was calculated by multiplying the relevant BMP cost by 1.35.

Since the CRWA study did not include cost estimates for porous pavement or sand filters, which are BMPs included in the Opti-Tool, relevant data was obtained from Jamie Houle of the University of New Hampshire Stormwater Center (UNHSC). He also provided additional cost estimates (as denoted by Footnote 4 in Table 1) for some of the other BMPs included in the tool. UNHSC can provide valuable data because they have been directly involved with the engineering, design and construction of numerous LID controls, as well as evaluating multiple stormwater treatment systems over multiple years at their primary field research facility in Durham, N.H. Since they could provide cost information for both porous asphalt pavement and pervious concrete, separately, the general category of porous pavement was divided into the aforementioned two sub-categories.

It should be noted that the costs used for the Opti-tool *assume linearity*, which will both allow for *and* incentivize the scaling to smaller-sized systems. For example, EPA has estimated that *smaller* capacity designs for BMPs, rather than large-sized BMPs, can increase both the technical and economic feasibility of installing controls, particularly for retrofits. The assumption of linearity was made for the following reasons: 1) Limited data currently exists on the cost of small capacity systems. Until a larger pool of cost data becomes available which will allow for the development of a non-linear cost curve, the current method is the best available alternative; 2) As the installation of smaller systems becomes more wide-spread, it is likely that economies of scale will develop and cost savings will occur. For example, if one entity is contracted to install multiple small systems at once, materials can be bought in bulk and the installation process can become more efficient and less expensive; 3) An undersized system built to treat a large area can be a very cost effective approach. As an example, there should not be a significant cost difference between a 1-inch system treating 1 acre and a 1/10-inch-system that treats 10 acres, since the absolute capacity of the system is the same in both cases. This topic of linearity will be revisited in the future when more data is available.

Since UNHSC typically calculates the capital costs per cubic foot (ft^3) *treated*, using WQv, Jamie Houle converted the costs to represent the capital costs per BMP storage volume (ft^3). This was necessary so the capital cost data would be consistent with the method used in the Opti-Tool. Also, all of the costs were converted to 2010, and ultimately 2015, dollars. As with the CRWA costs, the UNHSC capital costs were already adjusted to include the 35% design/engineering/contingency (D & E) cost. Details of all of these calculations, and any other assumptions made, are presented in Attachment B.

When developing cost estimates, another topic for consideration was whether or not to address the issue of inflation. CRWA's BMP cost estimates were based on capital costs from 2010. As previously stated, UNHSW's cost estimates have also already been converted to constant 2010 dollars using consumer price index inflation rates [U.S. Department of Labor (USDOL) 2014].[1] Therefore, there was the option of converting all of these 2010 costs to 2016 costs, using the U.S. Department of Labor's consumer price index inflation calculator. However, another suggestion was made to use the ENR Cost Index method to adjust for inflation instead because it more closely tracks construction work. At least one New England state (i.e., Vermont) also uses the ENR Cost Index method, so this could provide some consistency, as well. Therefore, the decision was made to ultimately convert all of the costs to 2016 values using the ENR Cost Index method. These values are reflected in Table 1.

To use the index, one calculates the quotient of the current index number (based on the month and year of *current* date) divided by the index number from a given date (e.g., June of 2010). Since the month was not known for the 2010 costs, the month of June was used as an estimate. This assumption was used because it falls mid-way between the construction season and would likely provide a reasonable estimate. Once the quotient was calculated, it was multiplied by the construction cost (found in the middle column in Table 1, above) to provide the 2016 construction cost value

B. Cost Adjustment Factor

Since the cost of installing a BMP will vary depending on the specific site location, the TAC subcommittee believed it was important for the Opti-Tool to include a scalable cost adjustment factor. The proposed cost estimates for the Opti-Tool (in Table 1) are all based on a Cost Adjustment Factor of 1. However, each Opti-Tool user has the option to choose and enter into the tool a cost adjustment factor that is appropriate for their site. This will adjust the storage volume cost function in the Opti-Tool.

For example, the CRWA report included the cost factors summarized in Table 2.

[1] Reference: U.S. Department of Labor (USDOL). (2014). Bureau of Labor Statistics consumer price index inflation calculator." ⟨http://www.bls.gov/data/inflation_calculator.htm⟩(Sep. 12, 2014)

Table 2: Example of Cost Adjustment Factors

BMP Type	**EXAMPLE** Cost Adjustment Factor
New BMP in undeveloped area	1
New BMP in partially developed area	1.5
New BMP in developed area	2
Difficult installation in highly urban settings	3

(Source: Table 4 of Appendix B of CRWA's Spruce Pond Brook Subwatershed Project for Town of Franklin)

The assumption made was that it would cost more to install a new BMP in a developed area (with more site constraints) than it would cost to install the same BMP in a previously undeveloped area. So in the above example, the cost adjustment factor would be 2 for installing a BMP in a previously developed area versus a cost adjustment factor of 1 for installing a BMP in an undeveloped area.

It should be noted that Table 2 (above) provides just *one example* of adjustment factors. The factor should be flexible enough so that another location (or Opti-Tool user) can adjust it, as needed. For example, the Charles River Watershed (in eastern Massachusetts) used an adjustment factor of 2 for installing a BMP in a developed area, while the State of Vermont uses an adjustment factor of 1.4 to estimate the cost of installing a BMP for existing development.

C. Maintenance (O&M) Costs

Originally, one goal was to include Operation and Maintenance (O&M) costs as part of the cost estimates for the Opti-Tool. These O&M costs would help to provide a more realistic reflection of the long-term expenses of structural storm water controls, which is obviously critical in the practical, real-world implementation of BMPs. However, it is difficult to obtain accurate maintenance costs and they will be highly variable depending on the size, location and equipment needed to perform long-term O&M.

This point was highlighted by a key finding in EPA's recent (2013) publication, *Case Studies Analyzing the Economic Benefits of Low Impact Development and Green Infrastructure Programs.* The report indicated that only a small percentage of the entities that implement LID and GI approach for stormwater management conduct economic analyses due to the "uncertainties surrounding costs, operation and maintenance (O&M) requirements, budgetary constraints, and difficulties associated with quantifying the benefits provided by LID/GI" and the need "to obtain better estimates of the O&M costs associated with different types of LID/GI projects" was a key finding of the report.

As previously mentioned, one article entitled, *Comparison of Maintenance Cost, Labor Demands, and System Performance for LID and Conventional Stormwater Management* (Houle *et al. 2013)*, did contain relevant information for BMP costs in the New England region. During initial discussions between EPA Region I (Mark Voorhees) and UNHSC (Jamie Houle), there was concern that not enough data existed on O&M costs to propose accurate values for each of the BMPs included in the Opti-Tool. There was also

the concern that the O&M costs were not scaleable. For example, initial O&M costs for each BMP were based on the cost of operation and maintenance per year per acre of IC treated. Scaled differences such as the annual O&M costs for treating 0.5 acres of IC or 2 acres of IC have **not** been evaluated and may or may **not** result in a simple linear relationship. Yet the Opti-Tool costs subcommittee also realized the importance of including some maintenance parameter in order to *initiate* the conversation on the importance of accounting for O&M to maintain the functionality of the BMPs. Therefore Table 3, below, presents these annual maintenance costs (in $) for select BMPs, as well as the annual maintenance hours. Although the O&M costs have been presented in this memo, only the O&M **hours** will be included (as a separate field) in the Opti-Tool.

Table 3: Maintenance Costs ($) and Hours per year for select BMPs – From UNHSC

BMP	Maintenance Cost ($) per year	Annual Maintenance Hours
Bioretention	$1,890.00	20.7
Chamber System	Not Assessed	Not Assessed
Detention Pond	$2,380.00	24.0
Gravel Wetland	$2,138.33	21.7
Porous Asphalt	$1,080.00	6.0
Pervious Concrete	$1,080.00	6.0
Retention Pond	$3,060.00	28.0
Sand Filter	$2,807.50	28.5

*Note: initial costs based on cost of maintenance per year per acre of IC treated

Annual maintenance strategies were evaluated by directly quantifying hours spent categorizing maintenance activities, and assessing difficulty of those activities. To better illustrate costs and anticipate maintenance burdens, activities were characterized into distinct categories and a standard cost structure was applied. This unit conversion can easily be adapted according to local conditions, current economic climate, and regional cost variations which is why we decided to go with maintenance **hours** as those were directly measured and should remain constant. These maintenance activity categories allow more accurate cost predictions and provide insight into the appropriate assignment of maintenance responsibilities.

Annual maintenance costs were normalized to 2012 dollars and calculated for all SCMs by both dollars and personnel hours per acre of IC treated per system per year. It is important to note that inflation was not considered in life cycle maintenance cost projections.

MEMORANDUM (DRAFT)

Tetra Tech, Inc.
10306 Eaton Place, Suite 340
Fairfax, VA 22030
Telephone (703) 385-6000
Fax (703) 385-6007

Date: October 29, 2015

To: Mark Voorhees, EPA Region I

From: Rui Zou, Khalid Alvi – Tetra Tech

Subject: Buildup and Washoff Calibration Approach and SW Nutrient EMC Data Analyses

---

A primary objective of Task 9 of WA 4-35 is to identify a methodology for calibrating continuous simulation runoff quality models as part of the procedure for developing long-term cumulative BMP performance estimates of nutrient load reductions.

This memo summarizes the literature review and SW nutrient EMC data analyses that will be used to support the selected approach for generating nutrient (TN and TP) runoff quality time series for impervious cover using the Storm Water Management Model (SWMM).

1. Literature Review

Urban storm runoff can result in significant water quality problems. In practice, Best Management Practices (BMPs) have been used to control urban storm runoff and associated water quality problems. To improve the efficiency of BMPs, a better understanding of the processes behind urban runoff and pollutant generation is necessary. In the past decades, multiple urban nonpoint source pollution models, such as HSPF (Johanson et al., 1980), and SWMM (Huber and Dickinson, 1988), have been developed and applied effectively in modeling urban storm water quantity and quality. In these urban nonpoint source pollution models, the process that pollutants accumulate on the land surface and then are washed off by entering storm water is generally represented by a combined buildup-and-washoff formulation.

In general, the buildup process is modeled as a first-order dynamic process using two parameters: accumulation rate, and the maximum unit loading capacity. This formulation (Overton and Meadows, 1976) was based on observed behavior of many pollutants, where the pollutant loads on land surface increase since the last major storm until reaching a maximum value due to wind or other factors preventing further increase in accumulation. This asymptotic formulation is most commonly used in practical modeling analysis, although some investigators also apply linear buildup models instead (Barbé et al., 1996). The widely used SWMM model provides both asymptotic and linear options, though it is generally considered more realistic to use the nonlinear buildup formulation for urban impervious surfaces. In the buildup model, the total amount of contaminants is thus a function of the initial mass on the surface area and the length of the antecedent storm dry period.

When a storm event occurs, the pollutant accumulated on the land surface may be carried away by stormwater. This process is modeled as a washoff process with a first-order formulation that results in exponential washoff function (Wang et al, 2011). A stormwater model such as SWMM

which is formulated with buildup and washoff processes needs to be calibrated before it can be used to support decision making. Traditionally, the standard calibration method is the trial-and-error method, which involves manually changing the values of parameters until a reasonable match between model results and observed data is achieved. This method, although widely used, suffers a number of drawbacks. First, a trial-and-error calibration process is somewhat subjective and overwhelmingly relies on the modeler's experience and insights (Little and Williams, 1992). Second, it is relatively slow and inefficient in terms of time and effort required. Third, it is not capable of identifying parameter pattern uncertainty, often producing misleading model projection results. Finally, when a storm water pollutant model is calibrated using many event based data, manually calibrating the parameters for a specific site based on data from different events would be cumbersome and difficult. Therefore, it is highly desirable to have a method that can overcome these deficiencies.

The essence of the trial-and-error calibration process is to find a set of parameter values that can reasonably reproduce the observed data. Obviously, the systematic counterpart of the calibration process, or alternatively so-called inverse method, can be formulated as a **nonlinear optimization problem** (NOP), of which the simulation errors regarding observed data are minimized, subject to the constraints imposed by the physical mechanism underlying the model or bounds of parameter values (Hopgood 2001; Zou and Lung, 2004). It initially appears to be a straightforward task to identify a set of parameter that best reproduce the observe data, however, due to the significant uncertainty which exists in the stormwater pollutant concentration data, as well as the assumption of uniform impervious land surface properties/loading/precipitation, a single set of parameters which reproduce the observed data with least error might not be the true representative parameters. In contrast, equal-finality might dominate the solutions, suggesting that multiple parameter patterns might be equally valid in reproducing the observed data when uncertainty is considered.

In light of this situation, instead of finding a unique parameter set, this study proposes to apply the **Multiple Pattern Inverse Modeling** approach (MPIM) (Zou and Lung, 2004; Zou et al, 2008) to calibrate the buildup and wash-off process, which will identify multiple distinct parameter patterns that will reproduce the observed data. Each of these patterns would represent a potentially possible system of mechanisms underlying the observed data. This approach provides a way to explicitly address uncertainty in parameter pattern resulting from limited availability and uncertainty in data, as well as other simplification assumptions.

The MPIM is different from the uncertainty based automatic calibration approach applied in Avellaneda et al (2009). In Avellaneda et al (2009), the authors apply a Simulated Annealing (SA) technology to solve an inverse storm water quality model to estimate the buildup and washoff parameters. The inverse model is applied on an event basis, and the parameter estimated for each event is dependent on the event characteristics. The multiple parameters derived from each event are then put together to derive a probabilistic distribution serving as the basis for a Monte Carlo uncertainty analysis. This approach suffers the following limitations; 1) estimating parameters based on a single event is unreliable since the parameter values that perform well in one single storm might not work for other storms, therefore, including such a parameter in deriving the probabilistic distribution is equivalent to including incorrect data in the process; 2) the Monte Carlo method suffers the limitation of generating a large number of unrealistic

combinations of parameters, therefore, the resulting distribution of results might not be representative.

The advantage of MPIM is that it only involves conducting model projection based on identified behavioral parameter combinations, therefore, each realization of the model prediction represents a highly possible condition of the real system, providing more reliable quantification of the model uncertainty. Since the inverse modeling in MPIM is conducted on all the available or selected representative events, therefore, the identified parameters are more robust and realistic than the parameters estimated based on a single event. A recent research on SWMM model calibration applies an approach consistent with the MPIM framework (Bowden and Nipper, 2012), which uses Evolutionary Strategy (ES) to identify multiple plausible buildup-washoff parameter values and retains them as likely simulators of the system.

In this study, a MPIM framework is proposed to investigate the calibration of impervious area buildup-washoff dynamics in the New England area based on EMC data. In order to effectively solve the inverse model for diversified solutions, a **genetic algorithm** (GA) is selected to solve the NOP problem. The GA is a population-based stochastic search algorithm that is widely used in the field of global optimization for solving complex nonlinear optimization models. The capability of GA has been proven by thousands of applications, showing it can solve a NOP model with diversified near optima.

2. Proposed Methodology

The subsequent text describes the proposed methodology for calibrating a buildup-washoff model consistent with the SWMM paradigm.

2.1 Inverse Model Formulation

Suppose a SWMM model is used to simulate multiple events, and the model accuracy is measured by the root mean square error (RMSE) in terms of event mean concentration (EMC). Let ε denotes the RMSE of the model with regard to observed data, and EMC_O_i represents the observed EMC value for event i, and EMC_M_i represents the corresponding model result. Hence we have:

$$\varepsilon = \sqrt[2]{\frac{\sum_{i=1}^{n}(EMC\_M_i - EMC\_O_i)^2}{n}} \quad (1)$$

To identify the proper parameter values that reproduce the observed data, the following optimization model is formulated:

$$\text{Min } \varepsilon \quad (2)$$

$$\text{s.t. } EMC\_M_i = f(x_{i1}, x_{i2}, \ldots x_{ik}, p_1, p_2, \ldots p_m), \forall\, i = 1,2,\ldots,n \quad (3)$$

Where f represents the simulation model relating EMC to storm characteristics and model parameters; x represents the storm characteristics; p represents parameters in the buildup-

washoff model. If a SWMM model is used to simulate the storm events, then function f represents the SWMM model specifically configured for the analysis.

Note that in Eq. (1), the objective function ε consists of n storm events, which means that to estimate the model parameters for a specific site, we need to configure n SWMM models each simulating a single event. In the meantime, it must be assured that all of them use the same parameter values. Apparently, doing this would be very cumbersome, especially in this study, since we would need to estimate parameters for multiple sites. At the first glance, this cumbersomeness might be bypassed by configuring all the n events in a single model, where the events are separated by the number of dry days based on data. However, the approach is subjected to significant limitation because the post-storm pollutant mass is a function of the buildup and washoff parameters. Therefore, the initial condition after each storm event is dependent on the parameter values. In a continuous simulation model this is not an issue because any event is preceded by its actual events, so the initial condition estimated is realistic with regard to the parameter values. However, in the model where the separate events are organized together to form a pseudo-continuous simulation, the initial condition resulted from the preceding event does not represent the real initial condition of the current event, causing inconsistency problem.

In this study, we propose an approach which would overcome the aforementioned limitations. This approach involves solving the buildup and washoff dynamics externally based on a process consistent with the SWMM representation. By solving the buildup and washoff externally, it avoids the cumbersome process of configuring multiple SWMM models for different events yet preserving same parameter values. In addition, it would enable a more convenient coupling with a population-based optimization engine for uncertainty-based parameter identification.

In SWMM, the pollutant buildup is modeled as an ordinary differential equation (ODE) as:

$$\frac{dN(t)}{dt} = \alpha - \beta N(t) \quad (4)$$

Where, N(t) is the accumulated load on a source area at time t (g/acre); α is the accumulation rate (g/acre/day); β is the first-order removal rate (/day); Here β is defined as the ratio between accumulation rate and the maximum load per unit area (g/acre) as:

$$\beta = \frac{\alpha}{M} \quad (5)$$

For an initial storage of N_0 at t=0, the solution to Eq. (4) is:

$$N(T) = N0e^{-\beta T} + M(1 - e^{-\beta T}) \quad (6)$$

Where T is the antecedent dry period before the current storm, and N_0 is the initial pollutant load after the preceding storm event (g/acre).

In SWMM, multiple different formulations for washoff are available, and the one used in the present study is the exponential representation that is equivalent to the ODE as below:

$$\frac{dN(t)}{dt} = -\gamma Q(t)^{\theta} N(t) \quad (7)$$

Where γ is a scaling factor introduced in the SWMM model, which serves as a calibration parameter. Note that when $\theta = 1$, this equation is reduced to the traditional first-order formulation and is analytically solvable. In such a case, the total washoff load of a specific event can be obtained using the total event runoff depth without needing the hydrograph information. On the other hand, if $\theta \neq 1$, the equation cannot be solved for solutions directly represented as a function of the total runoff, so a numerical method needs to be adopted to use the hydrograph information. The most straightforward method is to solve Eq. (7) using a finite difference method:

$$N^{t+1} = N^{t} - \gamma Q(t)^{\theta} N(t) \Delta t \quad (8)$$

In the present study, since the model is to be calibrated against EMC data, only the cumulative washoff load is of interest. Therefore, it is desired to derive a model which can directly relate the cumulative washoff load to the parameters and hydrograph. To achieve this, we consider Eq. (7) for a period Δt with constant runoff depth Q_t. Suppose the land surface pollutant mass at the beginning is N^t then at the end of the period the mass N^{t+1} can be analytically represented as:

$$N^{t+1} = N^{t}\, e^{-\gamma Q_t^{\theta} \Delta t} \quad (9)$$

As this particular study is intended to develop buildup-washoff parameters representative for impervious landuse only, the formulation can be further simplified by using the assumption that surface runoff depth can be approximated by event precipitation depth, i.e. $Q_t \approx r_t$. This assumption is justified by checking the previously calibrated SWMM hydrological model used to derive the unit area export ratio for the earlier phase of this project (Figure 1). As shown, the runoff depth closely approximates the corresponding rainfall depth except for a slight lag in time. Considering the length of antecedent dry days are usually multiple days, the slight lag in runoff time is not anticipated to cause significant uncertainty in the buildup/washoff model result.

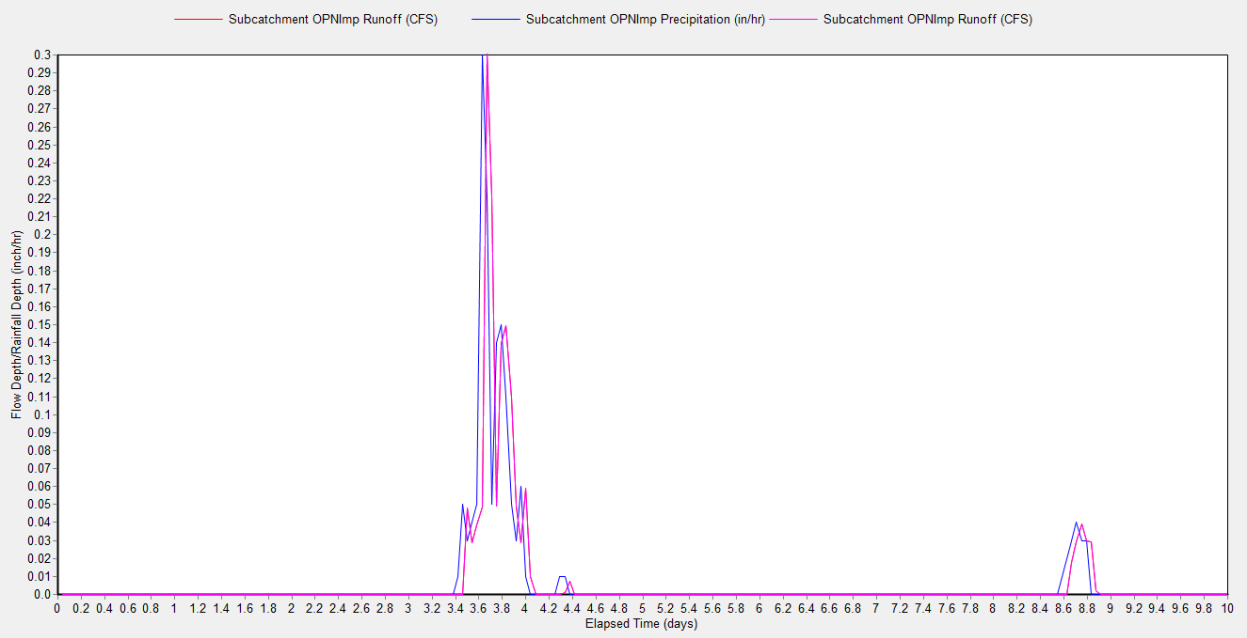

Figure 1. Comparing precipitation depth versus impervious area runoff depth simulated by the calibrated SWMM model

Applying Eq. (9) from the beginning of the storm to anytime during or at the end of the storm, and using the precipitation depth to substitute the runoff depth would lead to:

$$N(t) = N(T)e^{-\gamma \sum_{i=1}^{t/\Delta t} r_i^{\theta} \Delta t} \quad (10)$$

The cumulative washoff load W (t) at the end of time t is thus:

$$W(t) = N(T)(1 - e^{-\gamma \sum_{i=1}^{\frac{t}{\Delta t}} r_i^{\theta} \Delta t} \ ) \quad (11)$$

Assume the event end time is T_2 (hour), then the EMC can be represented as:

$$EMC = \frac{N(T)(1-e^{-\gamma \sum_{i=1}^{\frac{T2}{\Delta t}} r_i^{\theta} \Delta t} \ )}{\sum_{i=1}^{\frac{T2}{\Delta t}} r_i} \quad (12)$$

Combining Eq. (6) and (12), we obtain:

$$EMC = \frac{[N0e^{-\beta T} + M(1-e^{-\beta T})](1-e^{-\gamma \sum_{i=1}^{\frac{T2}{\Delta t}} r_i^{\theta} \Delta t})}{\sum_{i=1}^{\frac{T2}{\Delta t}} r_i} \quad (13)$$

Note that, on the right hand side of the equation, four parameters are used to predict the EMC from given antecedent dry days and storm hydrograph.

Note that, assuming for a specific impervious land, there are K events, so for each event, the predicted EMC would be:

$$EMC_k = \frac{[N_{0k}e^{-\beta T_k}+M(1-e^{-\beta T_k})](1-e^{-\gamma \sum_{i=1}^{\frac{T2k}{\Delta t}} r_{ik}^{\theta}\Delta t})}{\sum_{i=1}^{T2k} r_{ik}} \quad (14)$$

where the subscript k represents the event specific value. Apparently, the buildup and wash-off calibration of the model is essentially to identify the values of the parameters M, β, γ and θ which would predict the EMC value that match the observed value.

Combining model (2)-(3) with Eq. (14), and incorporating additional bound constraints which bracket the lower and upper bound of each parameter, the parameter calibration model for the SWMM equivalent buildup-washoff process is:

$$\text{Min } \varepsilon \quad (15)$$

$$\text{s.t. EMC\_M}_k=\frac{[N_{0k}e^{-\beta T_k}+M(1-e^{-\beta T_k})](1-e^{-\gamma \sum_{i=1}^{\frac{T2k}{\Delta t}} r_{ik}^{\theta}\Delta t})}{\sum_{i=1}^{T2k} r_{ik}}, \forall\, k = 1,2,\dots,n \quad (16)$$

$$(M_L, \beta_L, \gamma_L, \theta_L) \leq (\text{M}, , \gamma, \theta) \leq (M_U, \beta_U, \gamma_U, \theta_U) \quad (17)$$

where the subscripts "L" and "U" represent the corresponding lower and upper bounds.

Note that for the event based formulation, N_0 is unknown a priori, and it is event-dependent, therefore, it is not proper to directly treat it as a calibration parameter. Instead, N_0 will be treated as a source of uncertainty in deriving the parameters through a **stepwise calibration scenario construction** (SCSC) approach, i.e., in predicting the EMC of each event in a parameter estimation iteration, N_0 is treated as constant across the events, and the corresponding solutions are identified for different N_0 values for analyzing the sensitivity of the parameters to an uncertain initial condition. In such a construct, each round of parameter identification involves adding Eq (18) to model (15) to (17)

$$N_0=N_{0\_j} \quad (18)$$

where N_{0_j} is a prescribed initial condition for each round of optimization, which can be determined from a lower bound of 0.0 to an upper bound of 100% of the maximum load M, and a value can be taken in-between based on a step. For example, a 5% increment might be used to identify a series of initial conditions, and for each initial condition the optimization model is solved for corresponding parameter values. After obtaining all the solutions, the dependency of the parameter values to the assumption regarding initial condition can be evaluated for uncertainty analysis.

2.2 Parameter Pattern Identification

Solving model (15) to (18) can result in a large number of parameter combinations that might satisfy reasonable calibration criteria. In the case of calibration based on EMC data, two parameter combinations that result in exactly the same EMC might be due to different intra-storm dynamics (Bowden and Nipper, 2012). Therefore, it is crucial to preserve the diversity in the solutions for future scenario analysis for robust decision making. Following the MPIM paradigm, the solutions after implementing the SCSC procedure are evaluated to refine the estimate of the range of initial condition. This would likely result in much narrower range for the initial condition. Based on the new initial condition range, a few refined SCSC scenarios are designed, and the GA is used to solve the models. Then a parameter pattern identification (PPI) process is invoked as below:

Step 1; Rank the N individuals throughout the GA searches from the least to the largest;

Step 2: Set the one with the minimum objective function as the benchmark, then set a tolerance level, such as 10% to sift all the individuals, such that all the individuals with errors within 10% of the minimum are selected as the candidates for qualified solutions;

Step 3: Apply a clustering algorithm, such as K-means clustering algorithm, to identify distinct patterns from the candidate solutions, and then identify the elite member of each pattern as the representative parameter set.

Through these processes, all the likely parameter patterns that reproduce the observed EMC data equally well, but might be subjected to different intra-storm dynamics, are identified for being used in future projection analysis.

2.3 Implementation Plan

The proposed methodology as described above is a general framework that covers both the automatic calibration and the uncertainty analysis scopes. Since in the present stage of the project, a full exploration of the uncertainty aspect of the approach is unrealistic due to the limitation on time and resource, this project will focus on the calibration aspect of the approach, while leaving the possibility of further uncertainty analysis open in subsequent studies.

Another consideration is the availability of data. While it is ideal if EMC data are available for all impervious landuse types, which would allow estimation of parameter sets that represent the specific dynamics of each type of landuse, the reality prevents us from doing so, since data are only available for a subset of landuse types. Therefore, it is desired to reduce the complexity in parameter estimating by lumping all the data available for landuses together, and applying the proposed approach to derive a set of parameter that, on-average, represent the general impervious area.

The third consideration is about the regional representation. The EMC dataset provided by EPA also includes data from other areas in the U.S. which are outside of the New England region,

however, the purpose of the current study is to obtain representative parameters for the New England region alone. Therefore, only the data collected in the New England region is used in this study. Further considering that data collected before a certain year might not be suitable in the representing current conditions, therefore, the year 2000 is selected to be the threshold, i.e., any data collected before the year 2000 is not used in the current model calibration practice. Applying this criteria, it is determined that only the data from Massachusetts and New Hampshire will be used in this analysis.

The 4th consideration is the storm size to be focused in the calibration. Per the guidance from EPA, it is desired to focus the calibration on relatively small-sized rainfall events that are dominant in the New England region.

With the five considerations, the steps of implementing the proposed approach are as follows:

Step 1: Identify all sites in Massachusetts and New Hampshire;

Step 2: Identify all the Massachusetts and New Hampshire sites with impervious area fraction >80% associated with data collected after 2000;

Step 3: For all the identified sites, identify the precipitation events with total rain depth equal to or smaller than 1.0 inch to represent the moderate-to-small size precipitation events;

Step 4: Determine the pollutants that will be used for calibration, herein are TN and TP;

Step 5: For all the identified sites, obtain hourly precipitation data from other data sources such as NCDC data, or any other site-specific data;

Step 6: Formulate the inverse models for TN and TP for all the identified impervious sites;

Step 7: Develop computer code to solve the inverse model with GA, and identify the parameter pattern which best fits the observed EMC data as the identified parameter for use in the later time series generation.

3. SW Nutrient EMC Data Analysis

A large number of EMC data were organized in an Excel file, containing data collected at various land use sites from different locations in the United States. A preliminary analysis was done to identify whether there existed any apparent trend or patterns in that data. The analysis was divided into two major parts: an overall analysis for all data, and the same type of analysis for data in the New England region only. It was noted that the EMC values for both TN and TP were lower in New England area as compared to the data available from other parts of the country. The subsequent sub-sections present the findings from this preliminary analysis.

3.1 Drainage Area

The event mean concentration of TN and TP are plotted against their corresponding drainage area from all sites (Figure 2) and from New England region only (Figure 3). Although there is no clear trend line that can be fit for the data, there is a visible pattern that higher pollutant concentrations exist for smaller drainage areas, particularly for areas less than 100 acre. This trend is more prominent for TP in the overall dataset, and for TN in the dataset from New England region. It should be noted that there are several underlying uncertainty factors such as the land use type, percent imperviousness, rainfall intensity, and others which vary from one data point to another.

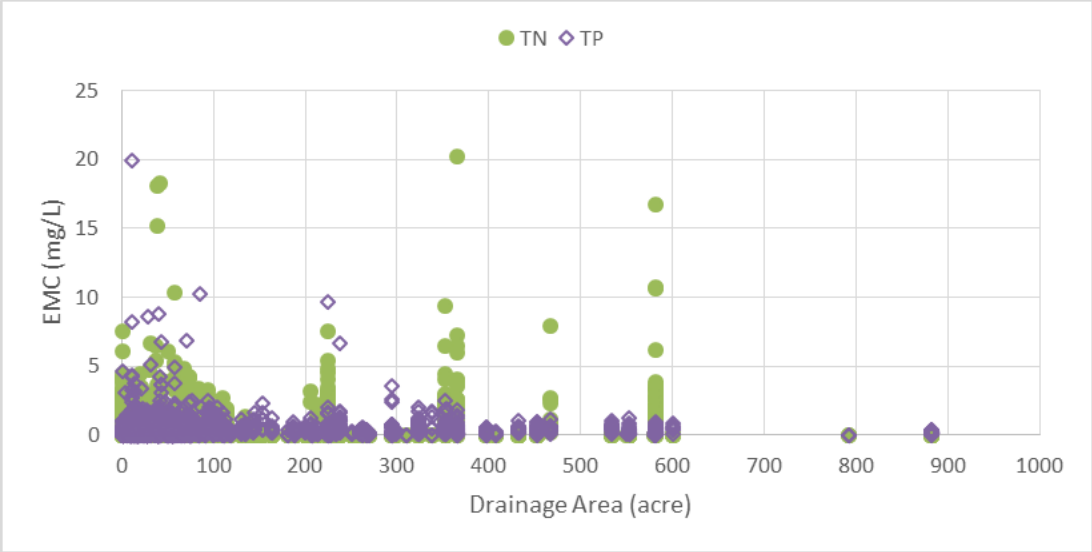

Figure 2. Comparing EMC for TN and TP versus drainage area (all locations)

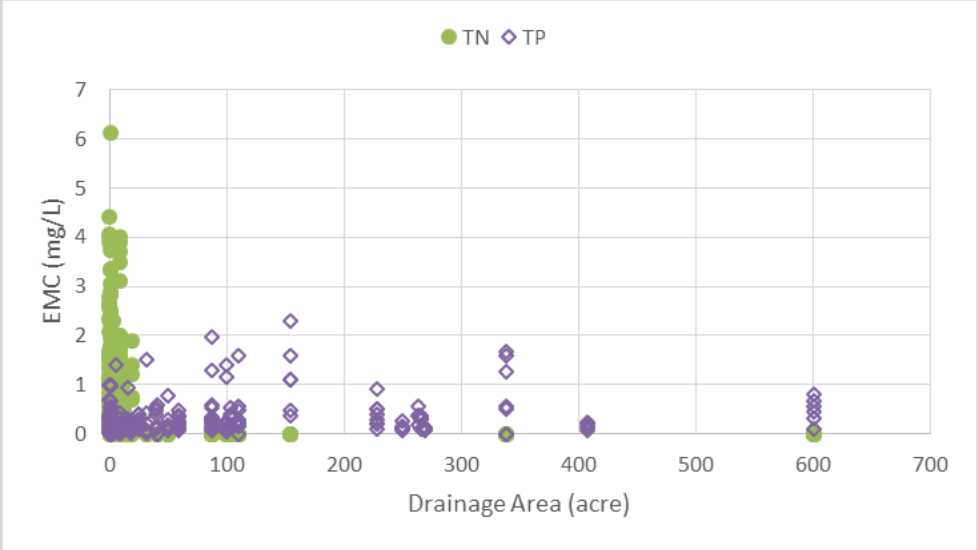

Figure 3. Comparing EMC for TN and TP versus drainage area (New England only)

3.2 Percent Impervious Land

In general, there is no conclusive relationship between impervious percentage and the pollutant EMC shown in Figure 4 and Figure 5. However, it seems the pollutant concentration increases with the increase in percent imperviousness. It should be noted that there are several underlying uncertainty factors such as the land use type, rainfall intensity, and others which vary from one data point to another.

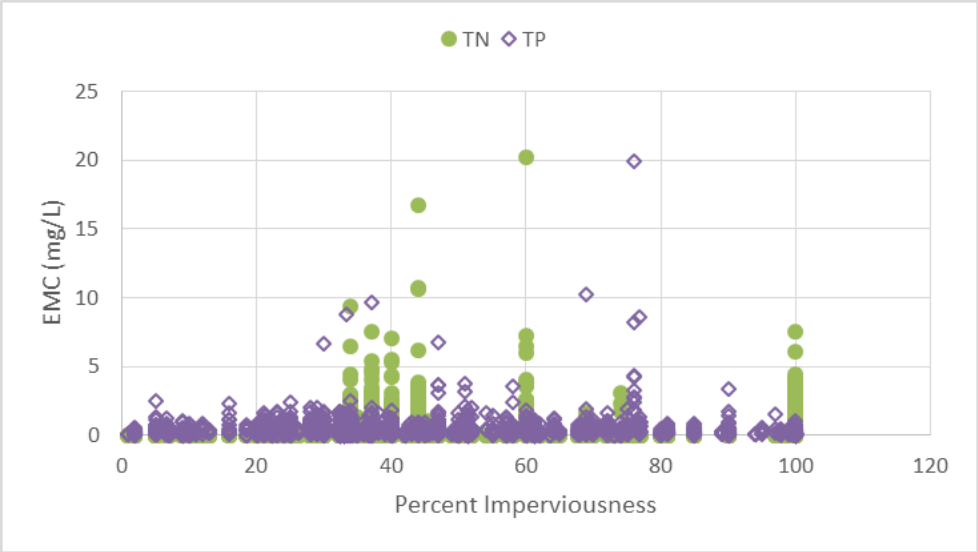

Figure 4. Comparing EMC for TN and TP versus percent imperviousness (all locations)

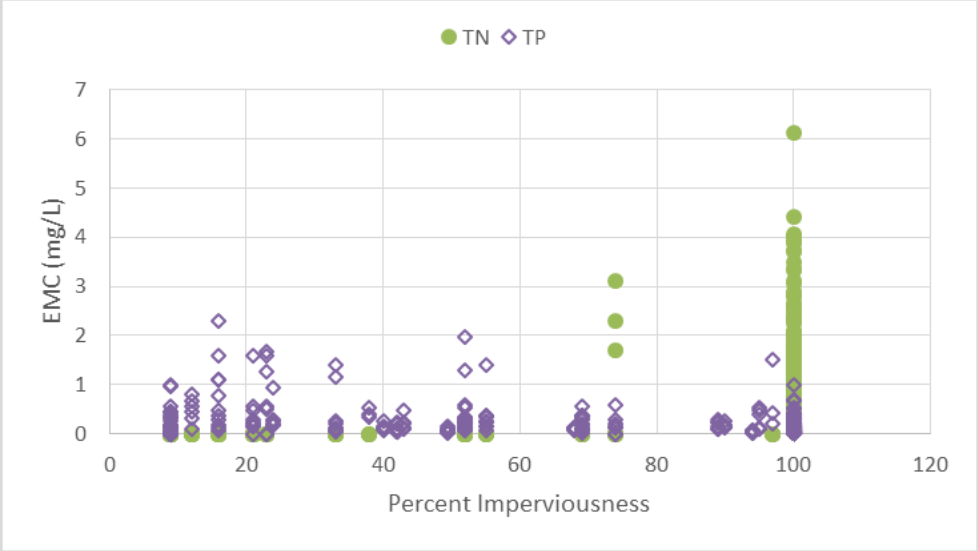

Figure 5. Comparing EMC for TN and TP versus percent imperviousness (New England only)

3.3 Land Use Type

The average EMC value for each pollutant (assigning 10% of the data set as outlier status) in each land use category is calculated. Figure 6 and Figure 7 show that open land has the lowest average EMC value for TN. Overall dataset shows that industrial land has the highest average EMC for TN whereas in the New England dataset, mixed land uses show highest average EMC for TP. The TN data for industrial, commercial mixed, and freeways mixed land uses are not available in New England region. It should also be noted that storm sizes, which can influence the average concentration, are not considered for this calculation.

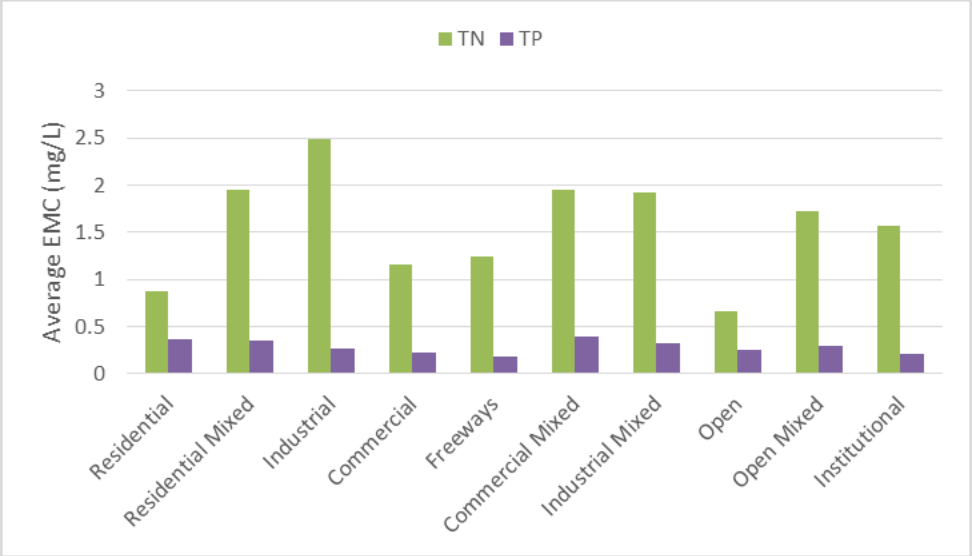

Figure 6. Comparing average EMC for TN and TP versus land use type (all locations)

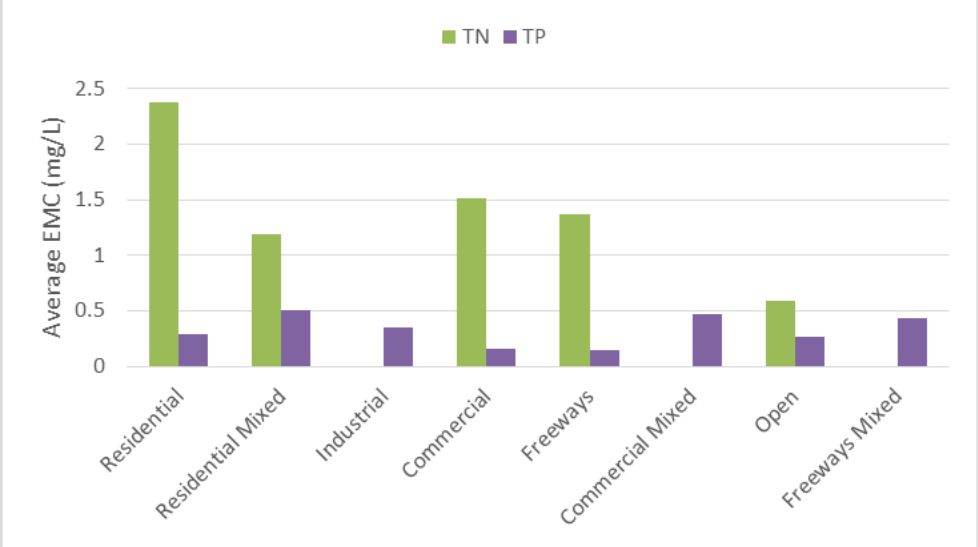

Figure 7. Comparing average EMC for TN and TP versus land use type (New England only)

3.4 Precipitation

Figure 8 and Figure 9 show storm sizes in inches versus EMC values for TN and TP from all sites in the database and from New England region only. Linear trend lines do not fit accurately but there is a clear relationship with pollutant concentrations decreasing as rain fall total in an event increases. The same trend is obvious in the box and whisker plots shown in Figure 10 and Figure 11. This trend is more obvious for TN as compared to TP and it seems like the first flush phenomenon is dominant, resulting in higher EMC values for smaller to medium storm sizes as compared to the large storms.

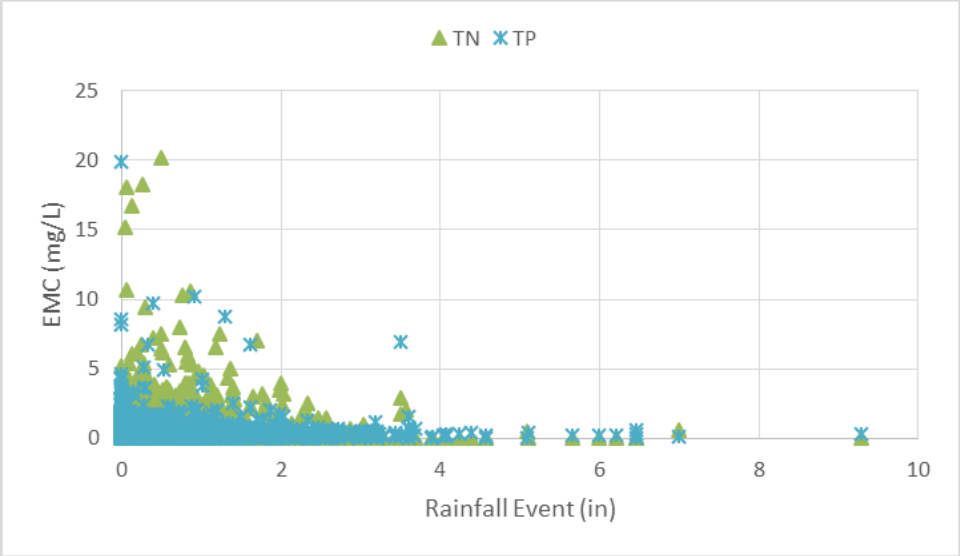

Figure 8. Comparing EMC for TN and TP versus rainfall event total (all locations)

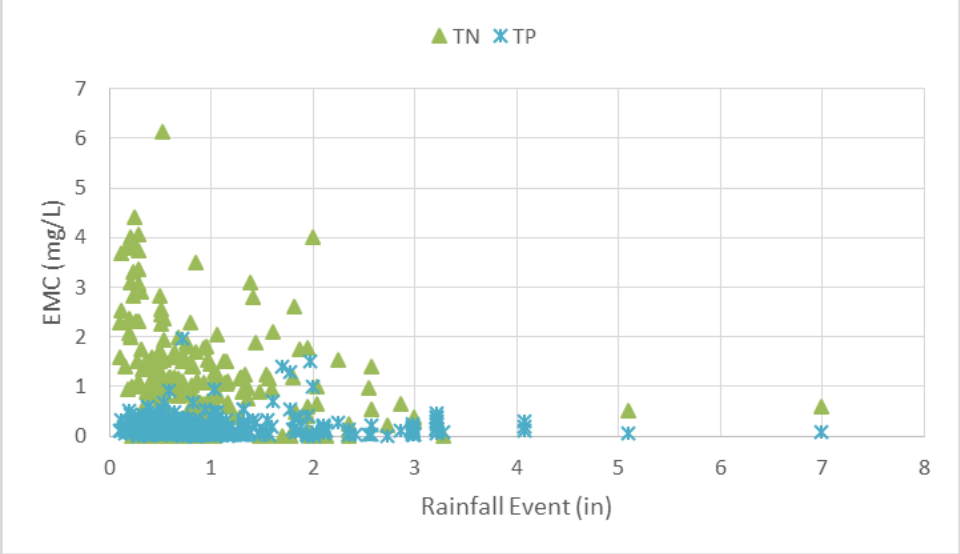

Figure 9. Comparing EMC for TN and TP versus rainfall event total (New England only)

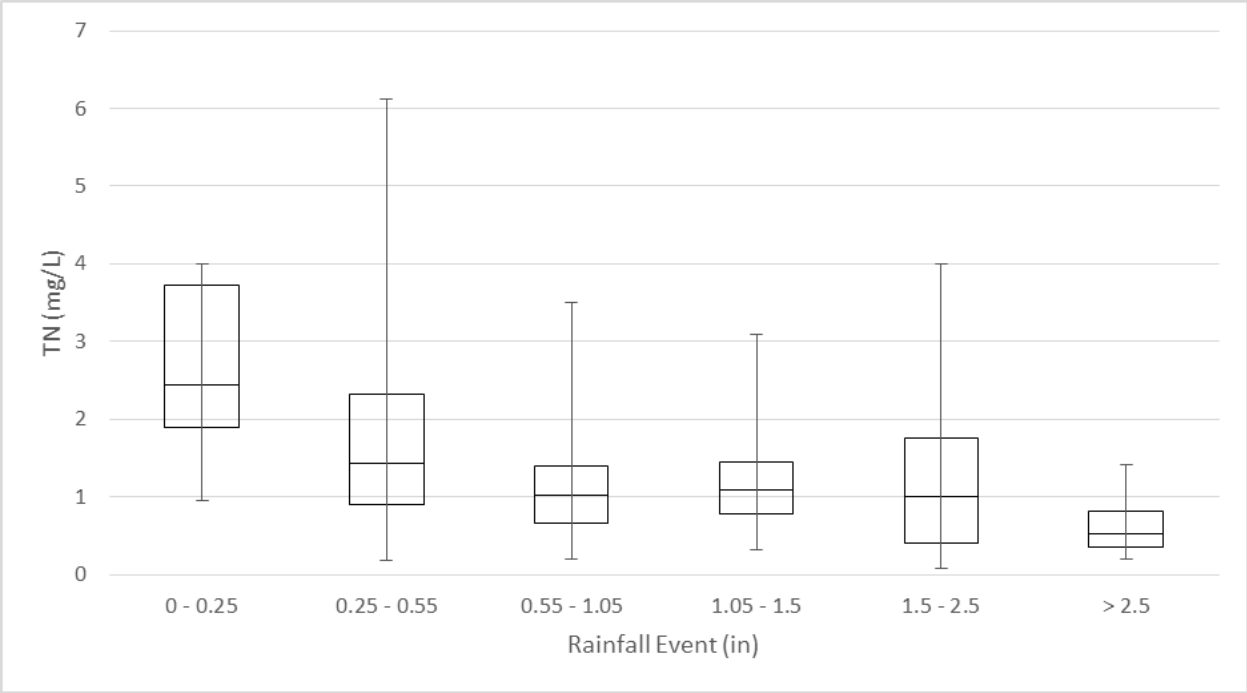

Figure 10. Box Whisker plot for TN versus rainfall event total (New England only)

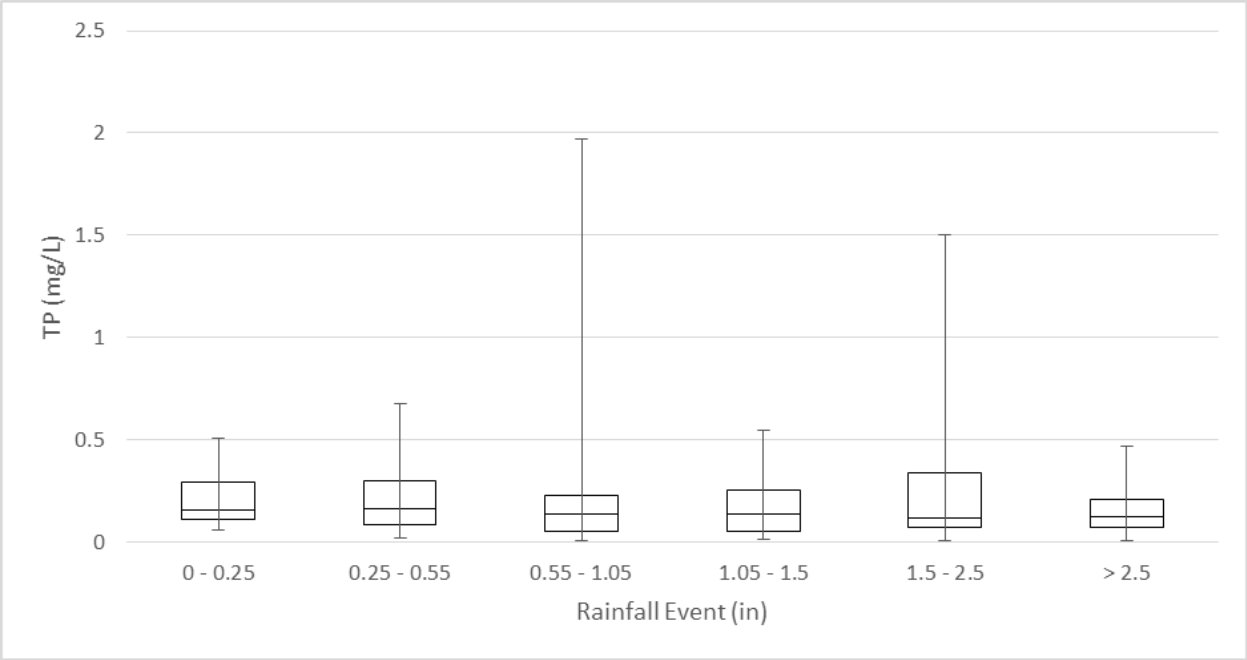

Figure 11. Box Whisker plot for TP versus rainfall event total (New England only)

References:

Avellaneda, P., Ballestero, T. P.; Roseen, R.M. and Houle, J.J (2009). On Parameter Estimation of Urban Storm-Water Runoff Model. Journal of Environmental Engineering, Vol. 135, No. 8, 596-608.

Barbé, D. E., J. F. Cruise, and X. Mo, 1996. Modeling the Buildup and Washoff of Pollutants on Urban Watersheds. Water Resources Bulletin 32(3):511-519.

Bowden, W.B., Nipper, J. (2012). Redesigning the American Neighborhood: Cost Effectiveness of Interventions in Stormwater Management at Different Scales. Project No. EM97155901. Prepared by: Rubenstein School of Environment and Natural Resources, The University of Vermont, Burlington, VT 05405-0088.

Huber, W.C., Dickinson, R.E., 1988. Storm water management model, version 4: User's manual. Rep. No. EPA 600/3-88/001a, Environmental Research Laboratory, US EPA, Athens, Ga.

Johanson, R.C., Imhoff, J.C., Davis, H.H., Jr., 1980. User's manual for hydrological simulation program Fortran (HSPF). Rep. No. EPA-600/9-80-015, US EPA, Athens, Ga.

Little, K.W., Williams, R.E., (1992). "Least-squares calibration of QUAL2E." *Water Environment Research*, 64, 179-185.

Overton, D. E. and M. E. Meadows, 1976. Stormwater Modeling. Academic Press, New York, New York.

Long Wang, Jiahua Wei, Yuefei Huang, Guangqian Wang, Imran Maqsood (2011). Urban nonpoint source pollution buildup and washoff models for simulating storm runoff quality in the Los Angeles County. Environmental Pollution, 159, 1932-1940.

Zou, R., and Lung, W.S. (2004). Robust water quality model calibration using an alternating fitness genetic algorithm. Journal of Computing in Civil Engineering, 130(6), 471-479.

Zou, R., Lung, W.S., and Wu, J. (2008). Multiple-pattern parameter identification and uncertainty analysis approach for water quality modeling. Ecological Modeling, 220 (5), 621-629.

MEMORANDUM (DRAFT)

Tetra Tech, Inc.
10306 Eaton Place, Suite 340
Fairfax, VA 22030
Telephone (703) 385-6000
Fax (703) 385-6007

Date: October 29, 2015

To: Mark Voorhees, EPA Region I

From: Rui Zou, Khalid Alvi – Tetra Tech

Subject: Buildup and Washoff Calibration Results and Long-term Continuous Hourly Timeseries

---

This technical memo summarizes the process and results of the systematic estimation of regional buildup and washoff parameters for TP and TN using the calibration approach described in memo 9.1 "Buildup and Washoff Calibration Approach". The resulting parameters were used to develop a long term continuous hourly timeseries of TP and TN loading for different impervious covers used in the opti-tool.

This memo consists of five sections; (1) Data preparation for the calibration model, (2) Development and verification of Event Based Buildup and Washoff (EBBW) model, (3) Genetic Algorithm (GA) based calibration of the model, (4) Robust parameter estimation, and (5) Development of long term continuous hourly timeseries for impervious cover.

1. Data Preparation

The data from the SW database provided by EPA were analyzed and a subset of data was identified as suitable for this study by following the steps shown below;

Step 1: All the events in Massachusetts and New Hampshire with precipitation depth less than 1 inch and no missing EMC data for TN and TP were extracted from the database;

Step 2: The data were then filtered such that data only after the year 2000 were kept;

Step 3: The hourly precipitation data were downloaded from National Climatic Data Center (NCDC) for the locations which were closest to the selected EMC monitoring sites;

Step 4: The hourly precipitation data were preprocessed to identify those events corresponding to the EMC data, and the total rainfall depths were compared with the site specific data in the SW database. The comparison showed that the total rainfall data from the SW sampling was not always consistent to that from the NCDC data, indicating that the rainfall pattern from the NCDC might not always have been representative of that from the SW sampling site. In order to construct site specific hourly rainfall pattern, the NCDC total rainfall which were within 50% difference from the sampling site data were maintained. It was assumed that the rainfall pattern from these NCDC record might have reasonably represented that of the sampling site condition.

Step 5: The hourly rainfall at the sampling sites were then reconstructed by using the total rainfall at the sampling site to rescale the corresponding NCDC data, such that the total rainfall

at the site matched the site-specific monitoring data, while the hourly distribution followed that of the NCDC data. Those site-specific events for which the NCDC rainfall total differed from the site rainfall total by more than 50%, were discarded as unreliable data to characterize that specific event.

After following the above steps, in total, 45 data sets were identified, 29 of them from MA sites, 16 from NH sites, and all of these sites were 100% impervious and met the study objectives, which were to estimate regional buildup and washoff parameters for impervious area, without differentiating land use types, due to a limited dataset.

Figures 1 and 2 show the EMC data for TN and TP for the selected rainfall events in this study.

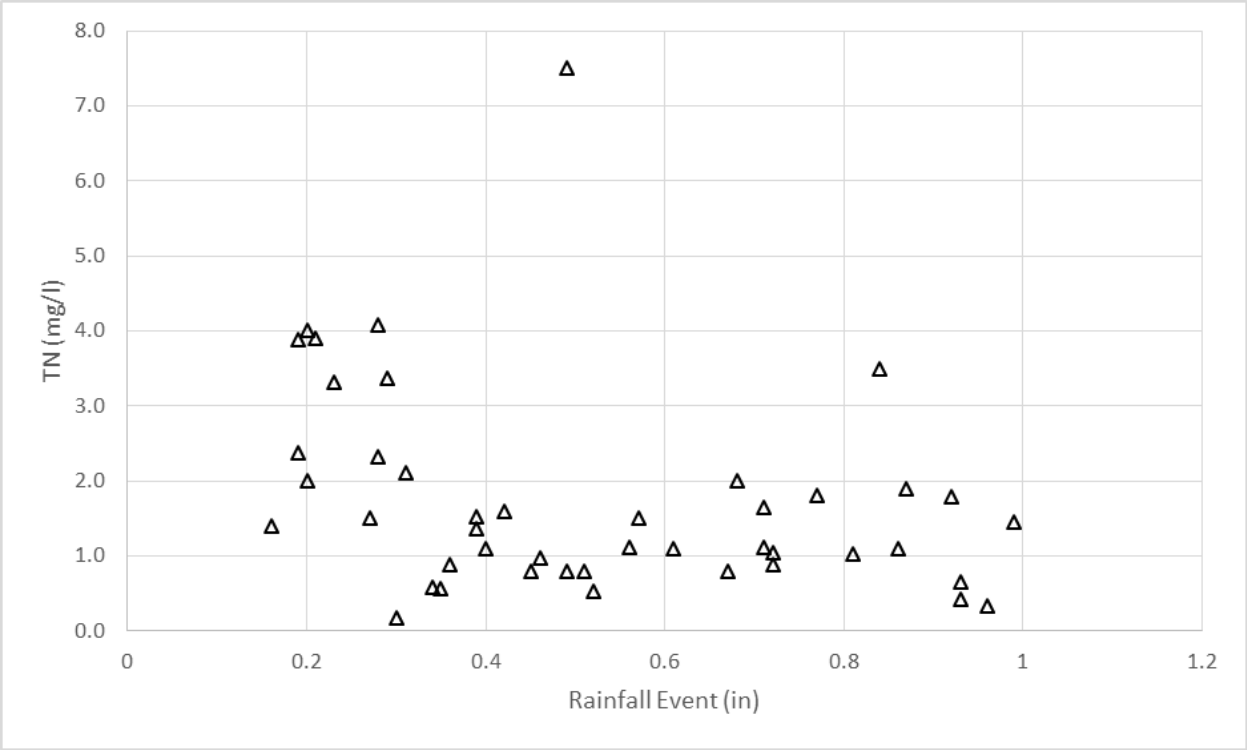

Figure 1. Observed EMC data for TN for the selected rainfall events.

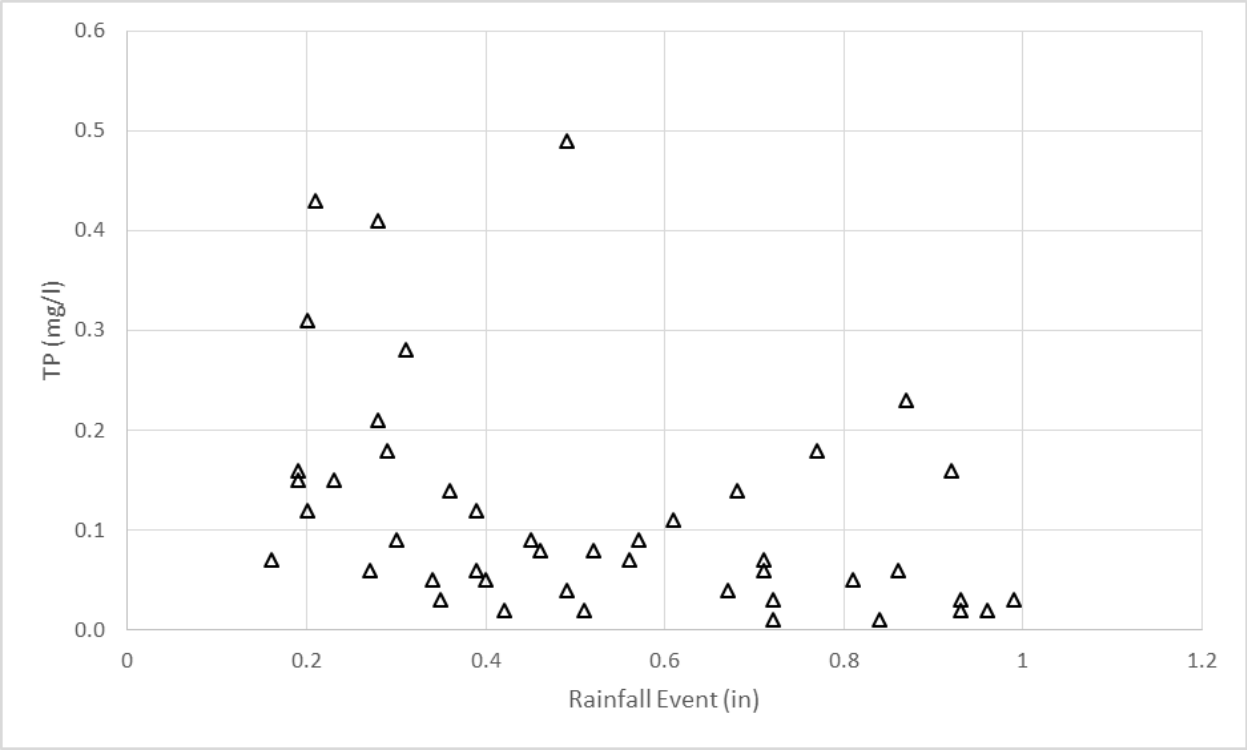

Figure 2. Observed EMC data for TP for the selected rainfall events.

2. Development and Verification of the Event-Based Buildup and Washoff (EBBW) Model

A computer simulation model was developed to simulate the buildup and washoff dynamics on an event basis. The purpose of this model was to replicate the behavior of SWMM model in terms of EMC prediction on an event basis, thus the parameters identified by this model would be directly applicable to the SWMM model for generating long term model results. The model was developed through solving the buildup and washoff equations as detailed in technical memo 9.1. The model inputs included initial land surface storage N_0, antecedent dry period length, two buildup parameters (Beta and M), and two washoff parameters (gamma and theta), as well as the hourly rainfall data. With these inputs, the model predicted the corresponding nutrient EMC.

The EBBW model was developed using the FORTRAN programming language, and the algorithm and code were then verified by comparing with the SWMM model results for a real event drawn from the dataset identified. The following steps were taken for the model verification.

- An event of 0.38 in of rainfall was randomly selected from the 45 data points. An hourly rainfall distribution for the selected event is shown in Figure 3.
- A specific set of model parameters was determined as: N_0=0.0 lb/acre; Antecedent dry days= 7.1, maximum storage capacity M=0.0133 lb/acre; the buildup accumulation exponent Beta=0.005; the washoff coefficient Gamma=1.719; and the washoff power coefficient Theta=0.918.
- A SWMM model for this event was configured and run, and the resulted simulated EMC was found to be 0.0612 mg/L.

- The EBBW model was run with the same parameters, and the resulted simulated EMC was found to be 0.0615 mg/L.

Apparently, the result from the EBBW model is equivalent to that of the SWMM, indicating that the parameter structure and numerical solution between the two models are consistent, therefore, the parameters identified using the event based model would be applicable to the SWMM model for long term simulation.

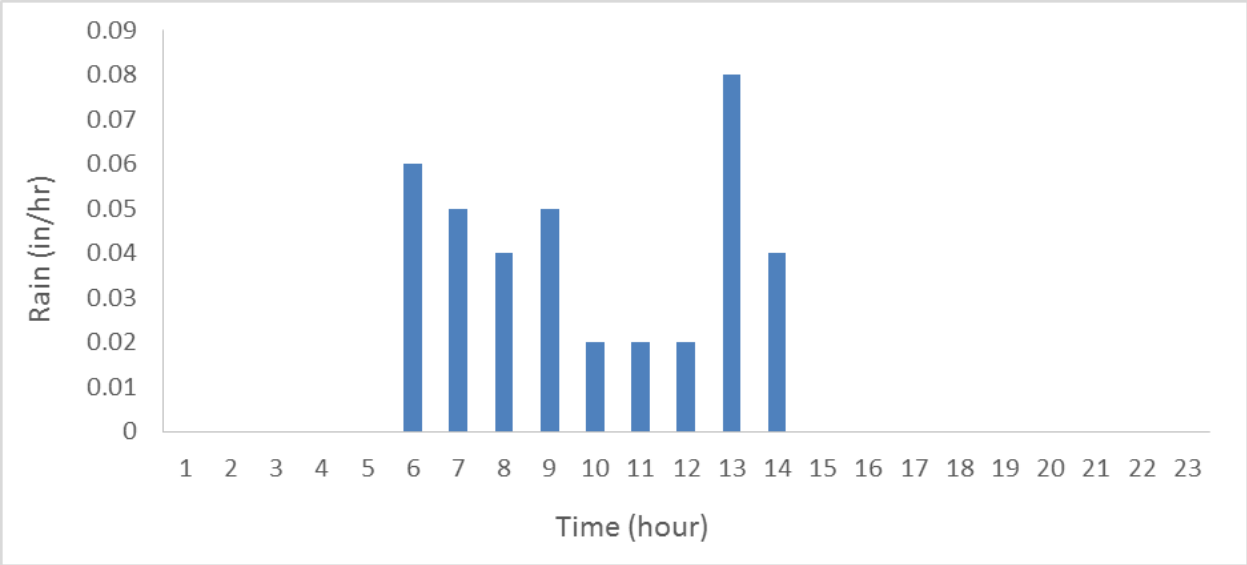

Figure 3 Rainfall distribution of the selected event for EBBW verification.

3. Genetic Algorithm (GA) Based Calibration

The Genetic Algorithm (GA) is a general-purpose stochastic search and optimization method inspired by the natural evolution process observed in the biological world. It has been widely applied in a variety of engineering optimization problems and has been shown to be capable of solving optimization problems with non-differentiable, nonlinear and multi-modal objective functions. The basic operations involved in a GA include four major operators including fitness evaluation/scaling, selection, crossover, and mutation. Due to its popularity, the implementation procedure of a GA has been covered widely and therefore is not repeated in this memo.

In this study, the EBBW model was coupled with a GA to form a computational platform for calibrating the buildup-washoff model using observed EMC data. Basically, the calibration model was formulated as a nonlinear optimization model where the objective function is the simulation error, and the decision variables are the four buildup and washoff parameters. The GA searched the entire parameter space to identify the combination of parameters that would result in the smallest model errors.

As described in memo 9.1, the initial storage N_0 was not considered as a calibration parameter. Instead, a range of N_0 was used to formulate different optimization models for calibrating the EBBW model. Therefore, for each specific N_0, a set of parameters which best reproduce the

observed EMC data in terms of **root mean square error** (RMSE) was identified. In this study, we applied 21 different N_0 values ranging from0.0 to 100% of the maximum storage M, with a step of 5%. For each of the two pollutants (i.e., TN and TP), 21 parameter optimization models were formulated and solved using the coupled GA-EBBW framework. The results for the EBBW model prediction using the identified optimal parameters, as well as the distributions of the identified parameters, are summarized below.

3.1 Result for TN

For each of the 21 GA-EBBW scenarios (each run with a different initial condition), the parameter combination which results in the lowest RMSE is identified, resulting in the 21 parameter combinations shown in Figure 4. As shown, while both the buildup parameters show significant variability, it appears that the majority of the values for Beta fall within a narrow range near 0.0, except for two parameters that significantly depart from this pattern. On the other hand, the variability in maximum accumulation storage M is more evenly distributed, though there is also the tendency to be more concentrated to the lower end. As for the washoff parameters, Figure 4 shows that Gamma has much less variability than Theta, suggesting the values of Gamma are less sensitive to the uncertainty in initial condition of the model. To gain further insight about the variability and distribution of the identified parameters, Figure 5 plots the histograms of each of the four parameters. Apparently, there is no continuous statistic distribution that can be used to characterize the parameters, and the values of all the parameters have clear gaps, particularly for Beta and Theta.

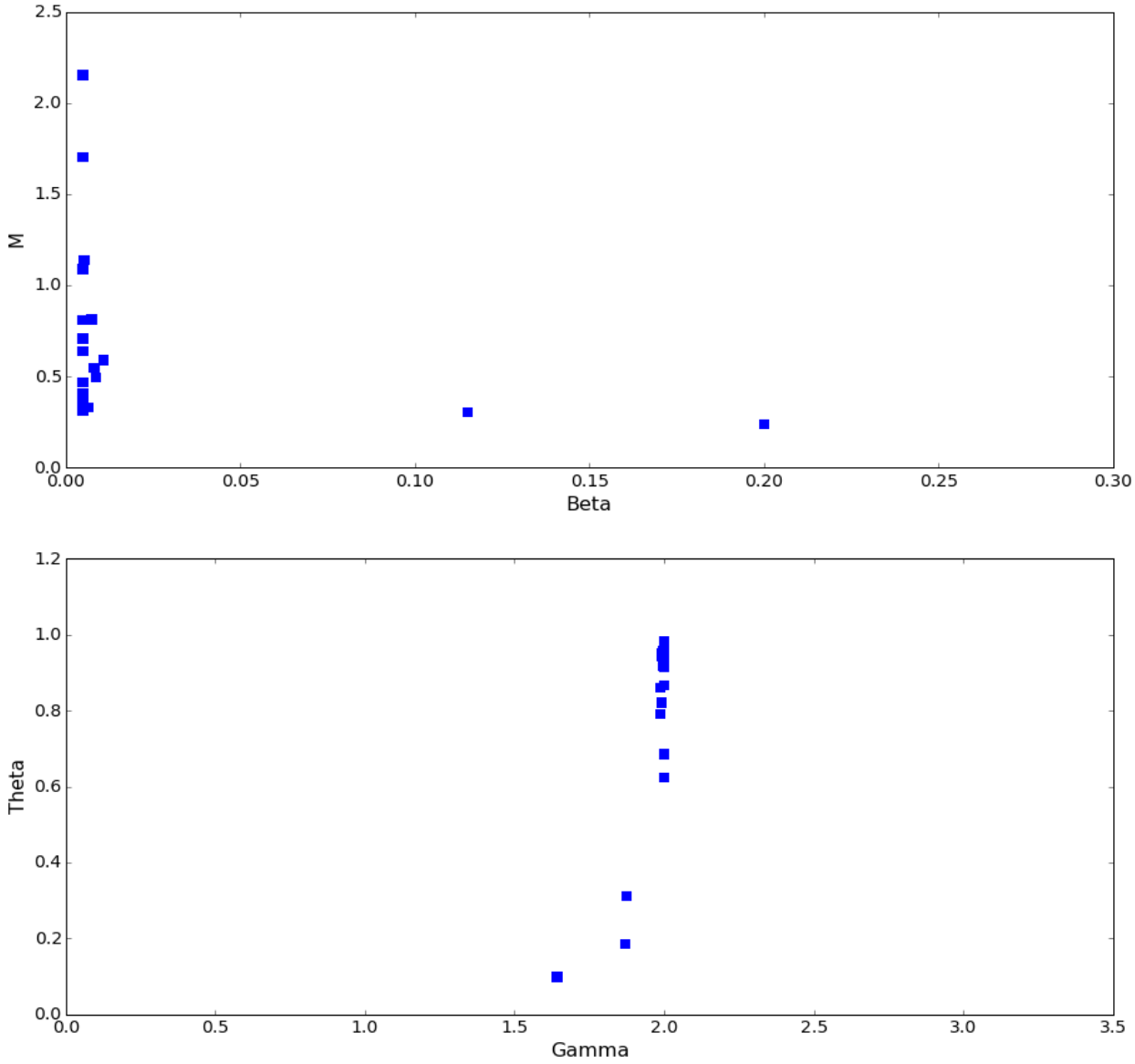

Figure 4 TN Parameter values identified using the GA-EBBW search

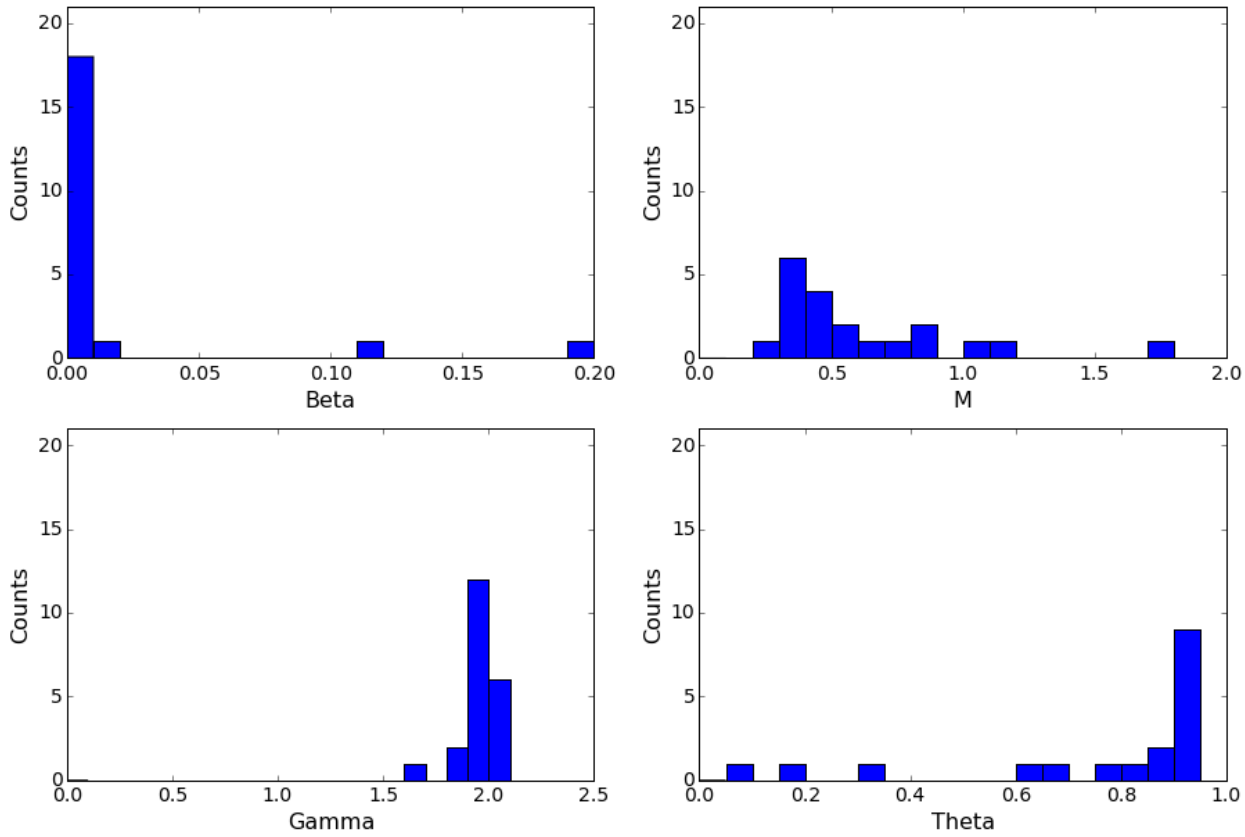

Figure 5 Distribution of the identified parameters for TN

While the 21 parameter combinations are highly variable, they were all identified through the optimization process, therefore, it is anticipated that they would perform similarly well in reproducing the observed data. Figure 6 plots the simulated EMC results using the 21 parameter combinations against the observed data. As shown, the predicted EMC results differ from each other between different parameter combinations, but in general they all perform well in mimicking the observed data, suggesting that they can all be considered calibrated parameters.

To further evaluate the model performance using the distinct parameter combinations, the simulated model results (21 scenarios) are compared with the observed data using boxplot as in Figure 7. The first plot in Figure 7 is for the observed data showing some extreme data points as outliers. It is observed that the model predicts a narrower range of EMC in comparison to the observed data, and in general, slightly over-predicts the median, 75th, and 25th percentile of the data.

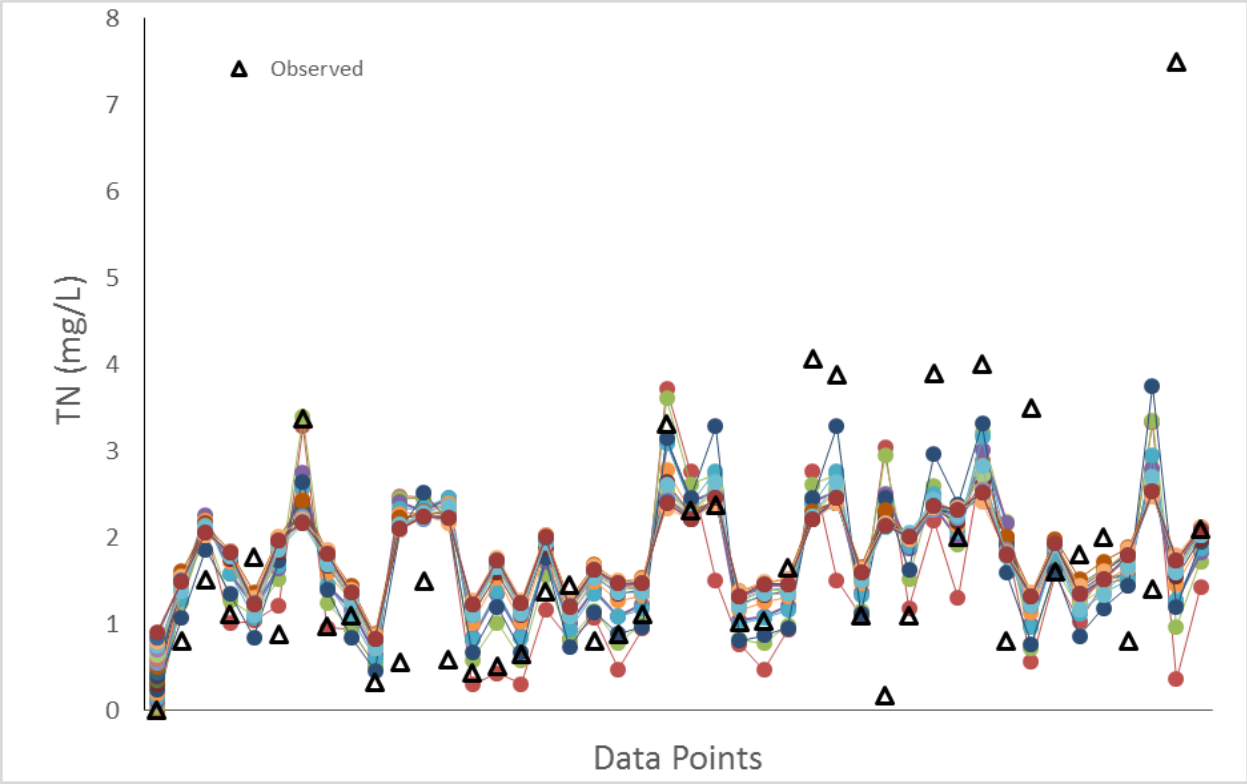

Figure 6 Comparing simulated TN EMC against observed values—point to point

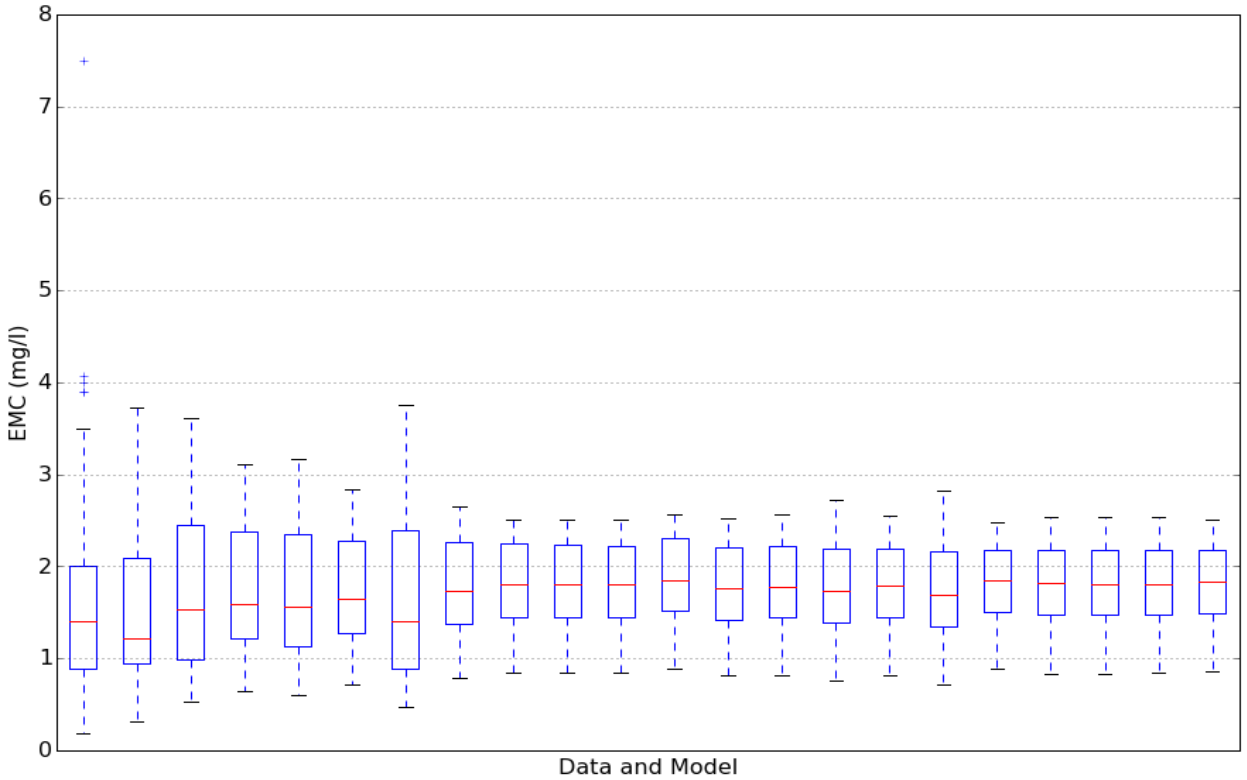

Figure 7 Comparing simulated TN EMC against observed values—boxplot

3.2 Result for TP

For each of the 21 GA-EBBW runs (each run with different initial condition), the parameter combination which results in the lowest RMSE for TP is identified, resulting in 21 parameter combinations as shown in Figure 8. Similar to that of TN, the buildup parameters for TP also show significant variability with the majority of the Beta values falling within a narrow range between 0.0 to 0.05, except for two parameters that have values of approximately 0.2. The variability in maximum accumulation storage M spans a near 10-fold range from about 0.03 to 0.3, though most of the values focus on the lower end below 0.1. Compared with the buildup parameters, the washoff parameters appear to be more evenly distributed, and both Gamma and Theta demonstrate similar range of variability. To gain further insight about the variability and distribution of the identified parameters for TP, Figure 9 plots the histograms of each of the four parameters. It is interesting to notice that M seems to follow a bell shape distribution for values under 0.1 if the two extreme values far on the right are not counted. Theta also shows a similar pattern if only the values between 0.6 to 1.2 are counted. For Gamma, the values tend to occur more frequently for the larger values, and most of the values focus on a narrow range between1.7 to 2.0. Beta values are heavily located at values below 0.01.

The performance of the TP EMC model using the optimally identified parameters is demonstrated in Figure 10 and 11, respectively. As shown by the point-to-point and boxplot comparison, the identified TP parameters allow the model to reasonably mimic the observed data, suggesting that they can all be considered calibrated parameters.

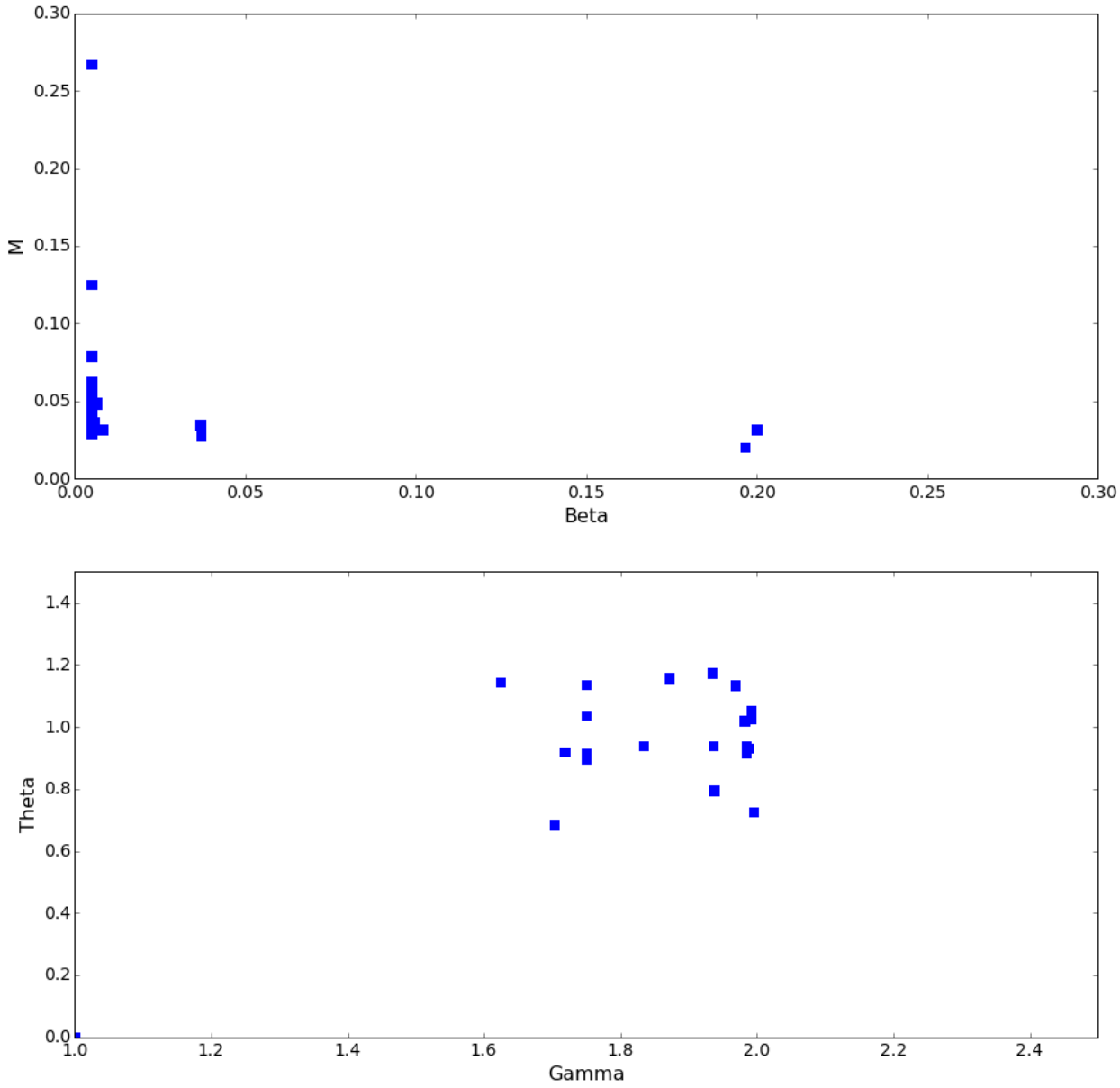

Figure 8 Parameter values identified using the GA-EBBW search for TP

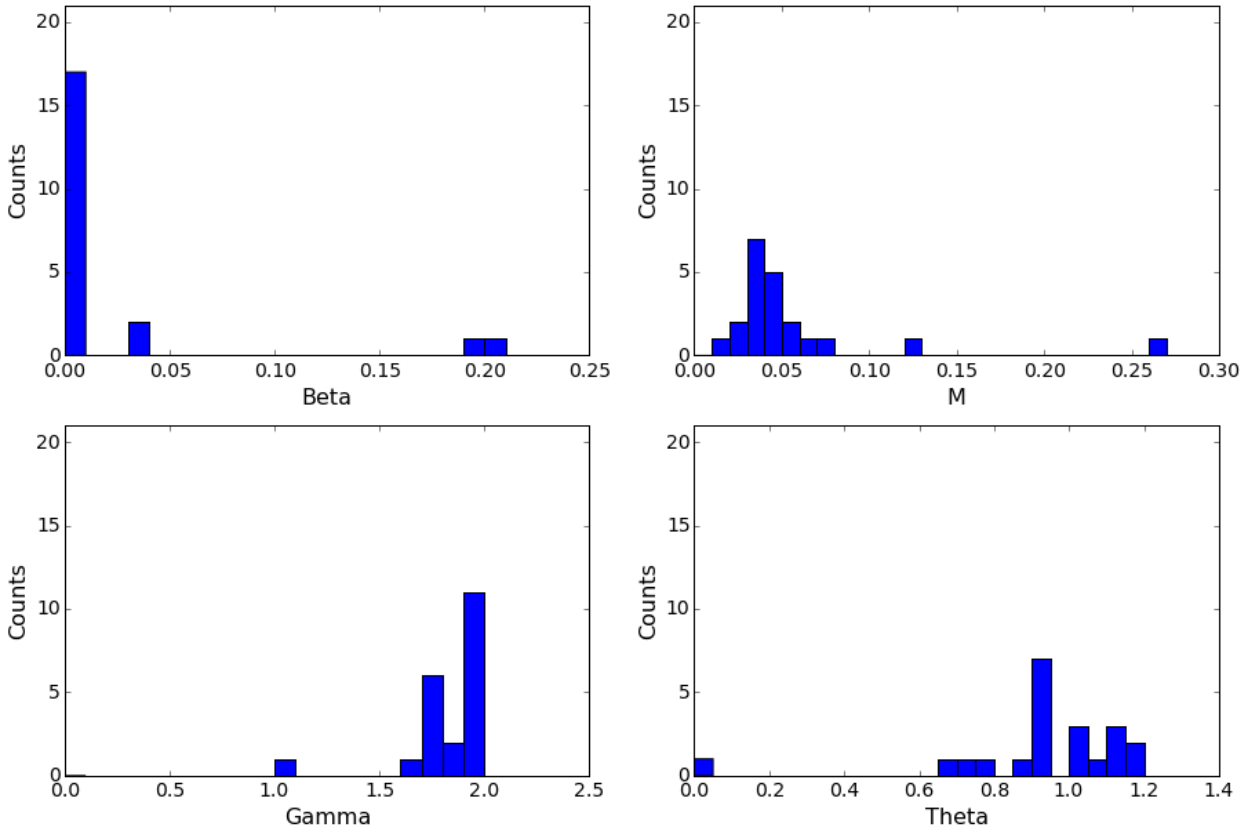

Figure 9 Distribution of the identified parameters for TP

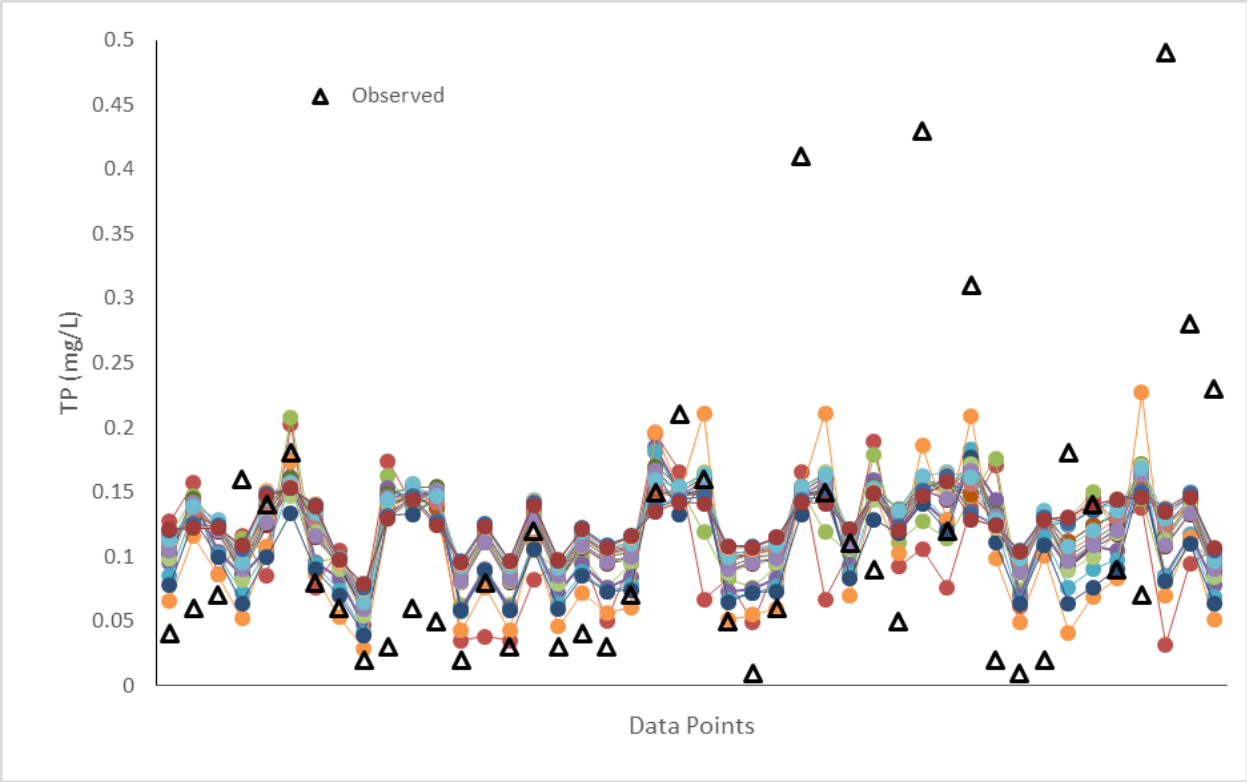

Figure 10 Comparing simulated TP EMC against observed values—point to point

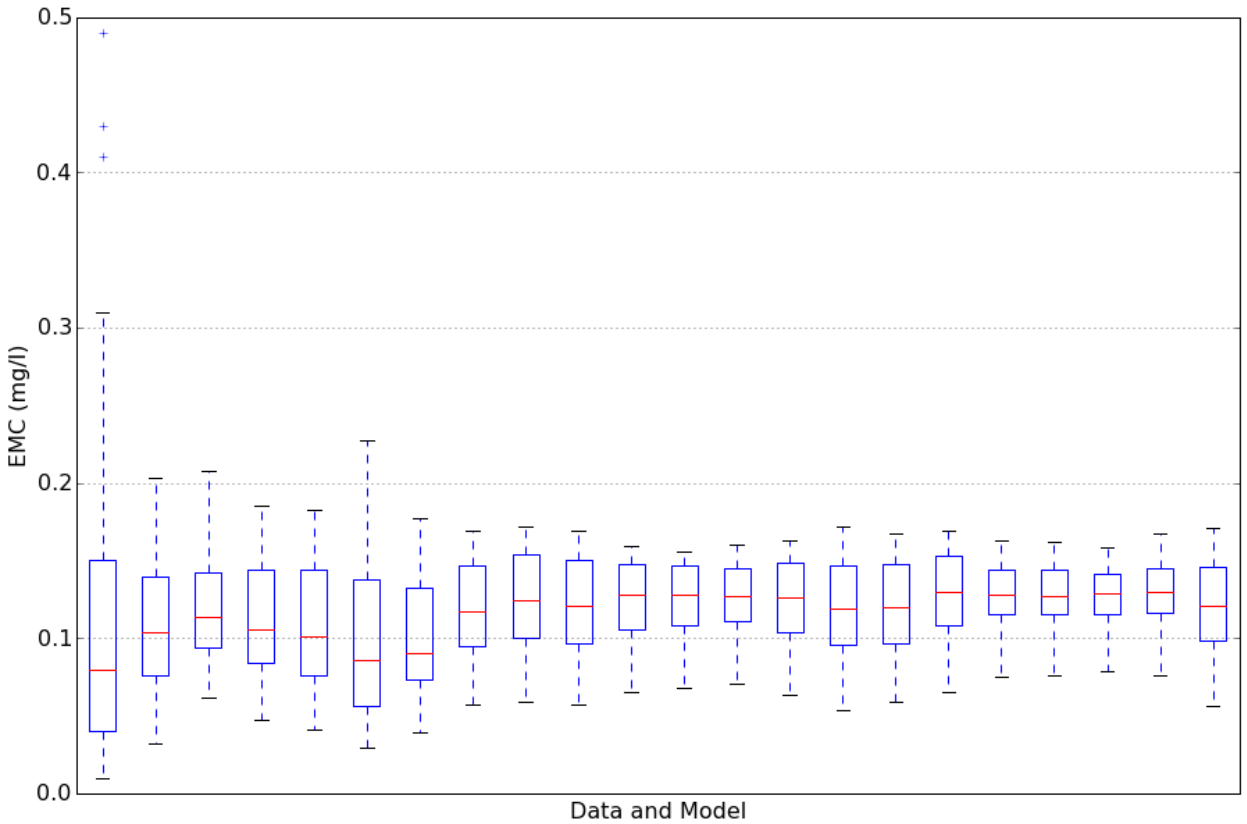

Figure 11 Comparing simulated TP EMC against observed values—boxplot

4. Robust Parameter Estimation

After applying the GA-EBBW modeling platform, 21 distinct parameter combinations were identified for predicting the TN and TP concentrations, and the previous section shows that all the parameters allow the model to reproduce the observed data reasonably well. Without further refinement, these parameters might be considered equally valid for being applied to a SWMM model for predicting stormwater associated pollutant loadings. In this section, however, an effort is made to further refine the parameters for more robust model prediction.

Considering that in the GA-EBBW process, the 21 parameters were identified using different assumption of initial condition, i.e., a particular set of parameters were identified which best reproduced the observed data with regard to the specific initial condition. As shown in the variability of the GA-EBBW results, the optimal parameter values are sensitive to the initial condition, therefore, the parameter identified under a specific initial condition might not work well for another initial condition. Due to lack of data to accurately quantify the initial condition for each event used in the model calibration, therefore, it is desired to identify the parameters which not only work for the specific initial condition used for the GA-EBBW process, but also work well for other initial conditions, i.e., to identify robust parameter sets which would work well under all or most of the conditions.

In order to achieve this goal, the 21 parameters were applied to all the 21 initial conditions to predict 441 sets of model results for each pollutant, and each of the results was compared with the observed data to obtain the corresponding RMSE. The results are described below.

4.1 Robust Parameter Identification for TN

Figure 12 plots the distribution of simulated error of the 21 parameters with regard to the 21 initial conditions (R_N0), and the parameter set is marked by its corresponding initial condition (0.0 to 1.0). For example, the parameter set at 0.2 means it was obtained through the GA-EBBW process with initial storage equal to 20% of the maximum storage. As shown in the preceding section, while it was not easy to differentiate the performance of those parameter sets through comparing their accuracy in reproducing the observed data, it is clear that some of the parameters behave significantly more robustly than the others. For example, while the parameter identified at 10% of the maximum storage works well for the corresponding initial condition, the prediction error using this parameter increases rapidly when the actual initial condition departs from 10%, suggesting that this particular set of parameters is not robust, and that to apply it to predict long term loadings can lead to significant uncertainties, given the high chance that the real initial condition would be different from the 10%.

Figure 12 also shows a pattern that the error is approximately lowest from the left bottom to the right upper corner following the diagonal line. This is easy to understand since the diagonal line represents the model RMSE for runs where parameter values and initial condition are matched, i.e. the parameter identified for initial condition of 0.2 is applied to the initial condition of 0.2, and the parameter identified for initial condition of 0.5 is applied to the initial condition of 0.5. Even with this pattern, it can be observed that the right part of the error surface is pretty flat,

suggesting that when these parameters are applied to simulate the entire range of initial conditions, the resulting errors are similar to the least error. Therefore, these parameters can be considered robust.

While Figure 12 seems to indicate that the parameters identified with low initial condition are not robust, this is not exactly the case, since the parameter identified with initial condition equal to 0.0 is also robust, as shown in Figure 13.

Apparently, the candidates for the final calibration parameters should be those producing the flat plains on the error surface plots, which are identified and plotted in Figure 14. Compared with Figure 4, it can be seen that the 13 robust parameter sets in Figure 14 show less variability than the entire parameter set of 21 individuals. For example, the maximum storage M is now highly concentrated around value 0.5 lb/acre. Interestingly, the variability in terms of Beta remains similar between the entire set and the robust set, suggesting that the entire range of the originally estimated Beta values are robust.

As for the washoff parameters, the robust set in Figure 14 covers the two extreme ends of combinations of the entire set. This phenomenon is of particular interest because in some previous studies, modelers attempted to obtain multiple sets of parameter values and then apply the average of the parameters as the final parameters. However, as shown in Figure 4 and 14, while the parameters located at the two ends of the parameters ranges are robust, those values in between actually are not robust and should be discarded. Therefore, it is not desired to apply the approach of averaging multiple parameter values in developing parameter values for model prediction.

Although it appears from visually inspecting Figure 14 that all the robust buildup parameters belong to three groups, and washoff parameters belong to two or three groups, it is not straightforward to categorize them based on the visual inspection because the four parameters are interactively linked, i.e. two buildup parameter sets in group 1 might respectively be associated with washoff parameter group 1 and 2. Therefore, to further identify the patterns in the robust parameters, a pattern recognition method needs to be applied.

In this study, we apply the k-means clustering algorithm to classify the parameters into four groups, where parameters in each of the groups represent a parameter pattern. Figure 15 plots the resulting parameter classes, with different colors for different classes. As can be seen, the buildup parameters dominate the differentiation between different parameter patterns for classes I to III, while the washoff parameters dominate that for class-IV. The distribution of parameters in each of the classes is shown in Table 1.

Based on the clustering analysis result, the final representative parameters for conducting future long term simulation analysis can be identified as the one parameter set from each of the four classes with the least mean RMSE and included in Table 2. The four parameter combinations can be used for uncertainty-based prediction analysis to obtain a range of prediction of pollutant loadings which reflect the parameter pattern uncertainty.

Table 1. Identified parameter patterns for the TN buildup-washoff model

Class ID	Beta	M	Gamma	Theta	Mean RMSE
I	0.0050	0.6408	1.9995	0.9453	1.6934
I	0.0109	0.5894	1.9921	0.9529	1.6061
I	0.0088	0.4952	1.9958	0.9180	1.5513
II	0.1152	0.3039	1.9978	0.9590	1.4260
III	0.0050	0.4670	2.0000	0.9162	1.5477
III	0.0051	0.4005	1.9884	0.8604	1.5362
III	0.0050	0.4063	1.9998	0.9230	1.5345
III	0.0066	0.3293	1.9905	0.8205	1.5365
III	0.0050	0.3922	2.0000	0.9816	1.5485
III	0.0050	0.3456	1.9990	0.9390	1.5629
III	0.0050	0.3267	2.0000	0.9387	1.5783
III	0.0050	0.3129	1.9922	0.9431	1.5948
IV	0.2000	0.2375	1.6418	0.0983	1.4525

Table 2. Final calibrated parameters for the TN buildup-washoff model

Beta	M	Gamma	Theta	Mean RMSE
0.0088	0.4952	1.9958	0.9180	1.5513
0.1152	0.3039	1.9978	0.9590	1.4260
0.0050	0.4063	1.9998	0.9230	1.5345
0.2000	0.2375	1.6418	0.0983	1.4525

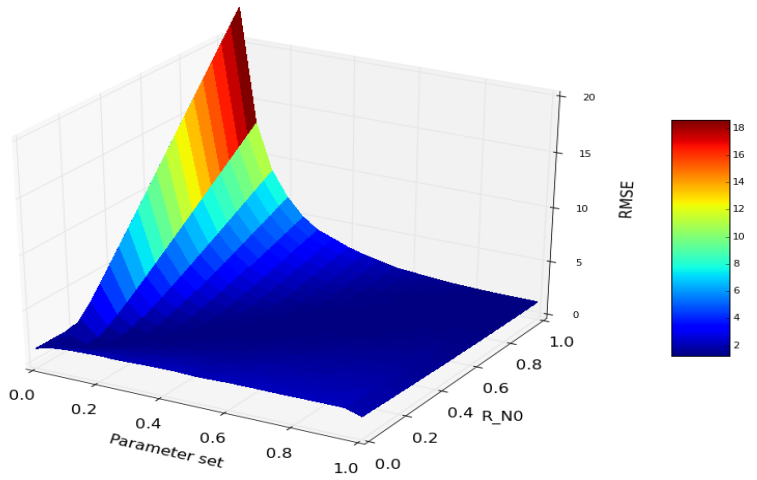

Figure 12 Simulation error surface for TN

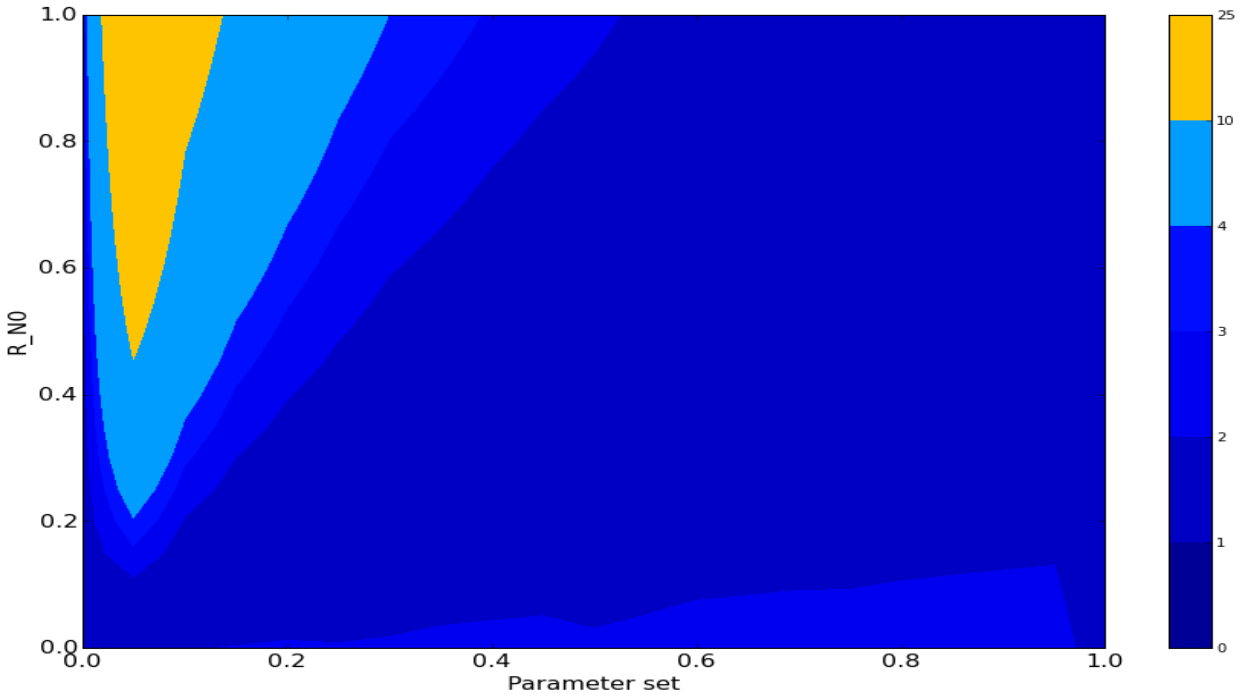

Figure 13 Simulation error contour for TN

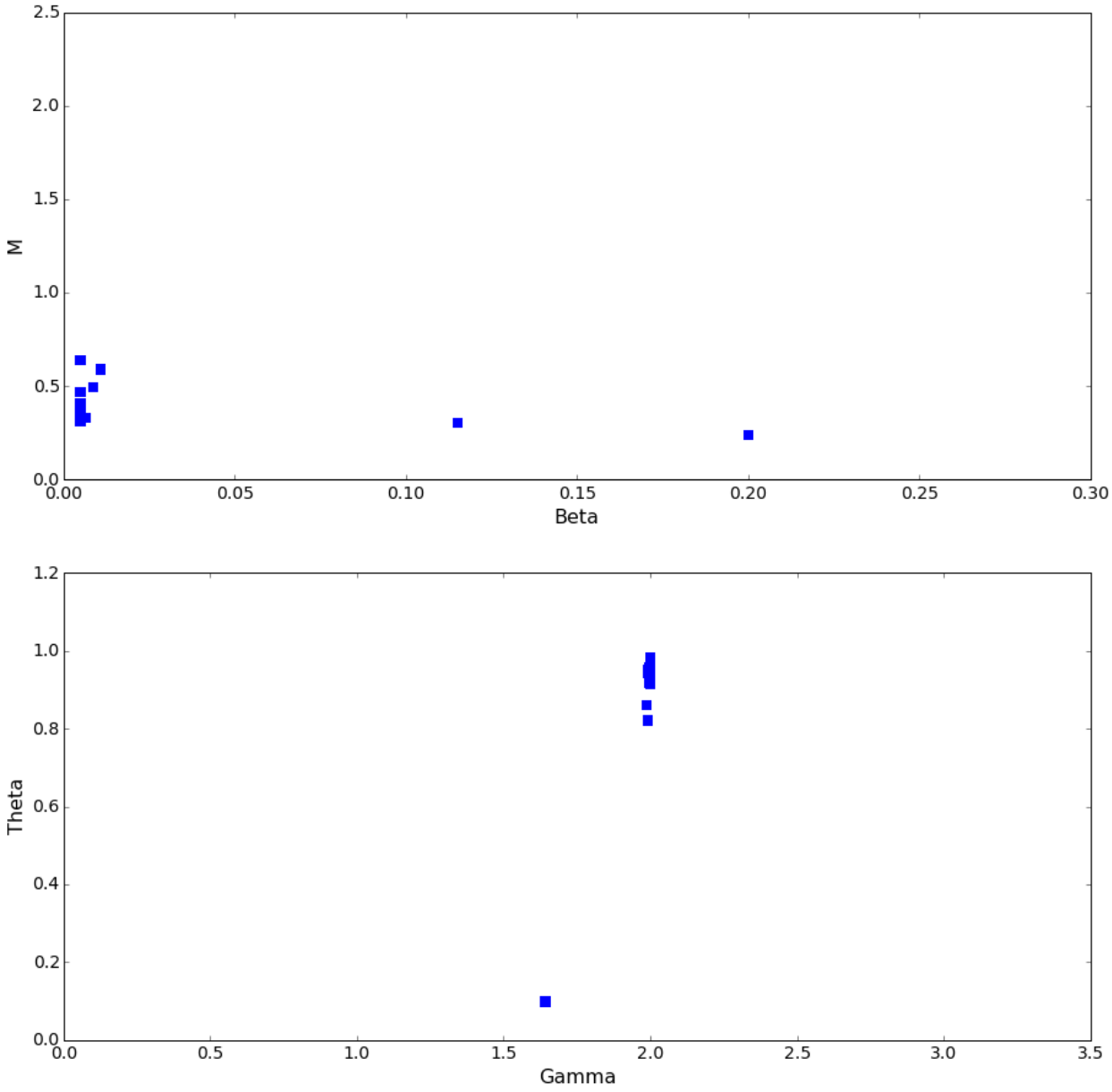

Figure 14 Robust parameter values identified for TN

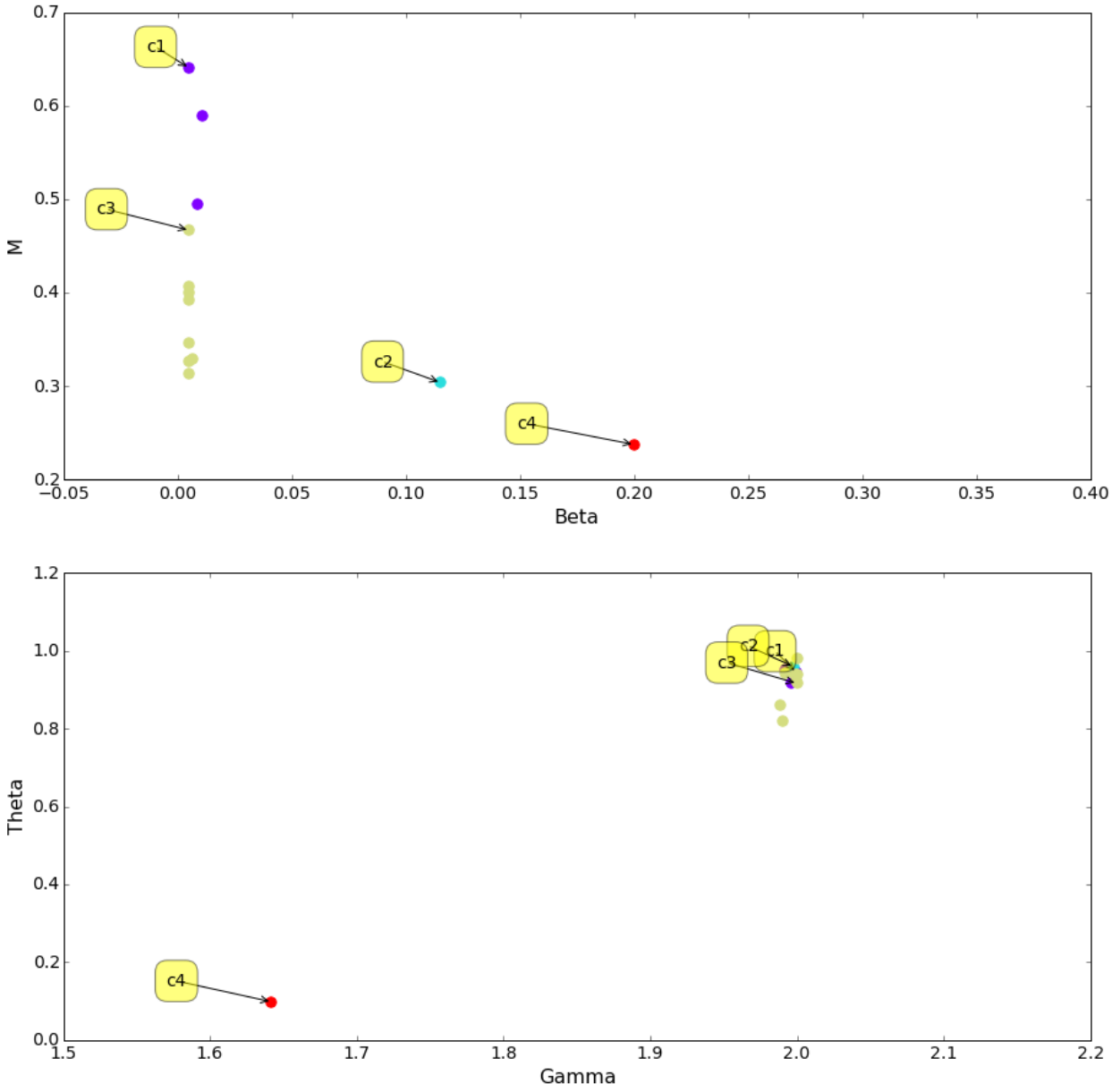

Figure 15 Clustered parameter patterns for the TN model

4.2 Robust Parameter Identification for TP

Figure 16 plots the distribution of simulated error of the 21 parameters with regard to the 21 initial conditions (R_N0) for TP. Same as for the case of TN, the parameters identified for TP also demonstrate significant variability in robustness. For example, while the parameter identified at 10% of the maximum storage works well for the corresponding initial condition, the prediction error using this parameter would increase rapidly when the actual initial condition departs from 10%, suggesting that this particular set of parameters is not robust, and to apply it to predict long term loadings could lead to significant uncertainties as there would be high chances that the real initial condition would be different from the 10%.

Figure 16 also shows the that the right part of the error surface is flat, suggesting that when these parameters are applied to simulate the entire range of initial conditions, the resulted errors are similar to the least error. Therefore, these parameters can be considered robust. It is interesting to notice that the error surfaces for TN and TP share the similar pattern, that is, there is a ridge of high simulation error for the parameters identified for low and medium-low initial conditions. However, at the low end (R_N0=0.0) and higher values (R_N0>0.5), the surface becomes flat for both TN and TP. The reason of such a common pattern is unknown, and future research might be needed to further investigate the underlying cause of such a robustness distribution pattern.

Using the same approach as in the case of TN, the 14 candidates for the final calibration parameters for TP are located in the plain areas on the error surface plots. These 14 parameters are shown in Figure 18. Compared with Figure 8, it can be seen that the 14 robust parameter sets show less variability than the entire parameter set. For example, the maximum storage M is now highly concentrated around value 0.05 lb/acre. Interestingly, the variability in terms of Beta remain similar between the entire set and the robust set, suggesting that the entire range of the originally estimated Beta values are robust. This phenomenon is, again, similar to that of TN.

As for the washoff parameters, the robust set in Figure 18 covers the similar area as the entire set, though those parameters with lower Theta values are eliminated due to their lack of robustness.

Results of applying the k-means clustering algorithm to classify the TP parameters into four groups are shown in Figure 19. As can be seen, the buildup parameters dominate the differentiation between different parameter patterns for classes II, III, and IV, while both the buildup and washoff parameters dominate that for class I. The distribution of parameters in each class are shown in Table 3.

Table 3 Identified parameter patterns for the TP buildup-washoff model

Class ID	Beta	M	Gamma	Theta	Mean RMSE
I	0.0050	0.0479	1.9844	0.9375	0.1368
I	0.0050	0.0510	1.9921	1.0502	0.1294
I	0.0066	0.0487	1.7500	1.0352	0.1243
I	0.0065	0.0478	1.9687	1.1328	0.1213
II	0.0050	0.0371	1.9824	1.0179	0.1202
II	0.0058	0.0365	1.8720	1.1564	0.1204
II	0.0050	0.0352	1.7500	1.1355	0.1214
II	0.0370	0.0346	1.6250	1.1430	0.1176
II	0.0085	0.0313	1.9351	1.1718	0.1223
III	0.0050	0.0289	1.9843	0.9130	0.1195
III	0.0372	0.0275	1.7499	0.9146	0.1145
III	0.0058	0.0313	1.9920	1.0261	0.1193
IV	0.2000	0.0313	1.8338	0.9375	0.1121
IV	0.1966	0.0197	1.9882	0.9301	0.1087

Based on the clustering analysis result, the final representative parameters for conducting future long term simulation analysis can be identified as the one with the least mean RMSE. These parameter sets are included in Table 4. The four parameter combinations can be used for uncertainty-based prediction analysis to obtain a range of prediction of pollutant loadings which reflect the parameter pattern uncertainty.

Table 4 Final calibrated parameters for the TP buildup-washoff model

Beta	M	Gamma	Theta	Mean RMSE
0.0065	0.0478	1.9687	1.1328	0.1213
0.0370	0.0346	1.6250	1.1430	0.1176
0.1966	0.0197	1.9882	0.9301	0.1087
0.0372	0.0275	1.7499	0.9146	0.1145

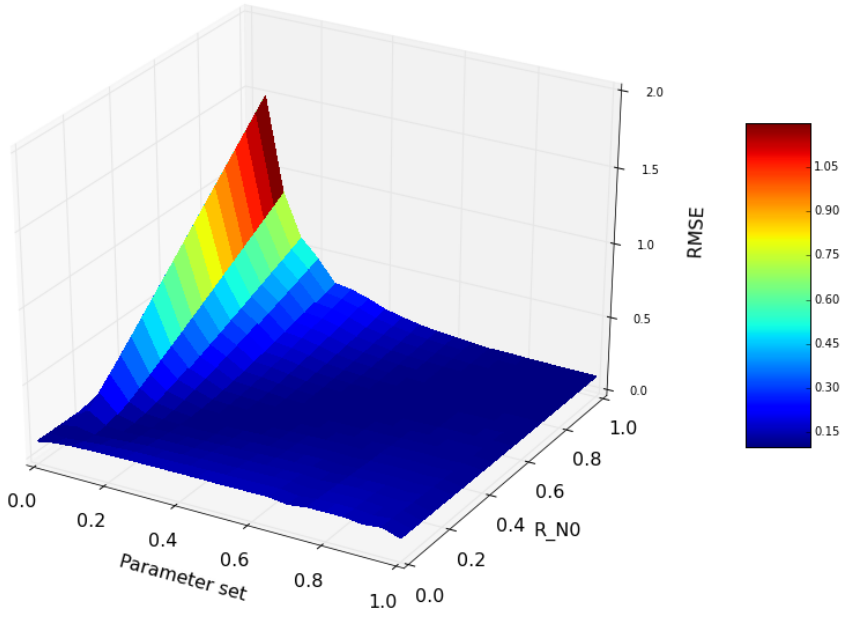

Figure 16 Simulation error surface for TP

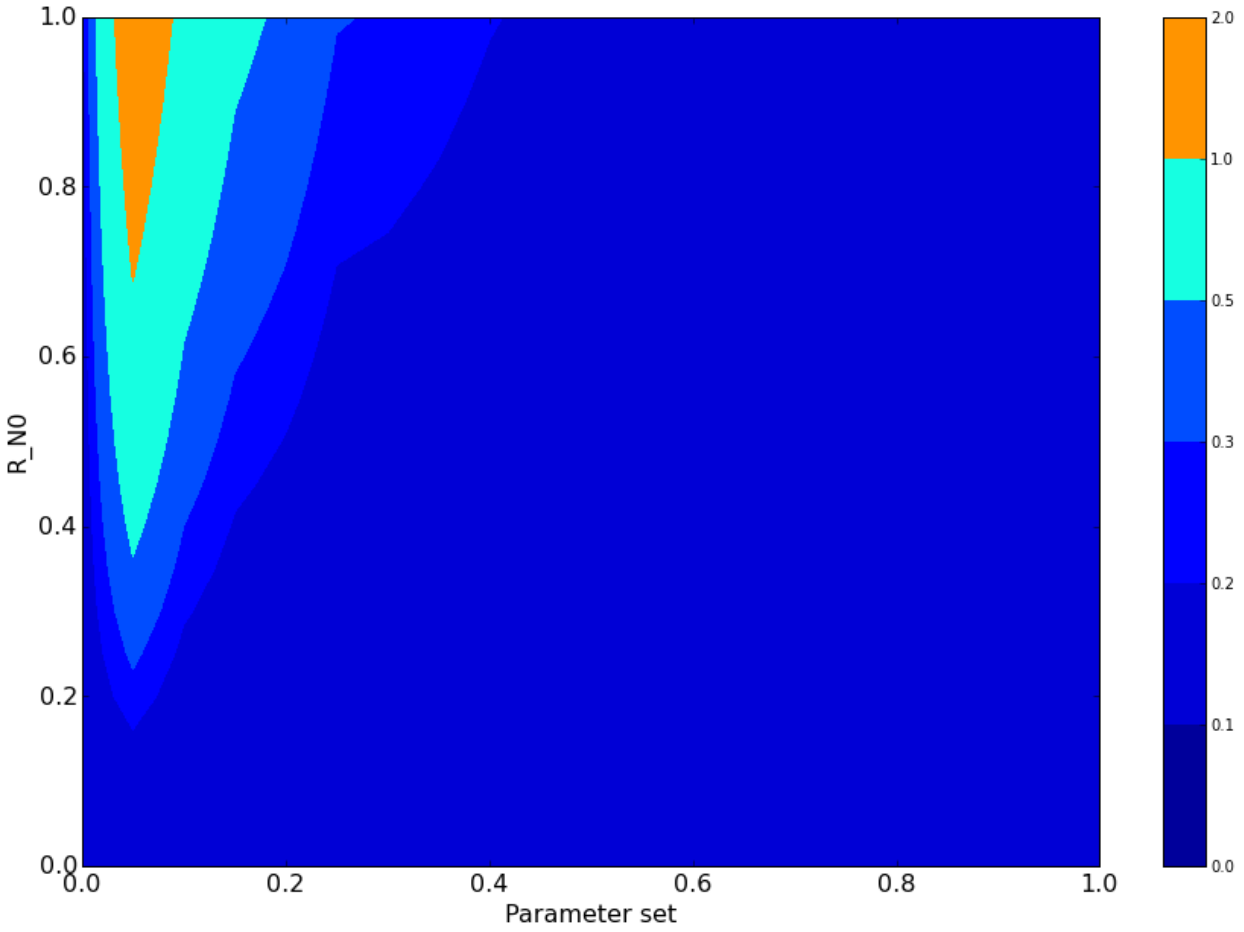

Figure 17 Simulation error contour for TP

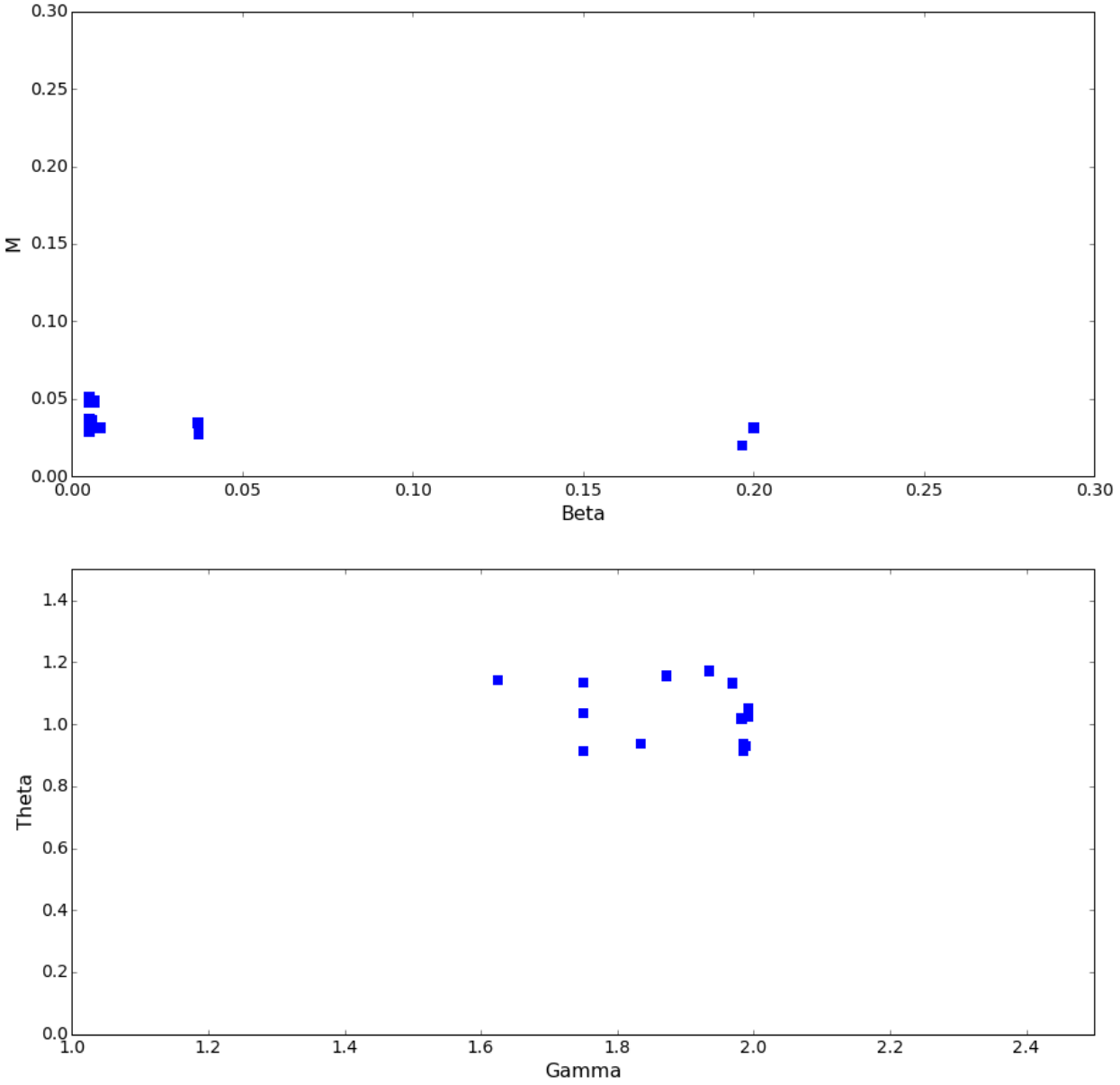

Figure 18 Robust parameter values identified for TP

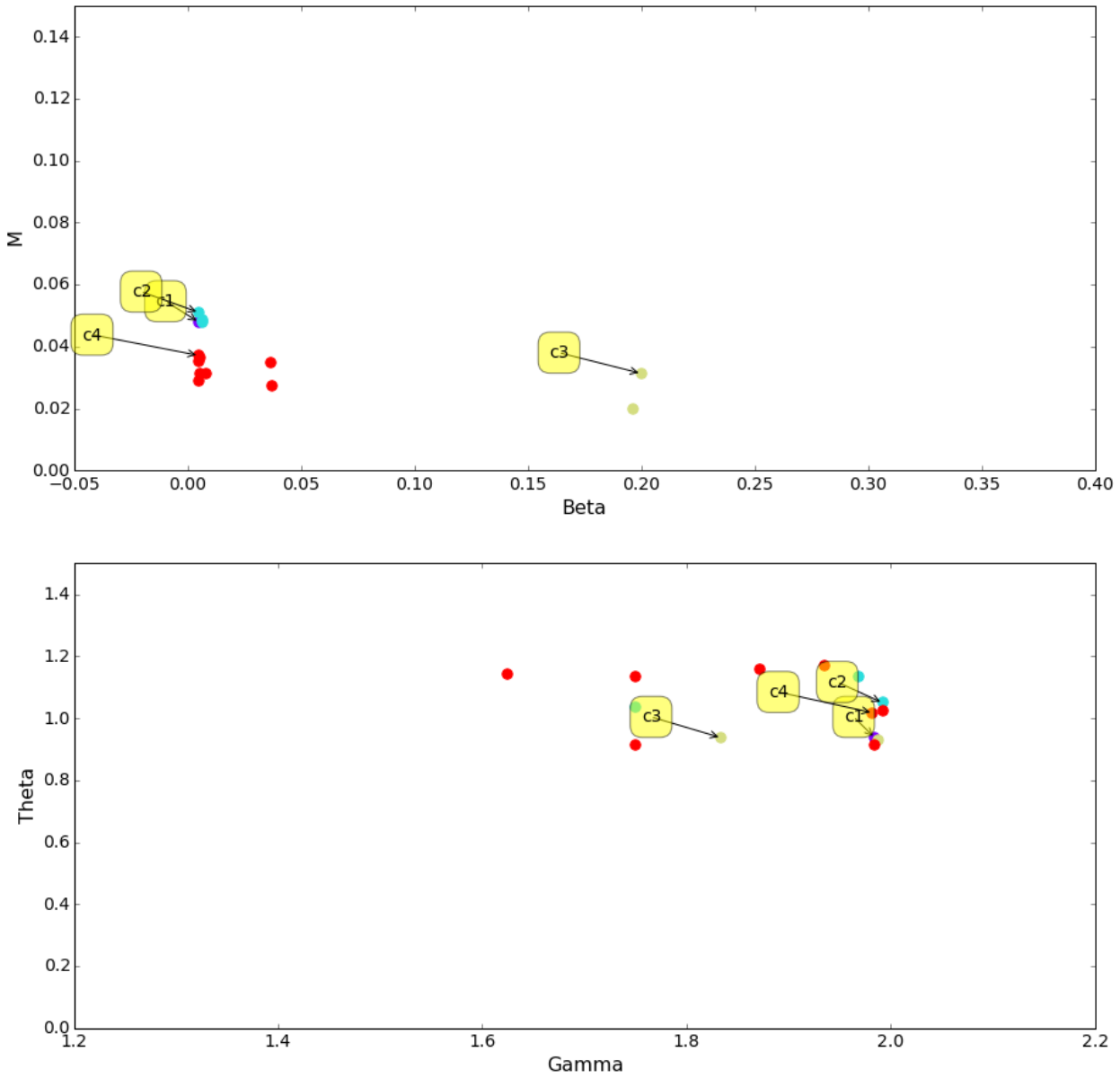

Figure 19 Clustered parameter patterns for the TP model

5. Develop Long-term Continuous Hourly Timeseries for Impervious Land Uses

The parameter set resulting in the lowest mean RMSE value (Table 2 for TN and Table 4 for TP) was selected as a calibrated parameter set for developing the long term continuous hourly timeseries for impervious land uses.

This particular set of parameters for TN is: Beta=0.115, M=0.304, Gamma=1.998, and Theta=0.959

This particular set of parameters for TP is: Beta=0.1966, M=0.0197, Gamma=1.988, and Theta=0.930

Due to the limited observed dataset from 100% impervious land covers, the observed data was not differentiated for land use types, and instead, the calibration was performed on a generic impervious land use category. A scaling factor was introduced to the maximum buildup possible under different impervious land use categories to further calibrate the annual average loading rates for TN and TP for developing the long-term timeseries. The continuous hourly simulation for 23 years (1992 to 2014) was performed using the selected calibrated buildup and washoff parameters in SWMM model. Figure 20 and Figure 21 show the box and whisker plots for the simulated annual loading rates for TN and TP, respectively, over 23 years. The green line shows the annual average value from the entire simulation period which is also the annual load export rate target. For comparison purposes, the selected calibrated buildup and washoff parameters were also simulated for 23 years without changing the maximum buildup capacity, and are shown in the box and whisker plot as the "calibrated impervious" category. The long term simulation results show that using the calibration parameters "as is" align well with the TP loading rates for open land impervious surface and low density residential impervious areas, but produce lower annual average loads for TN. The statistical results (min, 25th percentile, median, mean, 75th percentile, and maximum) in box and whisker plots show a similar trend between the calibrated impervious land and the other impervious land categories after applying the scaling factor to meet the land use-specific annual average load export rate target.

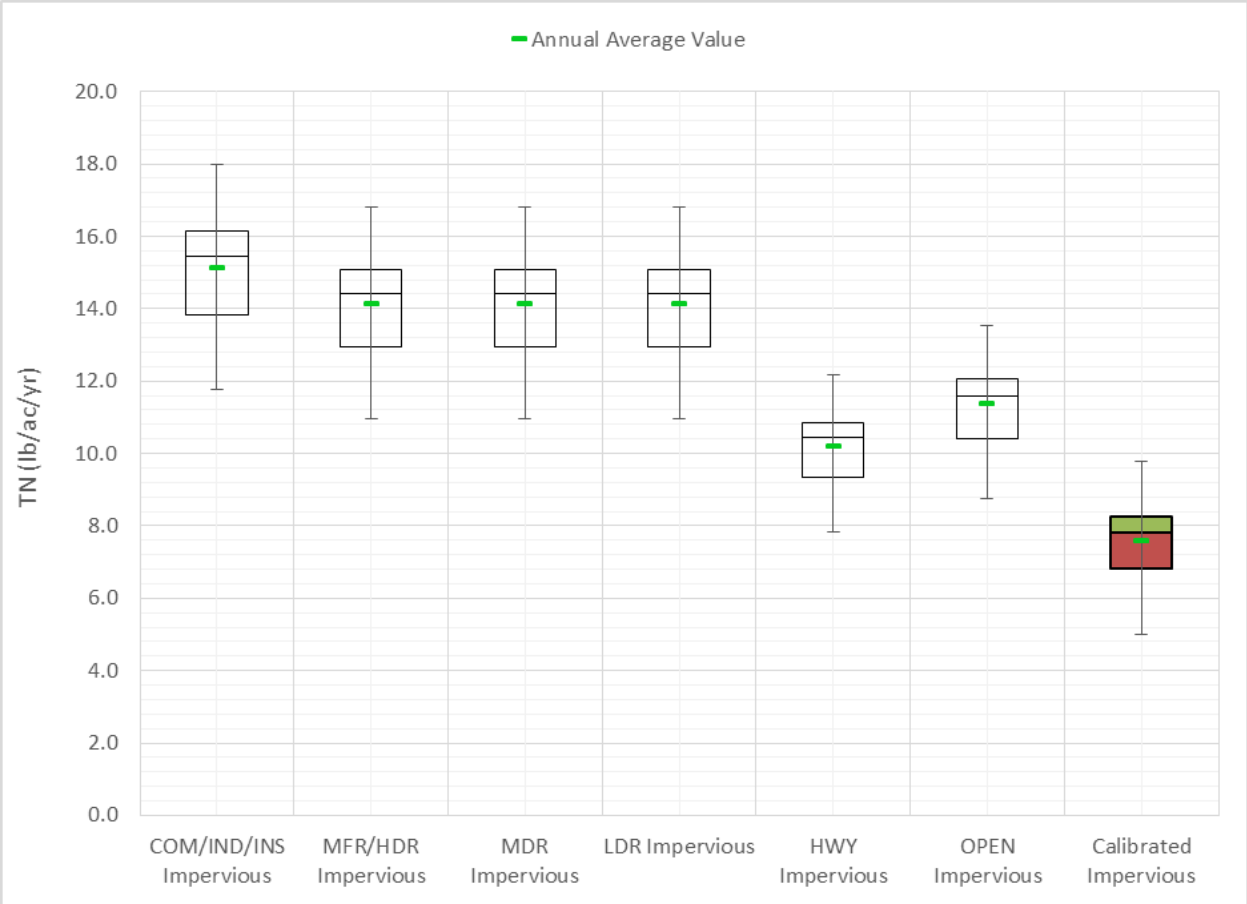

Figure 20 Box and Whisker plot for TN annual export rates in the continuous simulation model

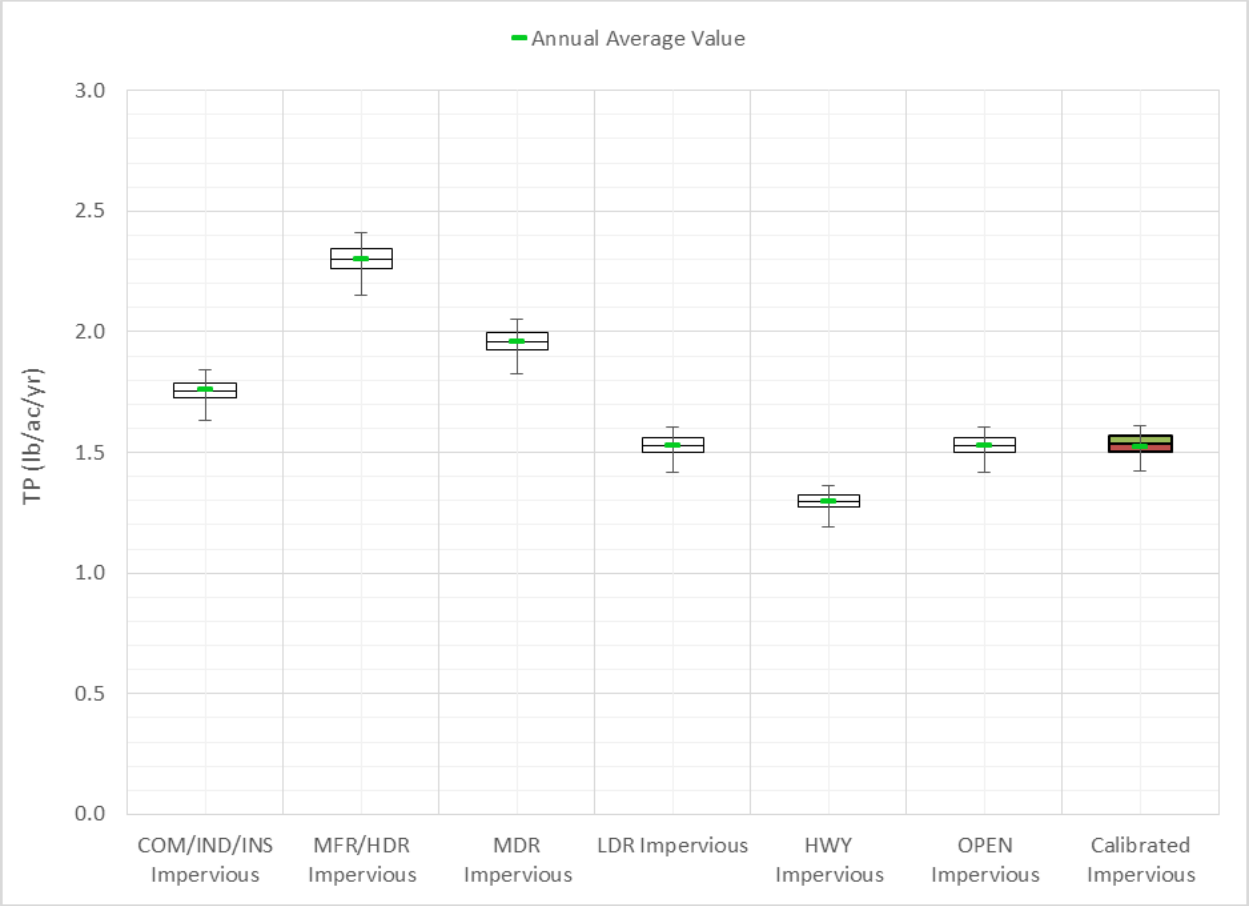

Figure 21 Box and Whisker plot for TP annual export rates in the continuous simulation model

MEMORANDUM (DRAFT)

Tetra Tech, Inc.
10306 Eaton Place, Suite 340
Fairfax, VA 22030
Telephone (703) 385-6000
Fax (703) 385-6007

Date: December 10, 2015

To: Mark Voorhees, EPA Region I

From: Guoshun Zhang, Khalid Alvi – Tetra Tech

Subject: BMP performance calibration approach sensitivity analysis

---

Task 10 of WA 4-35 requires that Tetra Tech conduct a sensitivity analysis of the long-term cumulative BMP performance estimates with regard to BMP model calibration approaches. The overall goal of the task is twofold: 1) to explore how factors such as rainfall event magnitude, inter-event dry days, seasons, and the number of calibration events could impact the development of long-term performance curves, and 2) to serve as a reference point for similar calibration efforts. Task 10 is set to investigate gravel wetland and biofiltration with internal storage reservoir (ISR) or enhanced biofiltration for nutrient pollutants (Total Nitrogen and Total Phosphorus). All the monitored BMP performance data in this memo are from the University of New Hampshire Stormwater Center (UNHSC).

This memorandum documents the sensitivity analysis results of BMP performance calibration methods. The steps of rainfall event selection, BMP calibration, and performance curve generation and comparison, and the final recommendations are discussed.

1. Overview of the Sensitivity Analysis Strategy

An overview of the sensitivity analysis strategy is shown in Figure 1. As shown, the sensitivity analysis starts with analysis of the available monitored data. Based on the data review, candidate events are selected for three calibration methods. In the first calibration method, three to five candidate events are selected, and the BMP hydrologic and water quality performances are calibrated against the observed data. The calibrated BMP parameters are then checked for cumulative performances against the observed data, and then used for generating the long-term BMP performance curves. The long-term time series (1/1/1992 to 12/31/2014) used for the BMP performance curve generation are the latest set of time series that reflect nutrient loadings from typical land uses in the Region. Based on previous TMDL implementation knowledge, the BMP performance curves are generated for only one type of impervious (*Commercial_Impervious*) in this study, as the BMP performance curves from various impervious surfaces tend to follow a similar trend.

Similarly to the first calibration method, the calibration efforts were carried out for calibration method two and three, in which the calibration events were increased from eight to twelve and nine to fifteen, respectively. A set of BMP performance curves was also generated following each calibration method.

A final review of the calibration cumulative performances against the observed data and the BMP performance curves yields a recommended set of BMP performance curves, and a procedure of

developing BMP performance curves is also recommended. Details of the sensitivity analysis strategy are discussed in sections that follow.

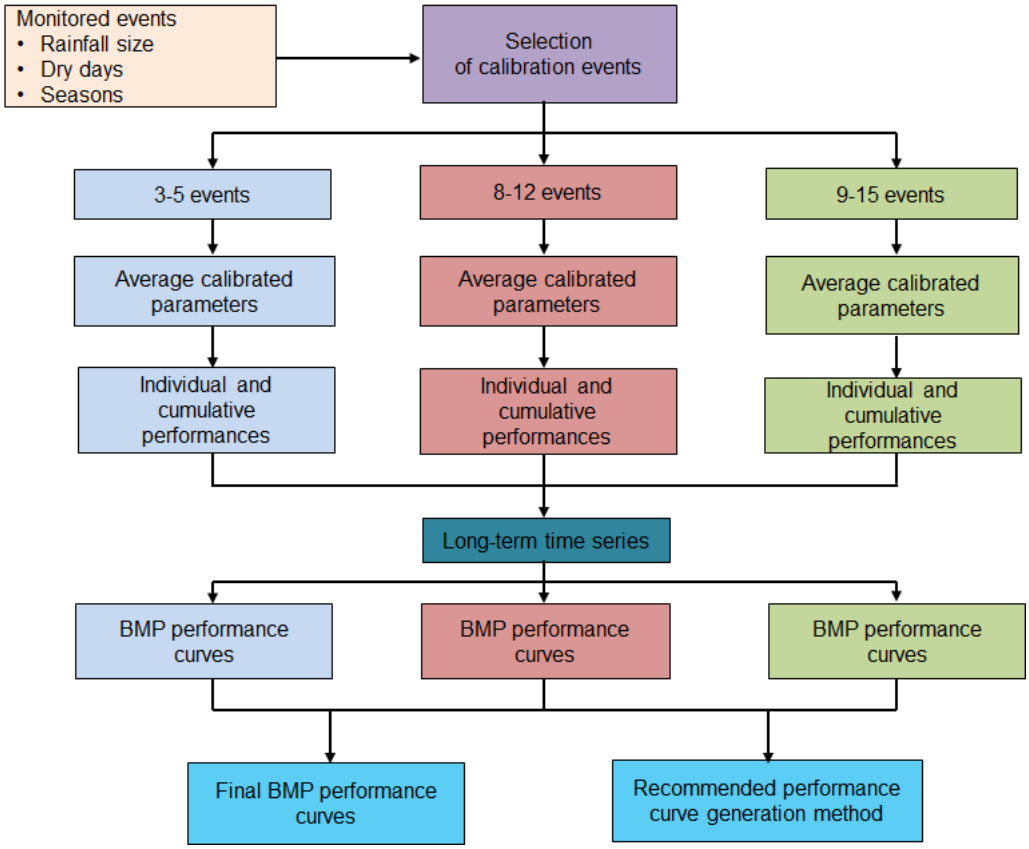

Figure 1. Overview of sensitivity analysis regarding BMP performance calibration approaches.

2. Evaluation of Monitored Rainfall Data

In this step, monitored events for gravel wetland and biofiltration with ISR were compiled and analyzed. For gravel wetland, there are a total number of 49 recorded events, and 30 for the biofiltration with ISR. Information about rainfall depth, antecedent dry period, inflow and outflow pollutant concentrations from gravel wetland and biofiltration with ISR can be found in the attached table. For some of the events, data for only one pollutant were available. The rainfall events to be used for the calibration process were selected from the candidate events. All 49 events form the cumulative performance validation dataset for gravel wetland, and similarly all 30 events for the biofiltration with ISR. For the purpose of developing a continuous and complete validation dataset, median inflow EMCs for the whole observed dataset for either TP or TN were assumed for events that are missing inflow EMC information for TP or TN.

During the data review process, events that did not have both TN and TP monitored performances at the same time were removed from the candidate list for selecting calibration events.. After the data reviewing process, 14 monitoring events were selected for the gravel wetland and 14 for the biofiltration with ISR. The list of events are shown in Table 1 and Table 2.

Table 1. List of gravel wetland candidate monitoring events.

Date	Rainfall Depth (in)	Peak Intensity (in/5-min)	Antecedent Dry Period (days)
6/4/2008	0.40	0.02	3
4/3/2009	0.79	0.11	3
4/6/2009	1.07	0.07	2
5/5/2009	0.72	0.03	12
6/18/2009	1.47	0.09	3
8/22/2009	0.76	0.38	8
9/11/2009	0.95	0.06	12
9/27/2009	0.51	0.02	14
11/20/2009	0.42	0.01	5
4/16/2010	1.16	0.04	6
6/10/2010	0.67	0.04	3
6/23/2010	0.29	0.02	12
7/21/2010	0.45	0.23	6
9/16/2010	0.49	0.03	3

Table 2. List of biofiltration with ISR candidate monitoring events.

Date	Rainfall Depth (in)	Peak Intensity (in/5-min)	Antecedent Dry Period (days)
11/10/2011	0.98	0.06	10
6/22/2012	0.71	0.20	8
7/17/2012	0.19	0.08	1
8/10/2012	0.53	0.07	4
9/8/2012	0.26	0.08	2
11/17/2013	0.27	0.04	6
6/25/2014	0.87	0.11	11
7/13/2014	0.19	0.07	3
07/27/2014	0.39	0.12	2
7/31/2014	0.12	0.03	2
9/2/2014	0.56	0.12	19
9/13/2014	0.12	0.01	5
10/4/2014	0.21	0.02	2
11/1/2014	0.35	0.01	8

3. First Calibration Approach

3.1 Gravel Wetland

In the first calibration approach for gravel wetland, four calibration events were selected, with at least one event for each season (spring, summer, and fall), and with varying magnitudes of storm

sizes (0.42 inch to 1.47 inch). The events used for gravel wetland calibration are shown in Table 3.

Table 3. List of gravel wetland candidate monitoring events following the first calibration approach.

Date	Rainfall Depth (in)	Peak Intensity (in/5-min)	Antecedent Dry Period (days)	Removal Efficiency (RE)	
				TN	TP
6/18/2009	1.47	0.09	3	11%	-150%
9/27/2009	0.51	0.02	14	-125%	75%
11/20/2009	0.42	0.01	5	31%	75%
6/10/2010	0.67	0.04	3	30%	95%

Individual SUSTAIN models were set up for the gravel wetland. For each event, the models were first calibrated for the hydrology, and then were calibrated to match the event mean concentration predictions for TN and TP, separately. The calibrated TN and TP performances are shown in Tables 4 and 5 below, with the calibrated parameters summarized at the end of the tables.

Table 4. Summary of calibration results for TN for gravel wetland following the first calibration approach.

Calibration events			**Values**
6/18/2009	Observed EMC (mg/L)	Inflow	0.9
		Outflow	0.8
	SUSTAIN prediction	Calibrated outflow	0.81
		Decay	0.03
		Perct. removal	0.12
9/27/2009	Observed EMC (mg/L)	Inflow	0.8
		Outflow	1.8
	SUSTAIN prediction	Calibrated outflow	1.8
		Decay	-0.08
		Perct. removal	0.05
11/20/2009	Observed EMC (mg/L)	Inflow	1.60
		Outflow	1.10
	SUSTAIN prediction	Calibrated outflow	1.021
		Decay	0.05
		Perct. removal	0.05
6/10/2010	Observed EMC (mg/L)	Inflow	1.00
		Outflow	0.70
	SUSTAIN prediction	Calibrated outflow	0.706
		Decay	0.13
		Perct. removal	0.12
Calibrated parameters (average)		**Decay**	**0.033**
		Perct. removal	**0.085**

Table 5. Summary of calibration results for TP for gravel wetland following the first calibration approach.

Calibration events			**Values**
6/18/2009	Observed EMC (mg/L)	Inflow	0.02
		Outflow	0.05
	SUSTAIN prediction	Calibrated outflow	0.047
		Decay	-0.21
		Perct. removal	0.06
9/27/2009	Observed EMC (mg/L)	Inflow	0.02
		Outflow	0.005
	SUSTAIN prediction	Calibrated outflow	0.005
		Decay	0.12
		Perct. removal	0.03
11/20/2009	Observed EMC (mg/L)	Inflow	0.02
		Outflow	0.005
	SUSTAIN prediction	Calibrated outflow	0.005
		Decay	0.1
		Perct. removal	0.13
6/10/2010	Observed EMC (mg/L)	Inflow	0.1
		Outflow	0.005
	SUSTAIN prediction	Calibrated outflow	0.005
		Decay	0.33
		Perct. removal	0.42
Calibrated parameters (average)		**Decay**	**0.085**
		Perct. removal	**0.160**

After the first calibration method is completed for TN and TP, the gravel wetland representation was validated using the cumulative dataset (09/2007 to 09/2010) formed by all 49 monitored events. The cumulative TN and TP EMC reductions by the calibrated gravel wetland model are then compared against the monitored data, and the results are summarized in Table 6.

Table 6. Validation of gravel wetland cumulative performances following the first calibration approach.

	First calibration method	Monitored	Difference%
TN removal percent	18%	45%	-27%
TP removal percent	34%	39%	-5%

As shown in the results, the calibrated parameters generate lower removal efficiency for TP and TN compared to the monitored data.

The calibrated parameters were then used for BMP performance curve generation. The long-term time series for the *Commercial_Impervious* land use and for the period of 01/01/1992 to 12/31/2014 were used for generating the BMP performance curve. The efficiency table is shown in Table 7, and the BMP performance curves for TN and TP are shown in Figure 2.

Table 7. Long-term gravel wetland performances following the first calibration approach.

	0.1in	0.2in	0.4in	0.6in	0.8in	1.0in	1.5in	2.0in
TN	15%	24%	36%	45%	51%	56%	64%	70%
TP	26%	39%	55%	65%	71%	75%	80%	84%

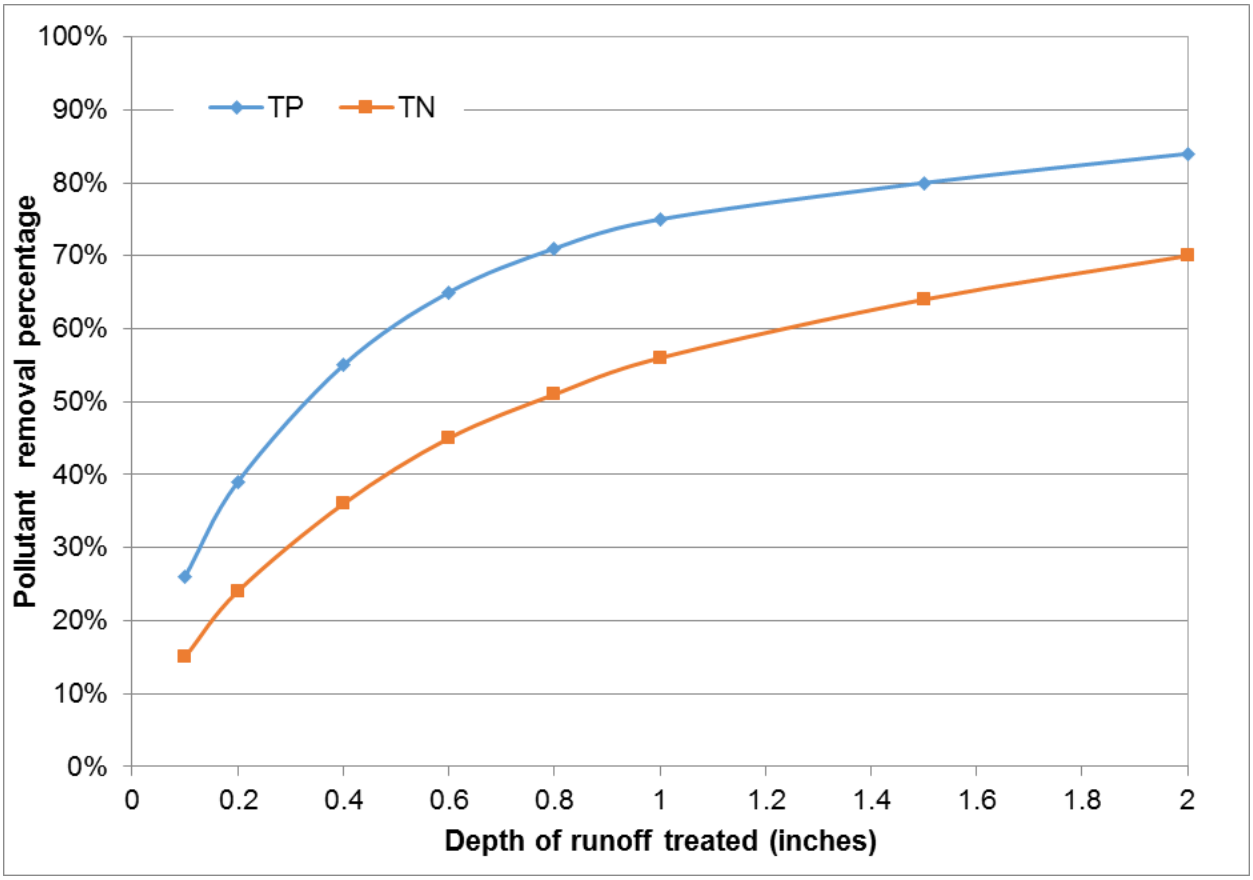

Figure 2. Gravel wetland performance curves for TN and TP following the first calibration approach.

3.2 Biofiltration with ISR

In the first calibration approach for biofiltration with ISR, four calibration events were selected from the summer, fall, and winter seasons, and with vary magnitudes of storm sizes (0.26 inch to 0.71 inch). The events used for biofiltration with ISR calibration is shown in Table 8.

Table 8. List of biofiltration with ISR candidate monitoring events following the first calibration approach.

Date	Rainfall Depth (in)	Peak Intensity (in/5-min)	Antecedent Dry Period (days)	Removal Efficiency (RE)	
				TN	TP
06/22/2012	0.71	0.20	8	56%	69%
09/08/2012	0.26	0.08	2	44%	53%

07/27/2014	0.39	0.12	2	-27%	33%
09/02/2014	0.56	0.12	19	-14%	-30%

Individual SUSTAIN models were set up for the biofiltration with ISR system. For each event, the models were first calibrated for the hydrology, and then were calibrated to match the event mean concentration predictions for TN and TP, separately. The calibrated TN and TP performances are shown in Tables 9 and 10 below, with the calibrated parameters summarized at the end of the tables.

Table 9. Summary of calibration results for TN for biofiltration with ISR following the first calibration approach.

Calibration events			**Values**
06/22/2012	Observed EMC (mg/L)	Inflow	2.5
		Outflow	1.1
	SUSTAIN prediction	Calibrated outflow	1.13
		Decay	0.16
		Perct. removal	0.06
09/08/2012	Observed EMC (mg/L)	Inflow	1.6
		Outflow	0.9
	SUSTAIN prediction	Calibrated outflow	0.92
		Decay	0.15
		Perct. removal	0.05
07/27/2014	Observed EMC (mg/L)	Inflow	1.5
		Outflow	1.9
	SUSTAIN prediction	Calibrated outflow	1.93
		Decay	-0.19
		Perct. removal	0.14
09/02/2014	Observed EMC (mg/L)	Inflow	1.4
		Outflow	1.6
	SUSTAIN prediction	Calibrated outflow	1.64
		Decay	-0.055
		Perct. removal	0.1
Calibrated parameters (average)		**Decay**	**0.016**
		Perct. removal	**0.088**

Table 10. Summary of calibration results for TP for biofiltration with ISR following the first calibration approach.

Calibration events			**Values**
06/22/2012	Observed EMC (mg/L)	Inflow	0.16
		Outflow	0.05
	SUSTAIN prediction	Calibrated outflow	0.047
		Decay	0.11
		Perct. removal	0.28
09/08/2012	Observed EMC (mg/L)	Inflow	0.15
		Outflow	0.07
	SUSTAIN	Calibrated outflow	0.072

	prediction	Decay	0.1
		Perct. removal	0.22
07/27/2014	Observed EMC (mg/L)	Inflow	0.09
		Outflow	0.06
	SUSTAIN prediction	Calibrated outflow	0.063
		Decay	0.14
		Perct. removal	0.65
09/02/2014	Observed EMC (mg/L)	Inflow	0.1
		Outflow	0.13
	SUSTAIN prediction	Calibrated outflow	0.126
		Decay	-0.09
		Perct. removal	0.16
Calibrated parameters (average)		**Decay**	**0.065**
		Perct. removal	**0.328**

After the first calibration method is completed for TN and TP, the biofiltration with ISR representation was validated using the cumulative dataset (10/2011 to 11/2014) formed by all 30 monitored events. The TN and TP EMC reductions by the calibrated biofiltration with ISR model were then compared against the monitored data, and the results are summarized in Table 11.

Table 11. Validation of biofiltration with ISR cumulative performances following the first calibration approach.

	First calibration method	Monitored	Difference%
TN removal percent	30%	26%	4%
TP removal percent	41%	37%	4%

As shown in the results, the calibrated parameters show slightly high removal efficiency for TN and TP as compared to the monitored data.

The calibrated parameters were then used for BMP performance curve generation. The long-term time series for the *Commercial_Impervious* land use and for the period of 01/01/1992 to 12/31/2014 were used for generating the BMP performance curve. The efficiency table is shown in Table 12, and the BMP performance curve is shown in Figure 3.

Table 12. Long-term biofiltration with ISR performances following the first calibration approach.

	0.1in	0.2in	0.4in	0.6in	0.8in	1.0in	1.5in	2.0in
TN	15%	24%	36%	45%	51%	56%	64%	70%
TP	26%	39%	55%	65%	71%	75%	80%	84%

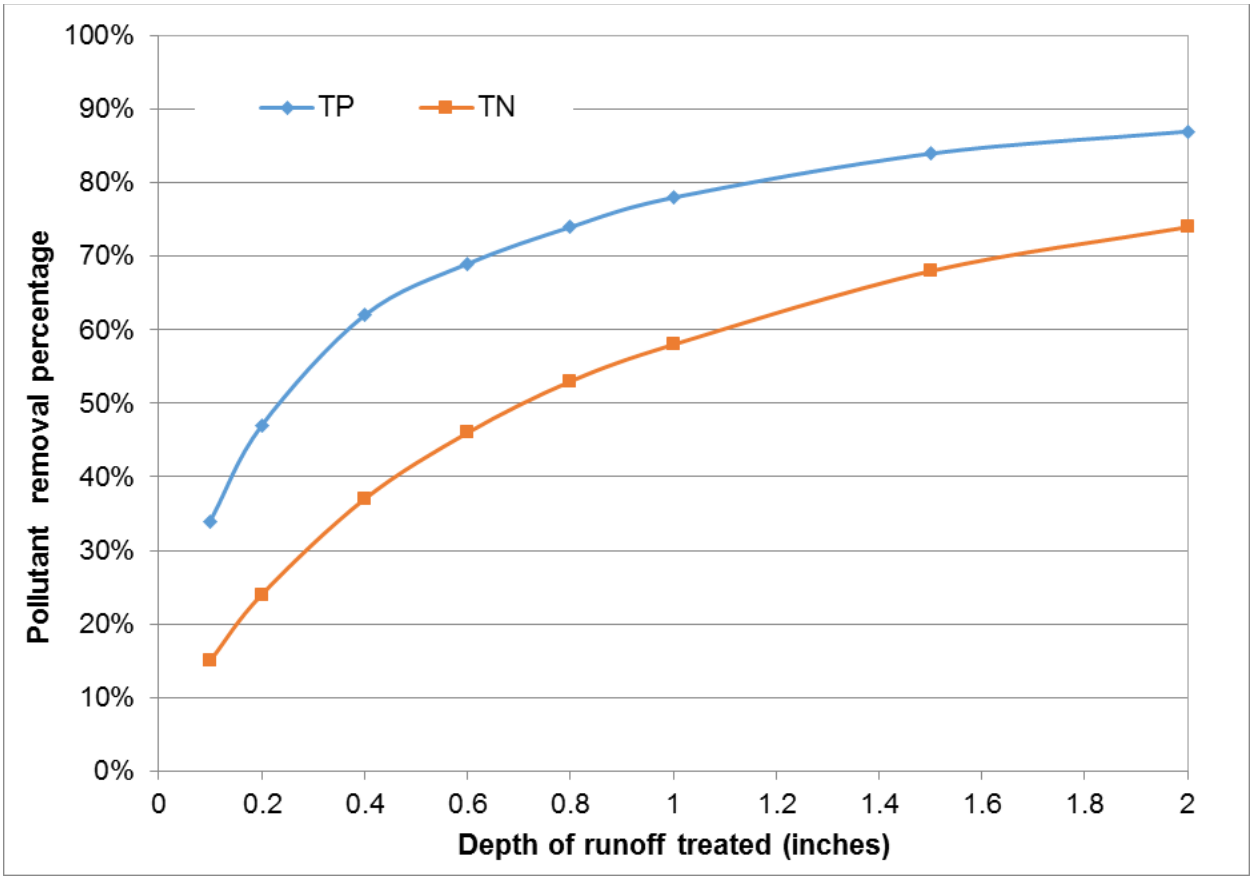

Figure 3. Biofiltration with ISR performance curves for TN and TP following the first calibration approach.

4. Second Calibration Approach

4.1 Gravel Wetland

In the second calibration approach for gravel wetland, a total number of eight events were selected for the calibration efforts. In addition to events shown in Table 3, four more events were added to the calibration dataset. Wider variations in season, rainfall depth, as well as the antecedent dry periods were incorporated during the selection process. The four new events are summarized in Table 13.

Table 13. Additional events added to the gravel wetland calibration dataset in the second calibration approach.

Date	Rainfall Depth (in)	Peak Intensity (in/5-min)	Antecedent Dry Period (days)	Removal Efficiency (RE)	
				TN	TP
04/06/2009	1.07	0.07	2	69%	56%
08/22/2009	0.76	0.38	8	68%	-33%
04/16/2010	1.16	0.04	6	18%	18%
06/23/2010	0.29	0.02	12	55%	90%

Similar to processes in the first calibration approach, SUSTAIN models were set up for each of the calibration events. The calibration was carried out first for hydrology and then for water quality. The calibrated TN and TP performances are shown in Tables 14 and 15 below, with the calibrated parameters summarized at the end of the tables.

Table 14. Summary of calibration results for TN for gravel wetland following the second calibration approach.

Calibration events			**Values**
04/06/2009	Observed EMC (mg/L)	Inflow	0.80
		Outflow	0.25
	SUSTAIN prediction	Calibrated outflow	0.244
		Decay	0.13
		Perct. removal	0.12
08/22/2009	Observed EMC (mg/L)	Inflow	1.90
		Outflow	0.60
	SUSTAIN prediction	Calibrated outflow	0.647
		Decay	0.12
		Perct. removal	0.27
04/16/2010	Observed EMC (mg/L)	Inflow	1.1
		Outflow	0.9
	SUSTAIN prediction	Calibrated outflow	0.86
		Decay	0.04
		Perct. removal	0.02
06/22/2010	Observed EMC (mg/L)	Inflow	1.10
		Outflow	0.50
	SUSTAIN prediction	Calibrated outflow	0.495
		Decay	0.11
		Perct. removal	0.12
Calibrated parameters (including the first four events)		**Decay**	**0.066**
		Perct. removal	**0.109**

Table 15. Summary of calibration results for TP for gravel wetland following the second calibration approach.

Calibration events			**Values**
4/6/2009	Observed EMC (mg/L)	Inflow	0.09
		Outflow	0.04
	SUSTAIN prediction	Calibrated outflow	0.038
		Decay	0.09
		Perct. removal	0.07
08/22/2009	Observed EMC (mg/L)	Inflow	0.03
		Outflow	0.04
	SUSTAIN prediction	Calibrated outflow	0.041
		Decay	-0.05
		Perct. removal	0.05
4/16/2010	Observed EMC (mg/L)	Inflow	0.017
		Outflow	0.014

	SUSTAIN prediction	Calibrated outflow	0.014
		Decay	0.11
		Perct. removal	0.15
6/22/2010	Observed EMC (mg/L)	Inflow	0.05
		Outflow	0.005
	SUSTAIN prediction	Calibrated outflow	0.005
		Decay	0.35
		Perct. removal	0.40
Calibrated parameters (including the first four events)		**Decay**	**0.105**
		Perct. removal	**0.164**

After the second calibration method is completed for TN and TP, the gravel wetland representation was validated using the cumulative dataset (09/2007 to 09/2010) formed by all 49 monitored events. The cumulative TN and TP EMC reductions by the calibrated gravel wetland model are then compared against the monitored data, and the results are summarized in Table 16.

Table 16. Validation of gravel wetland cumulative performances following the second calibration approach.

	Second calibration method	Monitored	Difference%
TN removal percent	22%	45%	-23%
TP removal percent	35%	39%	-4%

As shown in the results, the calibrated parameters generate lower removal efficiency for TN and exact match for TP as compared to the observed data.

The calibrated parameters were then used for BMP performance curve generation. The long-term time series for the *Commercial_Impervious* land use and for the period of 01/01/1992 to 12/31/2014 were used for generating the BMP performance curve. The efficiency table is shown in Table 17, and the BMP performance curve is shown in Figure 4.

Table 17. Long-term gravel wetland performances following the second calibration approach.

	0.1in	0.2in	0.4in	0.6in	0.8in	1.0in	1.5in	2.0in
TN	22%	33%	48%	57%	64%	68%	74%	79%
TP	29%	43%	59%	69%	74%	78%	83%	86%

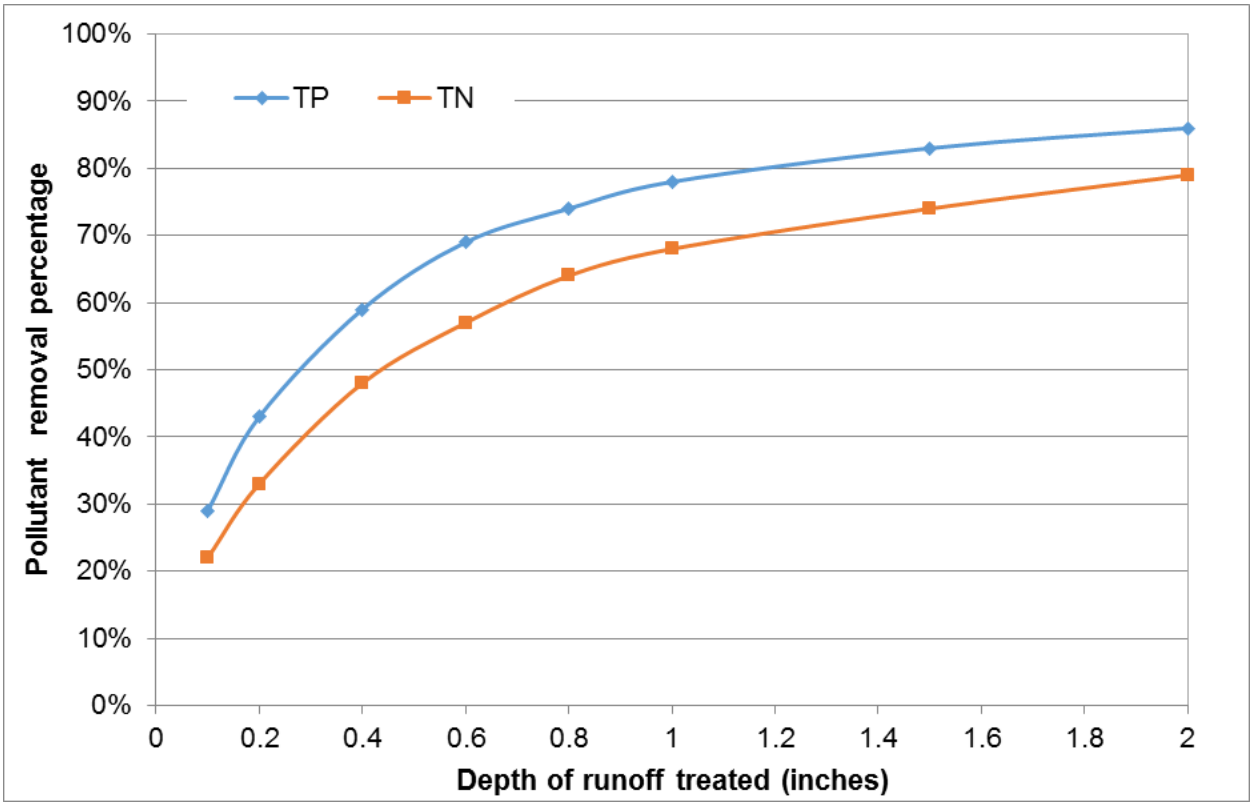

Figure 4. Gravel wetland performance curves for TN and TP following the second calibration approach.

4.2 Biofiltration with ISR

In the second calibration approach for biofiltration with ISR, a total number of eight events were selected for the calibration efforts. In addition to events shown in Table 8, four more events were added to the calibration dataset. Wider variations in season, rainfall depth, as well as the antecedent dry periods were incorporated during the selection process. The four new events are summarized in Table 18.

Table 18. Additional events added to the biofiltration with ISR calibration dataset in the second calibration approach.

Date	Rainfall Depth (in)	Peak Intensity (in/5-min)	Antecedent Dry Period (days)	Removal Efficiency (RE)	
				TN	TP
11/10/2011	0.98	0.06	10	20%	55%
7/17/2012	0.19	0.08	1	44%	65%
08/10/2012	0.53	0.07	4	-9%	-200%
11/17/2013	0.27	0.04	6	17%	43%

Similar to processes in the first calibration approach, SUSTAIN models were set up for each of the calibration event. The calibration was carried out first for hydrology and then for water quality. The calibrated TN and TP performances are shown in Tables 19 and 20 below, with the calibrated parameters summarized at the end of the tables.

Table 19. Summary of calibration results for TN for biofiltration with ISR following the second calibration approach.

Calibration events			**Values**
11/10/2011	Observed EMC (mg/L)	Inflow	1
		Outflow	0.8
	SUSTAIN prediction	Calibrated outflow	0.078
		Decay	0.47
		Perct. removal	0.79
7/17/2012	Observed EMC (mg/L)	Inflow	3.2
		Outflow	1.8
	SUSTAIN prediction	Calibrated outflow	1.82
		Decay	0.18
		Perct. removal	0.16
08/10/2012	Observed EMC (mg/L)	Inflow	1.1
		Outflow	1.2
	SUSTAIN prediction	Calibrated outflow	1.16
		Decay	-0.06
		Perct. removal	0.04
11/17/2013	Observed EMC (mg/L)	Inflow	1.8
		Outflow	1.5
	SUSTAIN prediction	Calibrated outflow	1.49
		Decay	0.09
		Perct. removal	0.04
Calibrated parameters (including the first four events)		**Decay**	**0.093**
		Perct. removal	**0.173**

Table 20. Summary of calibration results for TP for biofiltration with ISR following the second calibration approach.

Calibration events			**Values**
11/10/2011	Observed EMC (mg/L)	Inflow	0.2
		Outflow	0.09
	SUSTAIN prediction	Calibrated outflow	0.089
		Decay	0.16
		Perct. removal	0.2
7/17/2012	Observed EMC (mg/L)	Inflow	0.34
		Outflow	0.12
	SUSTAIN prediction	Calibrated outflow	0.118
		Decay	0.19
		Perct. removal	0.38
08/10/2012	Observed EMC (mg/L)	Inflow	0.002
		Outflow	0.06
	SUSTAIN prediction	Calibrated outflow	0.055
		Decay	-0.62
		Perct. removal	0.08
11/17/2013	Observed EMC (mg/L)	Inflow	0.07
		Outflow	0.04

	SUSTAIN prediction	Calibrated outflow	0.038
		Decay	0.25
		Perct. removal	0.26
Calibrated parameters (including the first four events)		**Decay**	**0.03**
		Perct. removal	**0.279**

After the first calibration method is completed for TN and TP, the biofiltration with ISR representation was validated using the cumulative dataset (10/2011 to 11/2014) formed by all 30 monitored events. The cumulative TN and TP EMC reductions by the calibrated biofiltration with ISR model are then compared against the monitored data, and the results are summarized in Table 21.

Table 21. Validation of biofiltration with ISR cumulative performances following the second calibration approach.

	Second calibration method	Monitored	Difference%
TN removal percent	42%	26%	16%
TP removal percent	36%	37%	-1%

As shown in the results, the calibrated parameters show slightly higher removal efficiency for TN and close match for TP as compared to monitored data.

The calibrated parameters were then used for BMP performance curve generation. The long-term time series for the *Commercial_Impervious* land use and for the period of 01/01/1992 to 12/31/2014 were used for generating the BMP performance curve. The efficiency table is shown in Table 22, and the BMP performance curve is shown in Figure 5.

Table 22. Long-term biofiltration with ISR performances following the second calibration approach.

	0.1in	0.2in	0.4in	0.6in	0.8in	1.0in	1.5in	2.0in
TN	32%	44%	58%	66%	71%	75%	82%	86%
TP	27%	39%	53%	62%	67%	71%	78%	83%

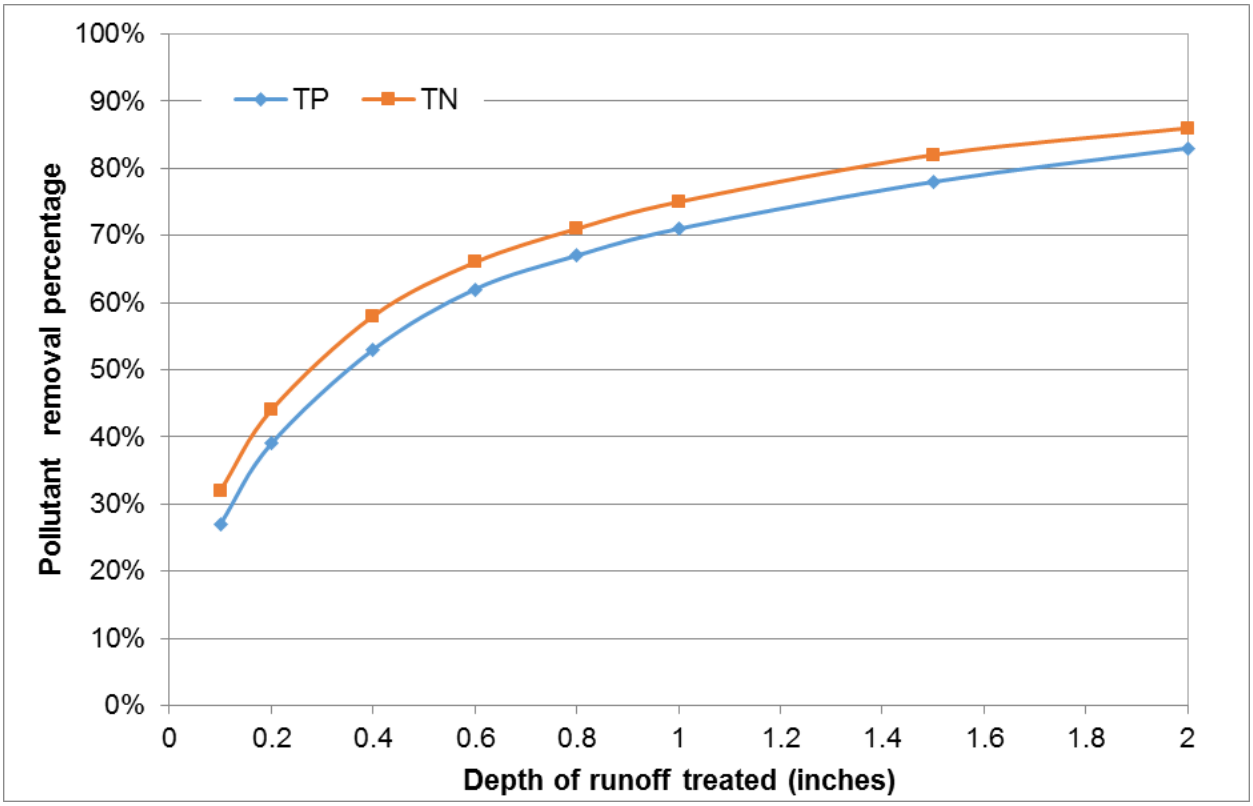

Figure 5. Biofiltration with ISR performance curves for TN and TP following the second calibration approach.

5. Third Calibration Approach

5.1 Gravel Wetland

In the third calibration approach for gravel wetland, all fourteen calibration events were used to calibrate the SUSTAIN representation. The six additional events used in the third calibration approach are summarized in Table 23.

Table 23. List of additional gravel wetland events for the third calibration approach.

Date	Rainfall Depth (in)	Peak Intensity (in/5-min)	Antecedent Dry Period (days)	Removal Efficiency (RE)	
				TN	TP
6/4/2008	0.40	0.02	3	45%	100%
4/3/2009	0.79	0.11	3	58%	81%
5/5/2009	0.72	0.03	12	53%	50%
9/11/2009	0.95	0.06	12	67%	92%
7/21/2010	0.45	0.23	6	69%	78%
9/16/2010	0.49	0.03	3	47%	33%

Similar to the first two calibration approaches, individual SUSTAIN models were set up to calibrate the gravel wetland hydrologic and water quality performances. The calibrated TN and TP

performances are shown in Tables 24 and 25 below, with the calibrated parameters summarized at the end of the tables.

Table 24. Summary of calibration results for TN for gravel wetland following the third calibration approach.

Calibration events			**Values**
6/4/2008	Observed EMC (mg/L)	Inflow	1.1
		Outflow	0.6
	SUSTAIN prediction	Calibrated outflow	0.58
		Decay	0.11
		Perct. removal	0.12
4/3/2009	Observed EMC (mg/L)	Inflow	0.6
		Outflow	0.25
	SUSTAIN prediction	Calibrated outflow	0.248
		Decay	0.05
		Perct. removal	0.04
5/5/2009	Observed EMC (mg/L)	Inflow	1.50
		Outflow	0.7
	SUSTAIN prediction	Calibrated outflow	0.73
		Decay	0.14
		Perct. removal	0.14
9/11/2009	Observed EMC (mg/L)	Inflow	1.80
		Outflow	0.25
	SUSTAIN prediction	Calibrated outflow	0.251
		Decay	0.2
		Perct. removal	0.22
7/21/2010	Observed EMC (mg/L)	Inflow	0.80
		Outflow	0.25
	SUSTAIN prediction	Calibrated outflow	0.246
		Decay	0.13
		Perct. removal	0.12
9/16/2010	Observed EMC (mg/L)	Inflow	1.50
		Outflow	0.80
	SUSTAIN prediction	Calibrated outflow	0.83
		Decay	0.03
		Perct. removal	0.05
Calibrated parameters (including the previous eight events)		**Decay**	**0.085**
		Perct. removal	**0.111**

Table 25. Summary of calibration results for TP for gravel wetland following the third calibration approach.

Calibration events			**Values**
6/4/2008	Observed EMC (mg/L)	Inflow	0.05
		Outflow	0.005
	SUSTAIN prediction	Calibrated outflow	0.005
		Decay	0.35
		Perct. removal	0.48

4/3/2009	Observed EMC (mg/L)	Inflow	0.16
		Outflow	0.03
	SUSTAIN prediction	Calibrated outflow	0.03
		Decay	0.14
		Perct. removal	0.13
5/5/2009	Observed EMC (mg/L)	Inflow	0.04
		Outflow	0.02
	SUSTAIN prediction	Calibrated outflow	0.019
		Decay	0.15
		Perct. removal	0.11
9/11/2009	Observed EMC (mg/L)	Inflow	0.06
		Outflow	0.005
	SUSTAIN prediction	Calibrated outflow	0.006
		Decay	0.33
		Perct. removal	0.48
7/21/2010	Observed EMC (mg/L)	Inflow	0.09
		Outflow	0.02
	SUSTAIN prediction	Calibrated outflow	0.02
		Decay	0.15
		Perct. removal	0.25
9/16/2010	Observed EMC (mg/L)	Inflow	0.03
		Outflow	0.02
	SUSTAIN prediction	Calibrated outflow	0.021
		Decay	0.02
		Perct. removal	0.03
Calibrated parameters (including the previous eight events)		**Decay**	**0.141**
		Perct. removal	**0.199**

After the third calibration method is completed for TN and TP, the gravel wetland representation was validated using the cumulative dataset (09/2007 to 09/2010) formed by all 49 monitored events. The cumulative TN and TP EMC reductions by the calibrated gravel wetland model are then compared against the monitored data, and the results are summarized in Table 26.

Table 26. Validation of gravel wetland cumulative performances following the third calibration approach.

	Third calibration method	Monitored	Difference%
TN removal percent	26%	45%	-19%
TP removal percent	40%	39%	1%

As shown in the results, the calibrated parameters show slightly higher removal efficiency for TN and TP as compared to monitored data.

The calibrated parameters were then used for BMP performance curve generation. The long-term time series for the *Commercial_Impervious* land use and for the period of 01/01/1992 to 12/31/2014 were used for generating the BMP performance curve. The efficiency table is shown in Table 27, and the BMP performance curve is shown in Figure 6.

Table 27. Long-term gravel wetland performances following the third calibration approach.

	0.1in	0.2in	0.4in	0.6in	0.8in	1.0in	1.5in	2.0in
TN	24%	38%	52%	62%	68%	72%	78%	82%
TP	33%	49%	65%	75%	80%	83%	87%	90%

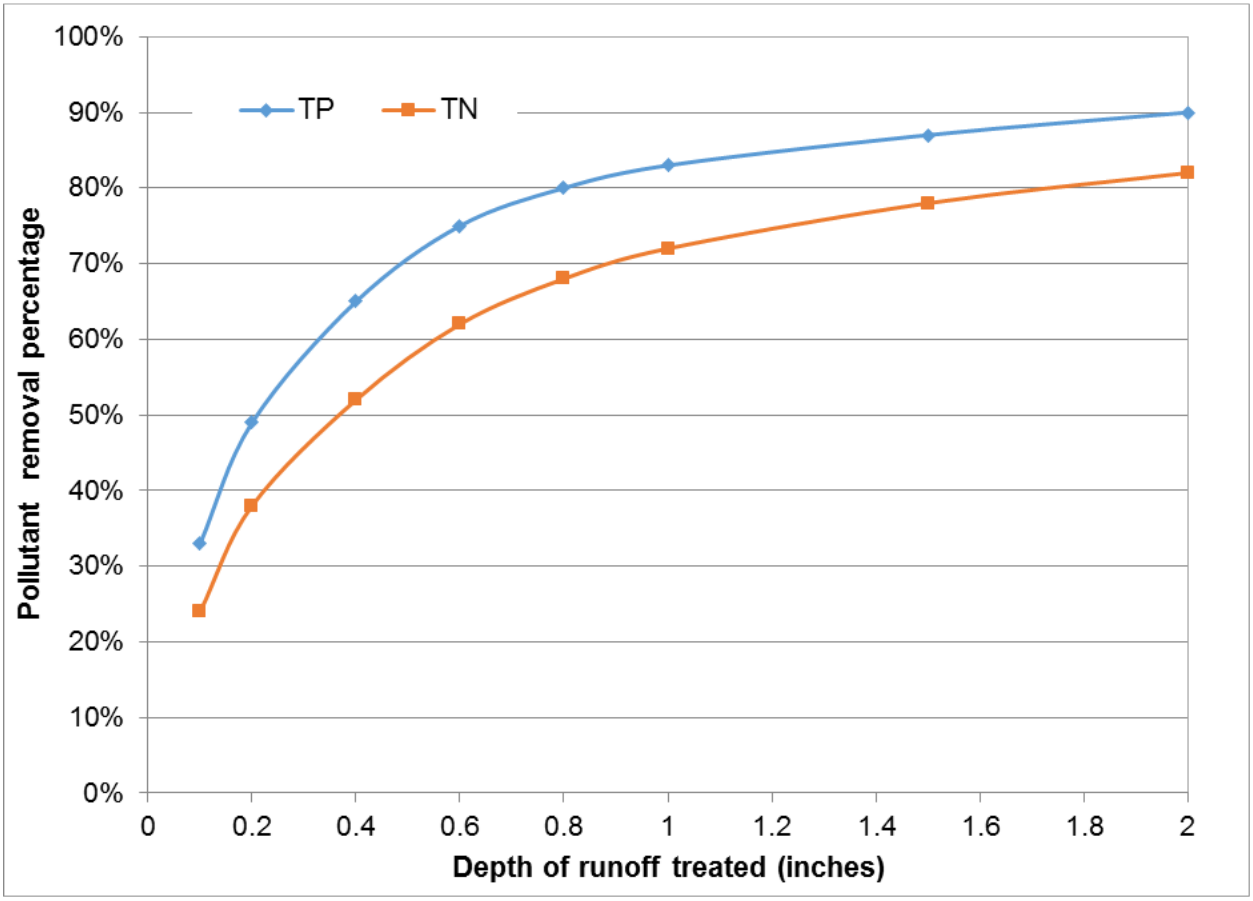

Figure 6. Gravel wetland performance curves for TN and TP following the third calibration approach.

5.2 Biofiltration with ISR

In the third calibration approach for biofiltration with ISR, all fourteen calibration events were used to calibrate the SUSTAIN representation. The six additional events used in the third calibration approach are summarized in Table 28.

Table 28. List of additional biofiltration with ISR calibration events for the third calibration approach.

Date	Rainfall Depth (in)	Peak Intensity (in/5-min)	Antecedent Dry Period (days)	Removal Efficiency (RE)	
				TN	TP
6/25/2014	0.87	0.11	11	21%	4%
7/13/2014	0.19	0.07	3	48%	89%

7/31/2014	0.12	0.03	2	48%	38%
9/13/2014	0.12	0.01	5	11%	58%
10/4/2014	0.21	0.02	2	59%	83%
11/1/2014	0.35	0.01	8	57%	75%

Similar to the first two calibration approaches, individual SUSTAIN models were set up to calibrate the biofiltration with ISR hydrologic and water quality performances. The calibrated TN and TP performances are shown in Tables 29 and 30 below, with the calibrated parameters summarized at the end of the tables.

Table 29. Summary of calibration results for TN for biofiltration with ISR following the third calibration approach.

Calibration events			**Values**
6/25/2014	Observed EMC (mg/L)	Inflow	1.9
		Outflow	1.5
	SUSTAIN prediction	Calibrated outflow	1.45
		Decay	0.09
		Perct. removal	0.04
7/13/2014	Observed EMC (mg/L)	Inflow	2.7
		Outflow	1.4
	SUSTAIN prediction	Calibrated outflow	1.45
		Decay	0.13
		Perct. removal	0.74
7/31/2014	Observed EMC (mg/L)	Inflow	2.5
		Outflow	1.3
	SUSTAIN prediction	Calibrated outflow	1.26
		Decay	0.30
		Perct. removal	0.24
9/13/2014	Observed EMC (mg/L)	Inflow	0.9
		Outflow	0.8
	SUSTAIN prediction	Calibrated outflow	0.76
		Decay	0.11
		Perct. removal	0.15
10/4/2014	Observed EMC (mg/L)	Inflow	2.2
		Outflow	0.9
	SUSTAIN prediction	Calibrated outflow	0.93
		Decay	0.21
		Perct. removal	0.19
11/1/2014	Observed EMC (mg/L)	Inflow	1.4
		Outflow	0.6
	SUSTAIN prediction	Calibrated outflow	0.57
		Decay	0.21
		Perct. removal	0.20
Calibrated parameters (including the previous eight events)		**Decay**	**0.128**
		Perct. removal	**0.21**

Table 30. Summary of calibration results for TP for biofiltration with ISR following the third calibration approach.

Calibration events			**Values**
6/25/2014	Observed EMC (mg/L)	Inflow	0.23
		Outflow	0.22
	SUSTAIN prediction	Calibrated outflow	0.205
		Decay	0.03
		Perct. removal	0.04
7/13/2014	Observed EMC (mg/L)	Inflow	0.18
		Outflow	0.02
	SUSTAIN prediction	Calibrated outflow	0.022
		Decay	0.14
		Perct. removal	0.65
7/31/2014	Observed EMC (mg/L)	Inflow	0.16
		Outflow	0.1
	SUSTAIN prediction	Calibrated outflow	0.096
		Decay	0.2
		Perct. removal	0.21
9/13/2014	Observed EMC (mg/L)	Inflow	0.12
		Outflow	0.05
	SUSTAIN prediction	Calibrated outflow	0.051
		Decay	0.2
		Perct. removal	0.26
10/4/2014	Observed EMC (mg/L)	Inflow	0.12
		Outflow	0.02
	SUSTAIN prediction	Calibrated outflow	0.021
		Decay	0.47
		Perct. removal	0.39
11/1/2014	Observed EMC (mg/L)	Inflow	0.12
		Outflow	0.03
	SUSTAIN prediction	Calibrated outflow	0.03
		Decay	0.37
		Perct. removal	0.36
Calibrated parameters (including the previous eight events)		**Decay**	**0.118**
		Perct. removal	**0.296**

After the third calibration method is completed for TN and TP, the biofiltration with ISR representation was validated using the cumulative dataset (10/2011 to 11/2014) formed by all 30 monitored events. The cumulative TN and TP EMC reductions by the calibrated biofiltration with ISR model are then compared against the monitored data, and the results are summarized in Table 31.

Table 31. Validation of biofiltration with ISR performances following the third calibration approach.

	Third calibration method	Monitored	Difference%
TN removal percent	45%	26%	19%
TP removal percent	44%	37%	7%

As shown in the results, the calibrated parameters show slightly higher removal efficiency for TN and TP as compared to monitored data.

The calibrated parameters were then used for BMP performance curve generation. The long-term time series for the *Commercial_Impervious* land use and for the period of 01/01/1992 to 12/31/2014 were used for generating the BMP performance curve. The efficiency table is shown in Table 32, and the BMP performance curve is shown in Figure 7.

Table 32. Long-term biofiltration with ISR performances following the third calibration approach.

	0.1in	0.2in	0.4in	0.6in	0.8in	1.0in	1.5in	2.0in
TN	37%	50%	63%	71%	76%	80%	85%	88%
TP	39%	53%	66%	73%	78%	82%	86%	89%

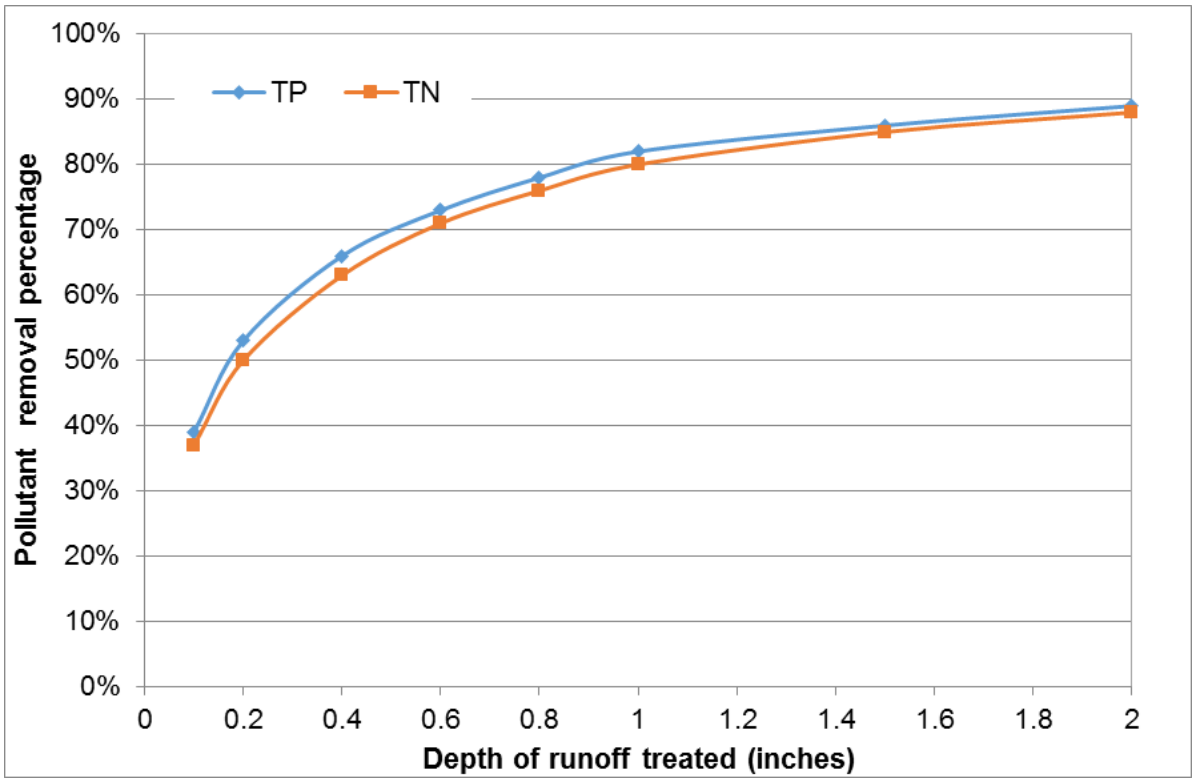

Figure 7. Biofiltration with ISR performance curve for TN and TP following the third calibration approach.

6. Evaluation and Recommendation

After the three calibration approaches were completed for gravel wetland and biofiltration with ISR, the resulting BMP performance curves from the three calibration approaches were plotted against each other for the two pollutants and are shown in Figures 8 to 11.

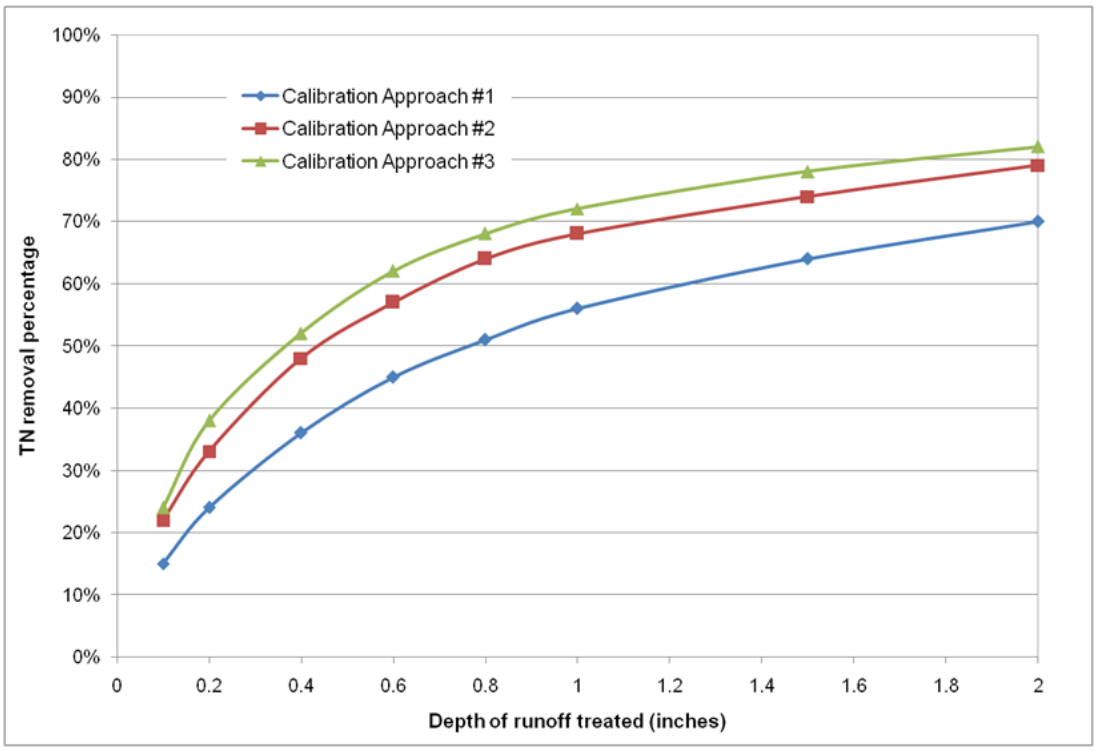

Figure 8. Comparison of gravel wetland performance curves for TN following the three calibration approaches.

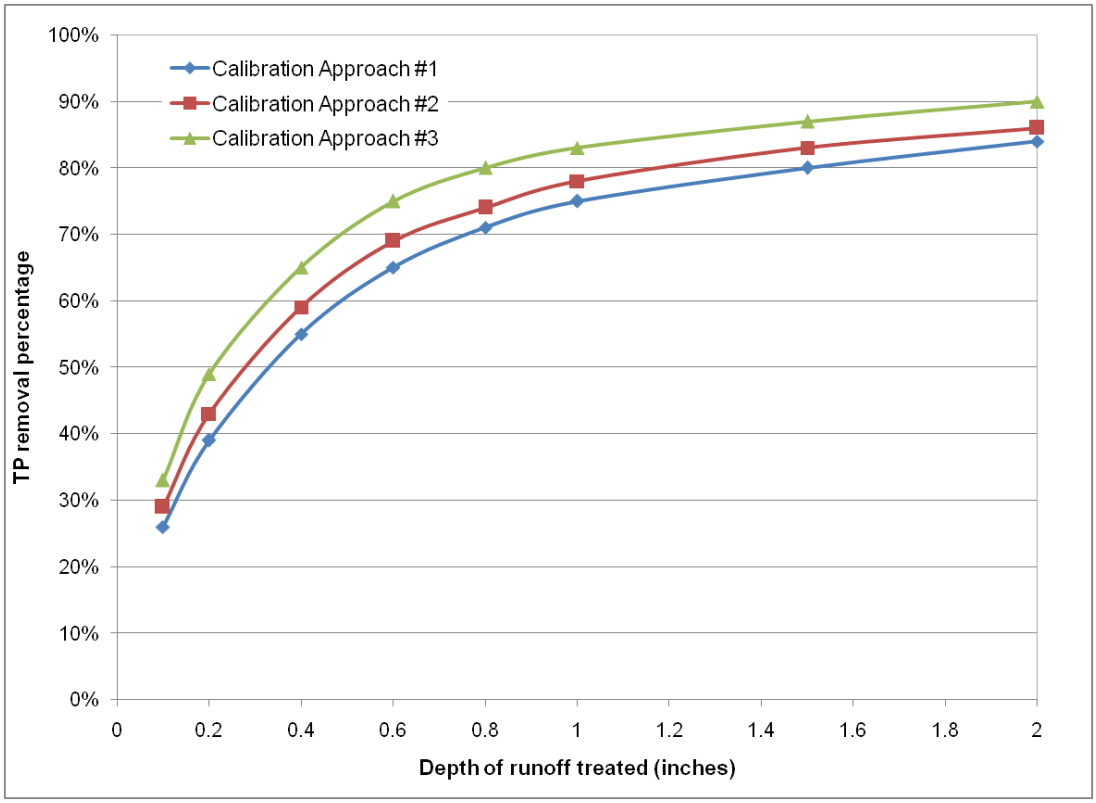

Figure 9. Comparison of gravel wetland performance curves for TP following the three calibration approaches.

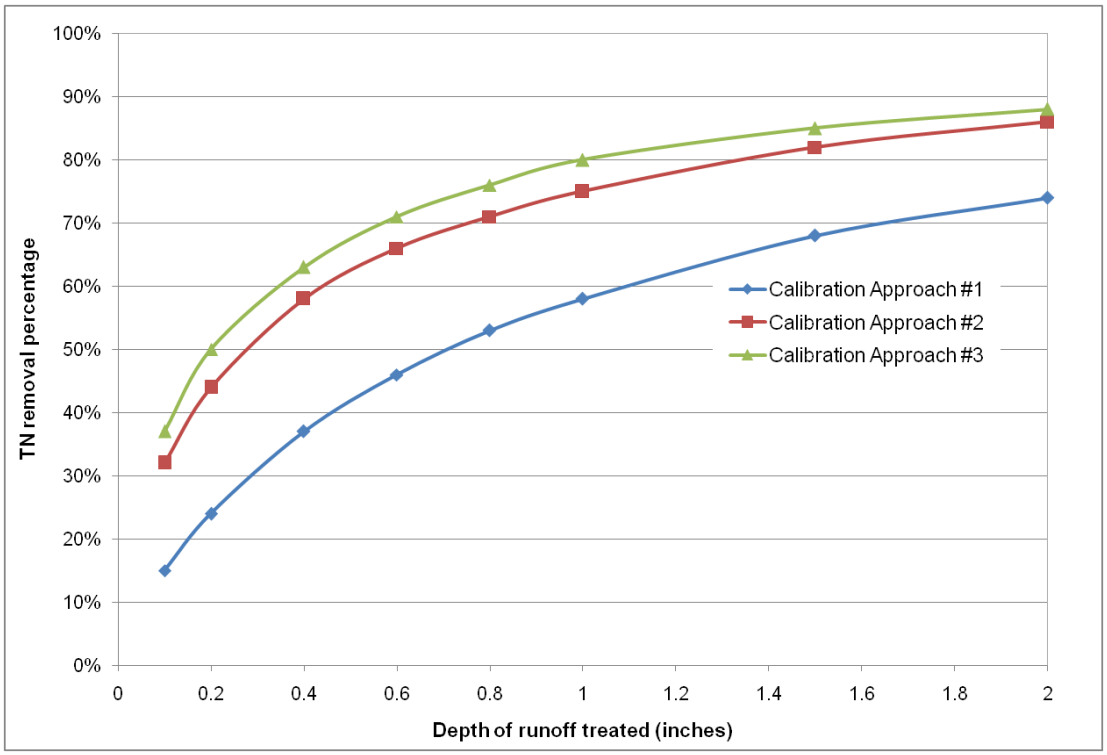

Figure 10. Comparison of biofiltration with ISR performance curves for TP following the three calibration approaches.

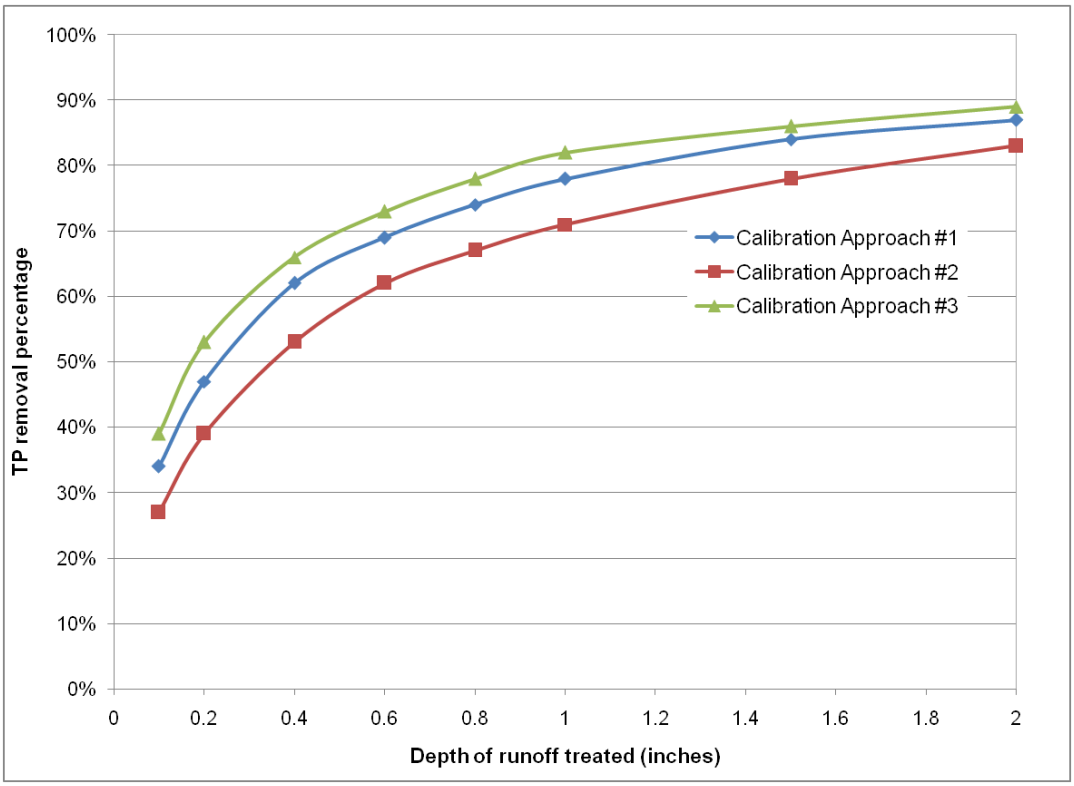

Figure 11. Comparison of biofiltration with ISR performance curves for TP following the three calibration approaches.

As shown in the figures, Approach #2 is a representative of the three calibration approaches for gravel wetland, with the average treatment efficiency differences from the other two approaches are about 10% for TN and 5% for TP. As for biofiltration with ISR, Approach #2 is a representative approach for TN and Approach #1 becomes the representative approach for TP. Overall, Approach #2 was selected as the approach that incurs intermediate level of efforts while achieving relatively high reliability.

From the performance curve generation processes for gravel wetland and biofiltration with ISR, the selection of model calibration events can be set to include 8 to 12 events, with at least one event from each season and at least two events for each size category (i.e. ≤0.5 in, 0.5-1.0 in, ≥1.0 in, depending on the actual rainfall distribution), and at the same time the events are representative of the antecedent dry period lengths. In addition, events that have negative removal efficiencies should also be included to have a comprehensive representation of the BMP performances.

Following these recommendations above on selection of calibration events, the Calibration Approach #2 could be used as a recommended approach for developing BMP performance curve generations, and the updated flow chart is shown in Figure 12.

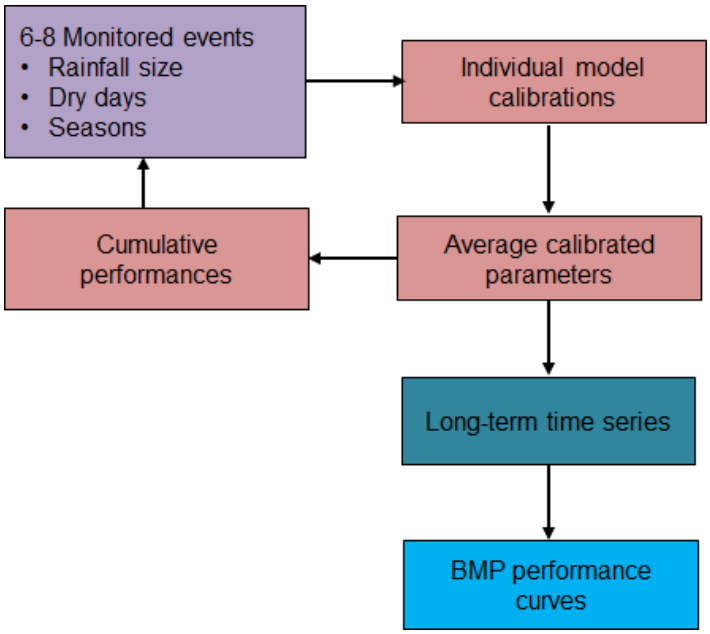

Figure 12. Recommended approach for developing long-term BMP performance curves.

7. Summary

The impacts of calibration strategies on the development of long-term BMP performance curves are evaluated in this study. Observed gravel wetland and biofiltration with ISR data from UNHSC were used for the calibration sensitivity analysis. SUSTAIN calibration models were set up for each individual event and the performances were calibrated. The calibrated BMP calibration parameters were then averaged for generating long-term performance curves. For sensitivity analysis purposes, the calibration events were divided into three groups: four events for the first

group, eight events for the second group, and 14 events for the third group. BMP performance curves were created for the commercial impervious land use.

The calibration results and final BMP performance curves indicate that six to eight calibration events with rainfall characteristic variations are reasonable for achieving good calibration results and for generating performance curves. Following the example analyses, the recommended procedures for generating long-term BMP performance curves are also provided in this study.